©2016

Shao-Yun Hsu

ALL RIGHTS RESERVED

THE FISCHER 344 SPINAL CORD CONTUSION MODEL AND EFFECTS OF CYCLOSPORIN-A ON THE MODEL

by

SHAO-YUN HSU

A dissertation submitted to the

Graduate School-New Brunswick

Rutgers, The State University of New Jersey

In partial fulfillment of the requirements

For the degree of

Doctor of Philosophy

Graduate Program in Neuroscience

Written under the direction of

Wise Young

And approved by

_____

_____

_____

_____

New Brunswick, New Jersey

May 2016

ABSTRACT OF THE DISSERTATION

The Fischer 344 Spinal Cord Contusion Model and Effects of Cyclosporin-A on the Model

By SHAO-YUN HSU

Dissertation Director:

Wise Young

The Multicenter Animal Spinal Cord Injury Study (MASCIS) standardized spinal cord injury (SCI) in Long-Evans hooded and Sprague-Dawley rats. In this thesis, we extended the MASCIS model to Fischer 344 (F344) rats for the following reasons. First, F344 rats are immune-compatible with each other. Cells can be transplanted from one F344 rat to another without immunosuppression. Second, our laboratory developed a strain of F344 rats that express green fluorescent protein (GFP). When transplanted into regular F344 rats, GFP F344 rat cells can be readily identified. Third, F344 rats are isogenic. They should have more uniform and replicable responses to injury and therapies. Finally, this F344 model allows us to assess effects of allogeneic cell transplants with and without

immunosuppressive drugs, such as cyclosporin-A (CsA), as well as the effects of immunosuppressive drugs on transplanted cells. We chose to assess olfactory ensheathing glial (OEG) cell transplants because many investigators have reported that these cells improve motor recovery in rat SCI models. Our results show that F344 rats can be reproducibly injured with the MASCIS model and that OEG transplants significantly improve locomotor recovery when transplanted without CsA. However, we encountered several unexpected findings. Female rats recovered more than male rats even though the animals were age-matched, studies of the spinal cords revealed no difference in size and anatomy of age-matched male and female rats, and 24-hour lesion volumes in male and female spinal cords were the same. OEG transplants improved recovery of male rats, almost as well as untreated female rats. CsA therapy improved recovery in both male and female rats. We conclude that the MASCIS model causes reproducible injury to spinal cords of F344 rats, age-matched female rats recover better locomotor function than male rats, OEG cells can be transplanted from GFP F344 rats to wild-type F344 rats without immune rejection, OEG transplants improve functional recovery particularly in male rats, CsA improved locomotor recovery in both male and female F344 rats. The MASCIS impactor model should be very useful for assessing mechanisms underlying gender differences, OEG and CsA effects on transplanted cells and recovery mechanisms.

ACKNOWLEDGEMENT

I would like to express my gratitude to Dr. Wise Young, who as my advisor fully supported my Ph.D. studies and related research. With his patience and vast knowledge, he helped to guide my research, and thesis. Also, I would like to thank the rest of my thesis committee: Dr. Jacqueline Bresnahan, Dr. Martin Grumet, and Dr. Shu-Chan Hsu. They provided me with a great deal of insight and direction. My sincere thanks also to Dr. Dongming Sun, Ms. Bor Tom, Mr. Hock Ng, and Mr. Sean O'Leary, who taught me a lot about the spinal cord injury model, which helped greatly with my research. Also, I appreciate the rest of my fellows in the W. M. Keck Center whom helped me to adapt and grow as an international student. In particular, I am grateful to Dr. Patricia Morton and Mr. Jim Bennett for their care and company. Lastly, I would like to thank my family: my parents and my husband. They encouraged me to pursue the degree and supported me through the struggles!

TALBE OF CONTENTS

LIST OF TABLES

LIST OF ILLUSTRATIONS

LIST OF ABBREVIATIONS

Ag-B	Antigen B
ANOVA	Analysis of variance
AUC	Area under the curve
BAD	Bcl-2 associated death promoter (a pro-apoptotic protein)
BBB	Basso-Beattie-Bresnahan (locomotor score)
BDA	Biotinylated dextran
BDNF	Brain-derived neurotrophic factor
BUF	Buffalo colony (rat)
Cd	Compression distance
CnA	Calcineurin A, phosphatase activity site
CsA	Cyclosporin-A
CST	Corticospinal tract
Cr	Compression rate (Cd/Ct)
Ct	Compression time
CVF	Cellular volume fraction
eGFP	Enhanced GFP
D1	Distal 5-mm spinal cord segment adjacent to the Imp segment
D2	Distal 5-mm spinal cord segment adjacent to D1
DMEM	Dulbecco's Modified Eagle's Medium (Sigma)
F12	Mixture of Dulbecco's modified Eagle and Ham's F12 media
F344	Fischer 344

FBS	Fetal bovine serum
FG	Fluorogold
FK506	Tacrolimus
FL-HL	Forelimb-Hindlimb
g	gram
GFAP	Glial fibrillary acidic protein
GFP	Green fluorescent protein
GVHD	Graft versus Host Disease
HBSS	Hank's buffered salt solution
IgG	Immunoglobulin G
ip	intraperitoneal
IFN	interferon
IL	interleukin
iv	intravenous
ImpV	Impact velocity
Imp	A 5-mm segment of spinal cord that has been contused
K	Potassium
[K]e	Extracellular potassium concentration
[K]I	Intracellular potassium concentration
LBN	Lewis-Brown-Norway (rat)
LV	Lesion volume
μl	microliter

mg	milligram
ml	milliliter
MASCIS	Multicenter animal spinal cord injury study
MPTP	Mitochondrial permeability transition pore
Na	Sodium
[Na]e	Extracellular sodium concentration
[Na]t	Tissue sodium concentration
Na-K	Difference of tissue Na and K concentration in mM.
NeuN	a neuron specific stain in vertebrates
NFAT	Nuclear factor of activated T-cells
ng	nanogram
NIH	National Institutes of Health
OEG	Olfactory ensheathing glia
ONL	Olfactory nerve layer
P1	Proximal 1 (5-mm spinal cord segment adjacent to Impact segment)
P2	Proximal 2 (5-mm spinal cord segment adjacent to P1)
P450	Microsomal P450 reductase, including cytochrome b5
P75	Low affinity neurotrophin receptor (TNFR superfamily, member 16)
RST	Rubrospinal tract
S100	low molecular weight proteins present in neural crest cells
sc	Subcutaneous injection
SCI	Spinal cord injury

SD	Sprague-Dawley
SEM	Standard error of mean
SMI-99	Purified mouse anti-myelin basic protein (antibody)
TNF-alpha	Tumor necrosis factor alpha
Vi	Intracellular volume
Vi/Vt	ratio of intracellular and tissue volume
ΔVi/Vt	change of the ratio of intracellular and tissue volume
Vt	Tissue volume
W	Wet weight (mg)
WNT	Wingless-related integration site (a family of signaling molecules)

CHAPTER 1 INTRODUCTION

1.1 History of the research

When we first started this project we had two main goals:

1. To establish a rat spinal cord contusion model for cell transplantation without using immunosuppression.
2. To determine the effect of immunosuppressant drugs on host and grafted cells after spinal cord injury (SCI).

Our laboratory had established a contusion model using the MASCIS Impactor on Long-Evans hooded and Sprague-Dawley rats. However, these two strains reject transplanted allogeneic (from a different individual of the same species or strain) cells and immunosuppression is necessary to prolong cell survival. To assess effects of an immunosuppressant drug on host and grafted cells, we chose Fischer 344 (F344) rats that allow cell transplants from other F344 rats to survive without immunosuppression. F344 is an inbred albino strain of rats that are immunocompetent but at the same time immune-compatible with each other. We first tested the contusion model in F344 rats using the standard MASCIS criteria. At the standard MASCIS criteria of 77±1 day old, F344 rats were smaller than Long-Evans hooded and Sprague-Dawley rats and had thinner dura that broke with weight drop contusions. We subsequently established a 100-day old criteria for the F344 contusion model and modified surgical exposure of the spinal cord to reduce dural breakage.

After establishing the contusion model, we studied immunocompatibility of cells from F344 rats transplanted into other F344 rats after SCI. We transplanted olfactory ensheathing cells (OEG) isolated from GFP F344 into other F344 rats after SCI and found that the OEG cells survived at least 16 weeks without immunosuppression. We then investigated the effects of CsA effect on F344 rats. The effective dose of CsA (10 mg/kg) in Sprague-Dawley was lethal for F344 rats. We therefore studied the pharmacodynamics of CsA in F344 rats and found the metabolism rate of CsA in the F344 was much slower than Sprague-Dawley rats. The effective CsA dose was 2 mg/kg in F344 rats. We then gave 2 mg/kg CsA daily to F344 rats for 6 weeks after SCI and assessed locomotor behavior and rubrospinal tract. The results were surprising. Untreated female F344 rats recovered much more than male rats. Previous studies in our laboratory had always used both male and female rats and showed no significant difference between male and female Long-Evans and Sprague-Dawley rats.

In summary, we thus achieved our first goal to establish the contusion model in F344 rats for cell transplantation. However, we also had several unexpected results. First, female F344 rats recover better than male F344 rats. Second, the pharmacodynamics and effective dose of CsA in F344 rats is much lower than for Sprague-Dawley and Long-Evans hooded rats. Third, CsA has significant beneficial effects on locomotor recovery after SCI in F344 rats. These results will be described below.

1.2 Contusion model

We assessed the effects of different parameters, including animal characteristics, surgical exposure, and impact parameters, on acute tissue damage, chronic histological changes, and functional recovery after graded spinal cord contusion. We collected data, including growth curve, spinal cord size and cell volume fraction to determine the age criteria for the contusion model. For validate the surgical procedure, we confirmed the contusion site and identified potential issues in F344 contusion model, including improper clamp position and dural breakage. We measured impact velocity, spinal cord compression distance (Cd), time (Ct), and rate (Cd/Ct). In addition, we calculated kinetic energy and average impact force from impact data. We measured 24-hour lesion volumes and chronic histological change, including spared white matter and neurons in spinal cords. Finally we observed behavioral and body weight changes for 8 weeks after SCI.

To optimize model parameters for F344 rats, we contused the spinal cords of 87 rats, using two different masses of falling weights (5-g and 10-g rods) and observing the effect of different impact parameters on acute tissue damage (24-hour lesion volume). Our results showed the Impactor with 10-g rod produced graded and consistent contusion injury. Therefore we used the Impactor device with 10-g rod for the rest of study, including chronic histological and behavioral change.

1.3 Contusion model for cell transplantation

This chapter describes immune-compatibility of cells transplanted from one F344 rat to another. We cultured primary OEG cells from GFP F344 rat pups, observed survival and migration of OEG cells after transplantation into contused spinal cords at 8 and 16 weeks, without immunosuppression. We also evaluated locomotor recovery of F344 rats once a week, using the Basso-Beattie-Bresnahan (BBB) scales. The results showed that OEG transplantation improved functional recovery in male rats only. The control female rats recovered much more than males. We proposed several hypotheses to explain this observation.

1.4 The cyclosporine effect on F344 rats after spinal cord injury

This chapter describes the effects of cyclosporine (CsA) on spinal-injured F344 rats. We first studied maximum tolerated CsA dose in F344 rats after SCI. Then we measured CsA blood levels at steady state and determined that the effective dose in F344 rats is 2 mg/kg/day by comparing blood CsA concentration with Sprague-Dawley that were given CsA 10mg/kg/day subcutaneously and confirming that this dose allowed survival of OEG cells collected from GFP Sprague-Dawley and injected into F344 hosts after SCI. Next, we gave 2 mg/kg/day CsA to spinal-injured F344 rats and evaluated hindlimb function and body weights every week. We traced rubrospinal tract with Fluorogold (FG) injured into the spinal cord below the injury site and counted the number of labeled neurons in red nuclei.

CHAPTER 2 F344 RATS CONTUSION MODEL

2.1 Introduction

2.1.1 Contusion model

Animal models are necessary to understand the pathology of SCI. Researchers use contusion, compression and transection SCI models. Although each model has limited ability to mimic all aspects of SCI in humans, the contusion model is a better model for human injury because most human SCI involve contusion of the spinal cord. Contusion models are the most widely used for research, and studies of contusion established the concepts of secondary tissue damage (*1*), demyelination (*2*), plasticity (*3*), and regeneration after SCI.

Several investigators have developed devices to contuse animal spinal cords. These include dropping a weight onto a piston [Wrathall] (*4, 5*), using air pressure to drive piston [General Motors] (*6*), applying an electromagnetic piston to the spinal cord [OSU] (*7, 8*), or dropping a rod [MASCIS] (*9-11*) or other weight [Infinite Horizon] (*12*) directly onto the spinal cord exposed by laminectomy. Contusion compresses the spinal cord rapidly enough to disrupt axons and other tissue elements.

A weight dropped onto the spinal cord exerts a force equal to the mass (m) times gravitational acceleration (g). The kinetic energy delivered to the spinal cord equals force times distance. Tissue will move longitudinally away from the indentation. When contusion velocity exceeds 0.5 m/s, deformation of tissues

disrupts blood vessels to cause hemorrhage, breaks axons, particularly myelinated axons at nodes of Ranvier and damages neurons (*13, 14*).

The Multicenter Animal Spinal Cord Injury Study (MASCIS) Impactor is the most popular device used to contuse rodent (rat and mouse) spinal cords. In 1989, Young et al. (*9*) at New York University (NYU) developed the Impactor device. In 1993, the National Institutes of Health (NIH)-funded MASCIS validated the model in eight SCI laboratories in the United States (*11*).

MASCIS obtained evidence justifying standardization of age of rats to 77±1 days, pentobarbital anesthesia (45 mg/kg and 65 mg/kg intraperitoneally for females and males respectively), timing of contusion to 1 hour after anesthesia, and weight drop heights to 12.5, 25.0, and 50.0 mm for mild, moderate and severe injuries. MASCIS also standardized many aspects of post-injury care, including care of the bladder and autophagia (*11*).

The Impactor created consistent and graded spinal cord injuries, manifested by consistent spinal cord lesion volumes (*9, 15*), spared white matter (*3*), and hindlimb locomotor activity using the Basso-Beattie-Bresnahan (BBB) locomotor score (*16, 17*). Over 100 laboratories have published studies applying the Impactor to several rat strains, including Long-Evans, Wistar and Sprague-Dawley. Few investigators (*18, 19*) have used the MASCIS Impactor to contuse F344 rats but no standardized model has been established.

2.1.2 F344 rats

Why we chose F344 rats

F344 rat is an inbred albino strain, originated by M. R. Curtis at Columbia University in 1920 (*20*). Inbred strains are produced by at least 20 generations of sibling mating and they are isogenic and homozygous. The latter means that the genes from the mother and father are located on the same chromosome, have the same DNA sequence, and have the same position on the chromosome. Isogenicity and homozygosity produce uniform and stable phenotypes (*21*).

These characteristics make F344 the preferred strain for certain types of research, such as aging, metabolism, and toxicology (*21-23*). For our study, the critical characteristic of F344 rat is immune-compatibility. Many studies have shown that F344 cell, tissue, and organ transplants survive in other F344 rats without immunosuppression (*24-29*).

This immune compatibility between F344 rats is not due to immune deficiency. F344 rat is immunocompetent. In 1978, Goodnight and colleagues (*30*) transplanted hearts and skin grafts from Lewis-Brown-Norway (LBN) and Buffalo colony (BUF) rats into F344 rats. The F344 recipients rejected heart grafts within a month and skin grafts within two weeks. They also reported that F344 rats showed strong immune responses to Antigen B (Ag-B) secreted by *Echinococcus granulosus metacestode*.

F344 rats are immune compatible because they are isogenic and homozygous. Cells or organs are transplanted from inbred, isogenic, and homozygous F344 rats to F344 rats are syngeneic transplants. The recipient rats do not require immunosuppression to prevent immune rejection of syngeneic transplants.

Our group had developed a F344 strain expressing the green fluorescent protein (GFP) by backcrossing transgenic male Sprague–Dawley rats [SD-Tg(CAG-EGFP)Cz-004Osb] carrying the eGFP transgene from Japan SLC., Inc. (Hamamatsu, Japan) with wild-type female F344 rats for 23 generations. We confirmed the resulting strain of GFP F344 rats are immune-compatible with wild-type F344 rats by showing that ovaries from GFP F344 rats can be transplanted into wild-type F344 rats. The wild-type F344 rats with GFP ovaries can give birth to GFP rat pups (*31*). The development of the GFP F344 rat and a contusion model using F344 rats allow transplantation of cells from GFP F344 rats into spinal-injured F344 rats without immunosuppression. Many immunosuppressive agents, particularly cyclosporin-A (CsA) and tacrolimus (FK506) inhibit calcineurin, a phosphatase known to activate nuclear factor of activated T-cells (NFAT) and Wingless Int (WNT)/beta-catenin (*32*), nuclear factors necessary for activation of growth, proliferation, and differentiation genes (*33*). Therefore, a SCI model in an inbred rat strain allows assessment of syngeneic transplants.

Why a model for F344 differs from other strains

Many investigators have studied contusion injuries in Sprague-Dawley (*34, 35*), Long-Evans (*3, 16, 34, 36*) or Wistar rats (*37*). While a few groups have used F344 rats for SCI research (*26-28, 38-41*), none established a standardized contusion model for F344 rats. F344 rat differs from other strains in several aspects.

The first and most obvious difference is that F344 rats have smaller body size compared to Sprague-Dawley and Long-Evans rats. According to growth charts from commercial breeders (Taconic/ Charles River), both male and female F344 rats are 50 g smaller at 6 weeks and 100 g smaller at 10 weeks than these two strains. Second, F344 rats are more sensitive to mechanical stimuli and show a higher incidence of autotomy (self-amputation of toes) in neuropathic pain models, compared to Lewis and Sprague-Dawley rats (*42*). Third, F344 rats differ significantly in motor cortex size, thresholds to elicit a movement, and performance of skilled reaching task comparing to Long-Evans rats (*43*).

2.2 Methods

2.2.1 Rat source

F344 rat is an inbred albino strain, originated by M. R. Curtis at Columbia University in 1920 (*20*). F344 rats can be purchased from commercial breeders. In our project, we purchased F344 rats from several companies including Charles River, Taconic and Simonsen. Also our lab developed a F344 rat strain

expressing the green fluorescent protein (GFP) by backcrossing transgenic male Sprague–Dawley rats [SD-Tg(CAG-EGFP)Cz-004Osb] carrying the eGFP transgene from Japan SLC., Inc. (Hamamatsu, Japan) with wild-type female F344 rats purchased from Taconic for 23 generations (October 2015). The offspring included GFP and non-GFP F344 rats. We called the rats expressing GFP " GFP F344" rats and the siblings without GFP expression "non-GFP F344 " rats.

2.2.2 Spinal cord contusion

I anesthetized pathogen-free 100-day F344 rats with isoflurane (5% initially and 2% maintenance). I shaved the rats, cleaned the skin on the back with betadine and alcohol wipes for three times, and made a midline incision of the skin using surgical scalpel with No. 15 blade, bluntly dissected and separated muscles attached on T7 to T12 vertebras by long surgical scissors to expose rat's spinal column. To expose the T13 spinal cord, I did a laminectomy, removing half of T9 and all of T10 rat vertebras using curved microrongeurs. I placed the rats on a sponge covered with sterile wrap and stabilized spinal cords by clamping on T8 and T11 spinous processes. After ensuring the rats' spinal cords were straight and horizontal, I dropped a rod from a height of 12.5- or 25.0-mm onto the T13 spinal cord. After injury, I placed subcutaneous fat from rats on the dural surface to prevent adhesion of dura to surrounding tissues. Finally, I closed the muscle by sterile 3-0 silk sutures and skin with stainless steel clips.

I used MASCIS Impactors to create SCI respectively with 5-g and 10-g rods. The device monitored rod and vertebral column movement with ± 0.001 mm and ± 0.01 msec precisions. By monitoring the rod trajectory and vertebral movement, the MASCIS Impactor measured four variables: impact velocity (ImpV), compression distance (Cd), compression time (Ct), and compression rate (Cr= Cd/Ct). Impact velocity was estimated by a regression line of rod trajectory during 2 sec before it contacted to the spinal cord. Compression distance, which was calculated by the "maximum depth of rod" subtracted the "movement of vertebral column" represented the maximum distance below the baseline. Compression time was the time in msec required for that the rod reach to the maximum distance after contacting to the spinal cord.

2.2.3 Care of spinal-injured rats

After injury, the rats were housed in separate boxes with sterile paper bedding (Alfa Dry). The rats received 5-10 ml sterile saline subcutaneously for 3 to 7 days if skin pinch tests indicated dehydration. All the rats had daily bladder expression and 7 days of prophylactic antibiotics (cefazolin 50 mg/kg) after injury to prevent wound and urinary tract infections. If the rats showed signs of urinary tract infections (urine becomes cloudy or hemorrhagic), Sean O'Leary (the animal care supervisor at the Keck Center) quarantined the infected rats and treated rats with a fourth-generation fluoroquinone enrofloxacin (Baytril 2.5 mg/kg) daily for

10 days. If the rats did not respond to enrofloxacin within 3 days, they were euthanized to avoid spreading fluoroquinone-resistant bacteria in the colony.

Sean O'Leary also examined rats daily for autotomy or autophagia. At the first sign of skin irritation in dermatomes below the injury site, we started acetaminophen (oral 65 mg/kg/day "Baby's Tylenol) daily until the end of study. If autophagia progresses, we euthanized the rat. In the F344 contusion model study, only one male showed mild autophagia and none showed autotomy (self-amputation of toes).

2.2.4 Tissue sample preparation

To determine cell volume fraction and lesion volume, Bor Tom (a senior technician at the Keck Center) and I collected fresh spinal cords without perfusion after euthanasia. First, we anesthetized F344 rats with 5% isoflurane for 10 minutes, decapitated, and collected blood samples. Second, we rapidly removed and cooled the spinal cord with powdered dry ice, and cut the cord into 5-mm pieces: one centered on the impact site (Imp), two 5-mm pieces from proximal end (P1 and P2) and two pieces from distal end (D1 and D2). Third, we weighed the samples before to obtain wet weight (W), sonicated and dried the tissue to obtain dry weights (D), and calculated water content from $(W - D)/W$. The samples were sonicated with an ultrasonic vibrator (Fisher) and diluted in deionized water. Then, we measured concentrations of sodium (Na) and

potassium (K) from the tissue suspensions using atomic absorption spectroscopy (AAnalyst 200, PerkinElemer).

2.2.5 Measurement of cell volume fraction and lesion volumes

To assess primary tissue damage, Bor Tom and I estimated cell volume fraction from total tissue sodium ion (Na) and potassium concentrations, using the Na-K method described by Young, et al. (*15, 44*). Briefly, intracellular volumes (Vi) and tissue volume (Vt) of living cell are linearly related to the difference of tissue Na and K concentrations by:

$$[Na]t - [K]t = [Na]e - [K]e + 2G \cdot Vi/Vt$$

$[Na]e - [K]e$ is the difference of extracellular Na and K concentrations, G means the average transmembrane ionic gradient and Vi/Vt represents the ratio of cell volume versus tissue volume.

G is the slope, a constant number that is approximately -124 mM for spinal cord. Tissue Na and K concentration can be readily measured by atomic absorption spectroscopy. Extracellular Na and K concentrations can be assumed to be similar to plasma Na and K concentrations and also measured by atomic absorption spectroscopy. Using these assumptions, we can calculate cell volume fraction (Vi/Vt) from normal or injured spinal cord.

The change in Vi/Vt ($\Delta Vi/Vt$) reflects the percentage of cells that lost the ionic gradients after SCI. To calculate the lesion volume (LV) in microliters, we used the equation:

$$\frac{\Delta Vi}{Vt} \cdot W = LV$$

To estimate $\Delta Vi/Vt$, we subtracted Vi/Vt of each cord sample from the normal cell volume fraction. W is the tissue wet weight in milligrams. The lesion volume is the sum of lesion volumes from the five pieces (P2, P1, Imp, D1, D2).

2.2.6 Euthanasia, perfusion and fixation

After SCI, Sean O'Leary and I kept F344 rats for 8 weeks to observe chronic changes. At the end of study, we anesthetized the rats with Pentobarbital (Sleepaway) 100mg/kg by intraperitoneal injection. Then we exposed rat hearts by opening the thorax cutting and injected 1% lidocaine into left ventricle. Then we perfused the rats by saline to wash out blood from the vasculature and then by 400 ml of 4% paraformaldehyde over 15 minutes. We used a peristaltic pump to regulate the perfusion rate. After removing the spinal cords from rats and post-fixation in 4% paraformaldehyde overnight, we transferred the tissue samples into PBS and send out the tissues to Neuroscience Associates (Knoxville, TN) for sectioning and staining. Neuroscience Associates made coronal 30 μm sections of 1.5-cm of the rat spinal cords centered on the impact site. They stained every 12th section with SIM-99 for showing white matter and NeuN antibody for neurons.

2.2.7 Locomotor assessment

We used the BBB score (*17*) to assess locomotor recovery in the rats weekly. Two experienced people scored the rats over a 4-minute period to come up with a 0-21 point BBB score for each side. Each observer scored the rat individually and then discussed and concluded a consensus score. TABLE 1 summarizes the criteria for the each BBB category.

2.2.8 Image analysis

We scanned stained sections with a slide scanner (Super Coolscan 8000, Nikon). Then, we measured total area of spared spinal cord tissue and spared white matter by Image J software. Spared cord tissue and white matter were measured every 12th section.

The NeuN stained sections were photographed with an epifluorescent microscope (Axiovert 200M, Zeiss, Germany). Neurons were counted every 36th sections from the photographic images by Image J software.

2.2.9 Statistics

We used repeated measures ANOVA did post-hoc testing (Scheffe's test) to assess differences of the spinal cord size including the cord length, cord weight and cell volume fraction between genders or strains. Second, we used linear regression to access the correlation between cord weight and length. Third, we used Chi-square test to evaluate the difference of probability of dural

breakage under different drop heights and rod weights. Fourth, to compare the impact parameters and lesion volumes with different rod weights and different drop heights, we used ANOVA and did post-hoc testing (Scheffe's test). Fifth, we used liner regression to assess the correlation between the lesion volume and kinetic energy and average impact force. Sixth, to compare the spared spinal cord, white matter and neurons between 12.5- and 25.0-mm groups, we used repeated measures ANOVA. Then we used t-test to compare the total neural counts between 12.5- and 25.0-mm groups. Finally, we use repeated measures ANOVA to assess BBB scores and weight changes over time. We used StatView to run ANOVA, repeated measures ANOVA, liner regression and used excel for Chi-square test and t-test. Results were expressed as mean ± standard errors of means (SEM).

2.3 Results

2.3.1 Animal parameters

Previous data from MASCIS showed that the size (weight) of the spinal cord correlate linearly with age of rats rather than body weight. Therefore, in contusion models of Long-Evans hooded and Sprague Dawley rats, age criteria (i.e. 77 days) was used rather than body weight. In F344 contusion model, we first wanted to determine whether the age criteria should be used for F344 rats and which days of the F344 rats we should choose. Thus, we documented growth curves of the male and female F344 rats and chose an age for contusion model. Second, we measured spinal cord size (weight and length) and cell volume fraction in male and female F344 rats. Third, we compared the spinal cord size between F344 and Sprague-Dawley rats.

Choice of age for the F344 contusion model

Male and female F344 rats grow at significantly different rates (Figure 1). Although both males and females start at similar body weights at 4 weeks, males grow two times faster than females. For first 80 days, males grew about 5 g per day while females only gained 2.5 g per day. Between 80 to 180 days, female grew 0.5 g per day and reached a plateau of 230 g at day 120. Male rats kept growing 1.5 g per day and reached to 460 g at day 180. Females grew significantly slower than males especially after 80 days.

Male F344 rats are younger than female rats at the same body weight. If we select animals by body weight, females could be from 80 days to 180 days or even older while male rats would be only 80-90 days old. In 2002, Young, et al. (*11*) compared impact parameters in rats of different ages. Based on these results, they chose 77 days as the standard age for contusion of Long-Evans rats. At 77 days old, Long-Evans males are usually 350 g while females are about 250 g. F344 rats grow slower than Long-Evans rats. At 77 days, F344 males are 250 g and females are only 170 g. The 77-day old females are too small to be used for contusion. Thus, we chose 100 days as the age criterion for F344 model instead of 77 days. At 100 days, F344 males are 350 g while females are 200 g.

Cord size and cell volume fraction

Spinal cords of male and female F344 rats were similar at 100 days of age. At 100 days, the lengths of spinal cord were 25.95 ± 6.4 mm, 5.83 ± 0.23 mm, 8.11 ± 0.28 mm, and 11.16 ± 0.27 mm respectively in T1-T8, T9/T10, T11/T12, and T13/L1 vertebral level (n=8) (Figure 2A). The spinal cords of F344 rats were 114.92 ± 3.99 mg, 25.34 ± 1.1 mg, 41.49 ± 2.16 mg, and 74.38 ± 2.54 mg respectively in T1-T8, T9/T10, T11/T12, T13/L1 vertebral level (n=8) (Figure 2C). Despite the large discrepancy in body weights of male and female F344 rats, repeated measure ANOVA showed no significant difference in age-matched cord size including weights and lengths between male and female F344 rats

(Figure 2B,D) (weight: F=5.82, p=0.524; lengths: F=3.504, p=0.1104; n=4 in both male and female groups).

The cell volume fractions of the spinal cords were also similar between genders in F344 rats. Cell volume fraction (CVF) is the ratio of cell to tissue volumes. At 100 days old, CVF of F344 rats were 76.83 ± 0.91%, 76.67 ± 0.56%, 74.17 ± 0.87%, 74.33 ± 0.42%, and 73.17 ± 0.6% in the five 5-mm long spinal cord segments (P2, P1, Imp, D1, D2) removed from the T8-T11 vertebra, centered on the T9-T10 vertebral interface (Figure 2E). Repeated measure ANOVA indicated the presence of significant differences among different spinal segments (F=5.853, p=0.0042, n=6). Post-hoc (Scheffe's) test showed a significant difference between P2 versus D2 (p=0.0283) and P1 versus D2 (p=0.039). However, CVFs between genders did not differ significantly (Figure 2F)(F=1.658, p=0.2674, n=3 in both male and female groups).

Comparing cord size between 100-day old F344 and 77-day old Sprague-Dawley

At 77 days, the weights of Sprague-Dawley rat spinal cords were 149.4 ± 7.2 mg, 34.38 ± 3.11 mg, 45.27 ± 3.08 mg, 73.95 ± 4.38 mg respectively in T1-T8, T9/T10, T11/T12, T13/L1 vertebral level (Figure 3A). The lengths of spinal cord were 31 ± 0.91 mm, 7.7 ± 0.41 mm, 9.7 ± 0.26 mm, 11.1 ± 0.33 mm in T1-T8, T9/T10, T11/T12, T13/L1 vertebral level (Figure 3B). Repeated measure ANOVA indicated that 77-day old Sprague-Dawley rats had significantly bigger spinal cords than 100-day old F344 rats (cord weight: F=13.52, p=0.0036; length:

F=32.526, p=0.0001; n=5 in Sprague-Dawley; n=8 in F344). The strain difference was most prominent in T1-T8 and T9/T10 vertebral level.

We correlated cord weight and length and found similar point distribution between Sprague-Dawley and F344 rats (Figure 4). The distribution of T1-T8 group differed from rest of spinal cords including T9/T10, T11/T12, and T13/L1. Thus we drew two liner regression lines. The red line included the data from Sprague-Dawley and F344 rats and represented the linear regression of cord weights and lengths in T1-T8 group. The red regression line showed correlation coefficient of 0.95 with y-intercept of -53.12 ± 19.11 and slope of 6.5 ± 0.68. The blue line included the data from Sprague-Dawley and F344 rats and represented the linear regression between cord weight and length in T9/T10, T11/T12, T13/L1 vertebral level. The blue regression line had correlation coefficient of 0.92 with y-intercept of -28.62 ± 5.50 and slope of 8.78 ± 0.61.

ANOVA indicated the significant correlation between cord weight and length in both red and blue liner regression lines ($p<0.0001$). Also the regression line fitted tightly for both F344 and Sprague-Dawley rats. In T1-T8 vertebral segments, cord weight increased 6.5 mg along with each mm of cord. In T9-L1 vertebral segments, each additional mm cord would add 8.78 mg.

2.3.2 Anatomical and surgical parameters

Several other parameters may affect outcome. First, rat source and selection may be important. We compared body weights of F344 rats from

different sources. Second, the anatomy of the spinal cords may differ among strains. So, we checked the roots of the spinal cord to ensure that the T9-10 laminectomy exposed the same spinal cord contusion sites in F344 rats. Third, body size may affect the system used to clamp the spinal column. We found that smaller body size, less than 160g, did not allow consistent clamping of the spinal column and this affected contusion injury. Fourth, we observed that F344 rats had more dural breakage from contusions than Sprague-Dawley rats. Closer examination of the spinal cords revealed that removal of the ligamentum flavum increased dural breakage. Each of these findings will be described in detail and discussed below.

Rat source and selection

F344 rat is a popular rat strain used for scientific study and can be purchased from several commercial companies. According to the growth chart from our own local colony and outside breeders, F344 rats from our local colony were bigger than those from outside breeders (Figure 5), probably because we do not restrict the food intake of the rats. At 100 days, local female F344 rats were about 200 g and males were about 350 g. At the same age, F344 rats from commercial source were about 170 g for females and 300 g for males. For 24-hour lesion volumes and impact parameters, we chose to purchase rats from outside source and used rats that weighed more than 160 g. For the long-term observation of BBB scores and weight changings, we used local F344 rats.

Contusion site

In the standard MASCIS Impactor model for Long-Evans and Sprague-Dawley rats, we remove T10 and half of the T9 lamina to expose the T13 spinal cord. The impact site is at the junction of the T9 and T10 vertebral segments. The T13 spinal root enters the spinal cord at that point, indicating that the T13 spinal cord is contused. Contusion injury of a different spinal segment would change injury severity and functional recovery. We traced the spinal roots in F344 rats to determine the spinal segment at the T9/T10 vertebral junction in 100-day old F344 rats. The anatomy of F344 rats did not differ from other strains, i.e. the T13 spinal cord was located at the T9/10 vertebra (Figure 6).

Clamp system (T7 vs. T8)

After exposing the T13 spinal cord, we placed the rats on a sponge covered with sterile wrap and clamped the T8 and T11 spinous processes to keep spinal cord stable, straight, and horizontal during the contusion. The F344 T8 spinous process sometimes was broken during laminectomy on smaller rats that weighed less than 160 g. When T8 spinous process was broken, we clamped the T7 process instead.

Dural breakage

We contused the spinal cords of F344 rats with the MASCIS Impactor using 5-g or 10-g rods. We observed that some F344 rats had dural breakage right after impact. The 5-g Impactor tore the dura in 27.27% of rats after 12.5-mm weight drop and 35.71% after 25.0-mm weight drop. The Impactor with 10-g rod tore the dura in 36.84% of rats after 12.5-mm weight drop and 43.48% after 25.0-mm weight drop (Table 2). Chi-square test showed greater drop height and rod weight significantly increased the percentage of dural breakage (both $p<0.0001$).

To reduce dural breakage, we have assessed several methods to protect dura during impact, including placement of membrane on the dural surface. Finally, we found that keeping the ligamentum flavum intact reduces dural breakage from contusions. Ligamentum flavum is a yellow ligament situated between lamina and spinal cord. During laminectomy, the ligamentum flavum can be easily and inadvertently removed. When the ligamentum flavum was left intact, we found no dural breakage shown after contusion injuries in F344 rats.

2.3.3 Impact parameters

The MASCIS Impactor connected to computer for recording the movement of falling rod. According to impact trajectory, we measured the impact velocity (ImpV), compression distance (Cd), compression time (Ct), compression rate (Cd/Ct) and kinetic energy delivered to the spinal cord.

Impact velocity

In F344 model, impact velocities of 12.5- and 25.0-mm weight drops were 0.485 ± 0.003, 0.69 ± 0.001 m/s with 5-g rod and 0.49 ± 0.002, 0.693 ± 0.002 m/s with 10-g rod (Figure 7A). ANOVA showed significant difference among different drop heights ($F=3155.49$, $p<0.0001$) but not with different rod weights ($F=2.05$ $p=0.1604$, 5-g rod: n=8 in 12.5-mm group; n=9 in 25.0-mm group, 10-g rod: n=12 in 12.5-mm group; n=13 in 25.0-mm group).

Compression distance

Compression distance (Cd or maximum depth of cord compression during the contusion) were recorded during the weight-drop contusion and corrected by the movement of the spinal column. The 12.5- and 25.0-mm groups respectively had compression distance of 1.52 ± 0.47 mm, 1.96 ± 0.05 mm with 5-g rod and 1.68 ± 0.05 mm, 2.11± 0.06 mm with 10-g rod (Figure 7B). ANOVA indicated compression distance was significantly increased along with higher drop height ($F=59.612$, $p<0.0001$) and bigger mass of falling weight ($F=7.506$, $p=0.0093$, 5-g rod: n=8 in 12.5-mm group; n=9 in 25.0-mm group, 10-g rod: n=12 in 12.5-mm group; n=13 in 25.0-mm group).

Compression time

Compression time is the time between first contact of the rod with the spinal cord and the deepest compression distance of the cord. The 12.5- and

25.0-mm contusions had compression times of 3.29 ± 0.11 sec and 2.99 ± 0.1 sec respectively with the 5-g rod and 3.91± 0.16 sec and 3.49 ± 0.14 sec with the 10-g rod (Figure 7C). ANOVA showed significant difference among different drop heights (F=6.184, p=0.0174) and rod weights (F=15.508, p=0.0003, 5-g rod: n=8 in 12.5-mm group; n=9 in 25.0-mm group, 10-g rod: n=12 in 12.5-mm group; n=13 in 25.0-mm group).

Compression rate

Compression rate is the ratio of compression distance and compression time. In the F344 model, 12.5- and 25.0-mm contusions resulted in compression rates of 0.46 ± 0.006 and 0.657± 0.007 m/s respectively with the 5-g rod and 0.43 ± 0.008 and 0.61 ± 0.015 m/s respectively with the 10-g rod (Figure 7D). ANOVA indicated significant difference between different drop heights (F=267.333, p<0.0001) and drop weights (F=12.312, p=0.0012, 5-g rod: n=8 in 12.5-mm group; n=9 in 25-mm group, 10-g rod: n=12 in 12.5-mm group; n=13 in 25-mm group).

Kinetic energy / Average impact force

The kinetic energy of the contusion can be calculated from the formula for kinetic energy of a free falling object, i.e. $^1/_2\, MV^2$. For the 5-g rod, mean kinetic energy were 0.586 ± 0.014 and 1.191 ± 0.005 mJ (millijoule) respectively from

12.5- and 25.0-mm contusions. For the 10-g rod, mean kinetic energy values were 1.202 ± 0.011 and 2.411 ± 0.094 mJ respectively from 12.5 and 25.0-mm contusions (Figure 7E).

Average impact force can be calculated from the work-energy principle, i.e. “average impact force” times “traveled distance” equals to “kinetic energy”. The compression distance can be considered traveled distance. The 12.5-mm and 25.0-mm weight drops had average impact force of 0.39 ± 0.02 and 0.61 ± 0.02 N (newton) with the 5-g rod and 0.72 ± 0.03 and 1.16 ± 0.04 N with 10-g rod (Figure 7F).

ANOVA showed significant differences between the drop heights and rod weights in kinetic energy (drop heights: $F=2309.58$, $p<0.0001$;rod weight: $F=2365.682$, $p<0.0001$) and average impact force (drop heights: $F=108.724$, $p<0.0001$;rod weight: $F=196.312$, $p<0.0001$,5-g rod: n=8 in 12.5-mm group; n=9 in 25.0-mm group, 10-g rod: n=12 in 12.5-mm group; n=13 in 25.0-mm group).

2.3.4 Primary tissue damage

We estimated tissue damage at 24 hours after SCI from tissue sodium and potassium concentration. Also we assessed the effect of different clamp positions and dural breakage on lesion volumes.

24-hour Lesion volume

To measure tissue damage, we used a method developed by Constantini, et al (*15*). This method is based on the distribution of sodium (Na) and potassium (K) ions between extra- and intra-cellular compartments after injury. Because Na is primarily an extracellular ion and K is primarily an intracellular ion, injury and loss of cells result in increasing of tissue Na concentration and decreasing of tissue K concentration. The difference of total tissue Na and K is linearly related to the volume of living cells in the spinal cord. Using this method, we measured the cell volume fraction (CVF) of the spinal cord at and around the contusion site. Differences of CVF between injured tissues and normal tissues give the percentage of cell loss, allowing us to calculate the lesion volume (as described in the Methods pp.13-14). Lesion volume provides a quantitative measure of tissue damage and the effects of contusion and other parameters on tissue damage. We chose to measure 24-hour lesion volume because the cell volume fraction at injury site is not yet influenced by infiltration of inflammatory cells. The 24-hour lesion volume represents the sum of primary and secondary tissue damage during the first 24 hours.

In the F344 rat contusions, mean values of lesion volumes were 20.56 ± 1.33 μl and 24.85 ± 1.27 μl respectively with 5-g rod and 28.96 ± 1.71 and 36.41 ± 1.2 μl respectively with 10-g rod after 12.5- and 25.0-mm contusions (Figure 8). ANOVA showed higher weight-drop caused more tissue loss ($F=15.98$, $p=0.0003$) and also 10-g rod leaded to more severe injury than 5-g rod ($F=46.21$,

p<0.0001, 5-g rod: n=8 in 12.5-mm group; n=9 in 25.0-mm group, 10-g rod: n=12 in 12.5-mm group; n=13 in 25.0-mm group).

Effects of T7 and T8 clamp positions on Lesion volumes

In early experiments, we sometimes damaged the T8 dorsal vertebral process during surgery and clamped the T7 dorsal process instead. This gave us an opportunity to assess the effects of clamp position on injury severity. For 5-g contusions, lesion volumes with clamp at T7 were respectively 15.78 ± 1.25 and 16.07 ± 0.29 μl after 12.5- and 25.0-mm weight drops. For 5-g contusions, lesion volumes with clamp at T8 were respectively 20.56 ± 1.33 μl and 24.85 ± 1.27 μl after 12.5- and 25.0-mm weight drops (Figure 9A). Compared with clamping T8 vertebra, clamping on T7 resulted in significantly less injury at 24 hours after contusion (12.5-mm: p=0.0331, 25.0-mm: p=0.012, T7: n=5 in 12.5-mm group; n=2 in 25.0-mm group, T8: n=8 in 12.5-mm group; n=9 in 25.0-mm group). Also lesion volumes in animals clamped at T7 showed no statistical difference between 12.5- and 25.0-mm groups (p=0.8963), suggesting the importance of clamp position in obtaining graded injury of the spinal cord.

Effect of dural breakage on lesion

For the F344 rats injured with the 5-g rod Impactor, mean lesion volumes with broken dura were 24.18 ± 2.82 (n=3) and 27.7 ± 1.99 μl (n=7) respectively

after 12.5- and 25.0-mm contusions. For the rats injured with the 10-g rod Impactor, mean lesion volumes of contused spinal cords with broken dura were 32.31 ± 3.33 μl (n=5) and 35.27 ± 1.82 μl (n=10) respectively after 12.5- and 25.0-mm weight drop. The lesion volumes in contused spinal cords with dural tears were slightly higher than those without dural tears except in the 25.0-mm group with 10-g rod. However t-tests indicated no significant difference in lesion volumes between dural breakage and non-dural breakage groups (5-g/12.5-mm: p=0.217, 5-g/25-mm: p=0.2274; 10-g/12.5-mm: p=0.334, 10-g/25.0-mm: p=0.593). T-test also showed that lesion volumes of spinal cords with dural tear had no statistical difference between 12.5- and 25.0-mm groups (5-g: p=0.335, 10-g: p=0.412). In the non-dural breakage group, lesion volumes of spinal cords were significant different between 12.5- and 25.0-mm groups (5-g: p=0.0337, 10-g: p=0.015).

Correlations of lesion volume vs. impact force vs. kinetic energy

We used linear regression to assess the relationships between tissue damage, impact force, and kinetic energy. Regression plot showed lesion volumes correlated linearly with kinetic energy with a correlation coefficient of 0.77 ($p<0.001$). The y-intercept was -0.601 ± 0.277 and the slope was 0.071 ± 0.009 (Figure 10A). Lesion volumes also correlated with average impact force with a correlation coefficient of 0.735 ($p<0.001$). The liner regression line showed the y-intercept of -0.089 ± 0.129 and the slope of 0.03 ± 0.004 (Figure 10B).

2.3.5 Chronic change

To access chronic morphological changes in the spinal cords, we fixed the animals by intracardiac perfusion with 4% paraformaldehyde (as described on pp.14) and collected 12 mm lengths of spinal cord centered from impact site at 8 weeks after injury. Serial coronal sections were cut and stained with antibodies for myelin basic protein (SMI-99) to show white matter area and NeuN to show neurons.

Total spinal cord and white matter sparing

The contusions caused significant tissue loss at the injury site. SMI-99 stained white matter of a 12-mm spinal cord showed total coronal spinal cord damage as well as white matter loss at injury site (Figure11). In the rostral injury site, the white matter loss was mainly in dorsal volume and the tissue loss gradually extended to gray matter and lateral column. In the injury epicenter, little white matter was present in the ventral area. Caudal to the injury epicenter, white matter was absent in both dorsal and lateral regions.

Compared with 12.5-mm group, 25.0-mm group showed more tissue and white matter loss on the coronal sections (Figure 12). Repeated measures AVOVA indicated significant differences between 12.5-mm and 25.0-mm groups in spared tissue ($F=15.938$, $p=0.0026$, $n=5$ in 12.5-mm group; $n=7$ in 25.0-mm group)(Figure 12A) and spared white matter ($F=14.057$, $p=0.0038$, $n=5$ in 12.5 mm group; $n=7$ in 25 mm group) (Figure 12B).

Neuron loss

To assess neuronal loss, we counted NeuN-stained cells in selected coronal sections (Figure 13). More neurons were present in rostral and caudal edges of the 12.5-mm contusion site than in the 25.0-mm contusion site. Both 12.5-mm and 25.0-mm groups showed complete loss of neurons at the lesion epicenter. The length of complete neural loss was 1 mm in 12.5-mm contused cords and 3 mm in 25.0-mm contused cords (Figure 14). Repeated measures ANOVA indicated significant difference of spared neurons between the two groups ($F=22.088$, $p=0.0008$, $n=5$ in 12.5-mm group; $n=7$ in 25.0-mm group)

2.3.6 Recovery

BBB scores

To assess behavioral recovery, we evaluated locomotor performance every week, using Basso-Beattie-Bresnahan (BBB) locomotor scores (*17*). Rats in both the 12.5-mm and 25.0-mm groups showed no hindlimb (HL) movement at day 2 after injury (BBB= 0 in 12.5-mm and 25-mm groups). At 4 weeks, rats injured with the 12.5-mm weight drop had frequent-to-consistent weight-supported plantar steps but no FL-HL coordination (BBB= 11). By 8 weeks, the 12.5-mm group rats started to show occasional FL-HL coordination (BBB= 12). The rats in the 25.0-mm contusion had slight movement of two joints and extensive movement of third one (BBB= 5) by 4 weeks and had extensive movement of three joints (BBB= 7) at 8 weeks after injury. Repeated measures

ANOVA showed BBB scores were significantly different between 12.5- and 25.0-mm contusions ($F=70.562$, $p<0.0001$, n=14 in 12.5-mm group; n=15 in 25.0-mm group)(Figure 15A).

Correlation between hindlimb function and spared white matter

Regression analysis showed that hindlimb function correlated with spared white matter and the correlation coefficient was 0.603 ($p=0.038$). The y-intercept was 51.728 ± 18.456 and the slope was 4.8 ± 2.011(Figure 15B).

Body weight and weight changes after injury

SCI causes significant body weight loss (*15*). Then body weight improves gradually over time, partly due to growth but also due to muscle formation. Figure 16A shows that the average body weights of 100 days F344 rats were 176.53 ± 4.09 g and 305.5 ± 4.91 g before injury respectively in females and males. After injury, both male and female rats lost weight and reached a nadir by 1 week. From 2 weeks, rats began gaining weight and kept increasing through 8 weeks. Repeated measures ANOVA showed significant difference of body weight between male and female F344 rats ($F=402.812$, $p<0.0001$, n=14 in male group; n=15 in female group).

After injury, female rats lost 16.13 ± 0.83 g at day 2 and 22 ± 3.20 g at 1 week. At 2 weeks after injury, female rats started to gain weight and kept increasing up to 173.13 ± 2.3 g at 8 weeks. Repeated measures ANOVA

indicated the body weight changes did not differ between 12.5- and 25.0-mm weight drop contusions ($F=0.006$, $p=0.9389$, $n=8$ in 12.5-mm group; $n=7$ in 25.0-mm group) (Figure 16B).

Male rats lost 28.93 ± 2.4 g at day 2 and 63.93 ± 4.27 g at 1 week after injury. By 2 weeks, weights started to increase until 8 weeks. Although group 12.5-mm and 25.0-mm showed similar decreasing at day 2 and 1 week after injury, in group 12.5-mm, body weights increased faster than 25.0-mm from 2 weeks to 8 weeks. At 8 weeks, mean body weight in 12.5-mm was 28.63 g heavier than 25.0-mm group. Repeated measures ANOVA revealed significance between 12.5-mm and 25.0-mm groups ($F=5.459$, $p=0.0376$, $n=6$ in 12.5-mm group; $n=8$ in 25.0-mm group) (Figure 16C).

Correlation between hindlimb function and body weight changes

Regression analysis showed the behavioral recovery correlated linearly with body weight changes (Female: $p<0.0001$, Male: $p<0.0001$) (Figure 17). Among female F344 rats, the correlation coefficient was 0.458. The y-intercept was 9.433 ± 0.397 and the slope of regression line was 0.139 ± 0.025. In male rats, the correlation coefficient was 0.78. The regression line showed y-intercept of 9.595 ± 0.262 and slope of 0.094 ± 0.007. The body weights of female F344 rats increased 1.51 g for each point improvement of BBB score and body weights of male F344 rats increased 6.46 g for each point improvement of BBB score.

2.4 Discussion

2.4.1 Animal parameters

Age criteria

We chose to standardize the model on 100-day old F344 rats for the following reasons. First, body weights differ significantly between male and female rats. The size of spinal cords in rats correlates with age and is similar in age-matched male and female F344 rats. Second, female F344 rats are smaller than other strains. If we use F344 rats that are 77-day old, the female rats would be too small, less than 120 g body weight.

Age affects several important factors that may alter both SCI and recovery. For example, age affects glutamate and related amino acids levels in the central nervous system (*45*), reduces spinal cord plasticity (*46*), amplifies and extends microglial activation (*47*). After SCI, older rats have larger lesion volume and more microglia infiltration in injury epicenter (*48*), bigger degree of demyelination, delayed recovery, bigger locomotor deficits and different inflammatory components (*49*). By standardizing the model to rats of the same age, we hope the model would be more consistent.

At 100 days, female F344 rats weigh about 200 g while males are 350 g and which are big enough for contusion model. Our results showed if rats are smaller than 160 g, T8 vertebra were easily broken during laminectomy. Following contusion injury failed because clamp system could not be used on T8

and T11 vertebra. The sizes and weights of spinal cord and cell volume fractions did not differ between 100-day old male and female F344 rats even though body weights differed by 150 g.

The weights of the whole spinal cords in 100-day old F344 rats were significantly lighter than spinal cords of 77-day Sprague-Dawley rats but the weights of the spinal cords per millimeter were similar, suggesting that the spinal cords of Sprague-Dawley rats were longer but not thicker than those of F344 rats. The cell volume fraction of 100-day old F344 rats were also similar to 77-day old Sprague-Dawley rats.

2.4.2 Surgical parameters

Clamp position

The vertebral clamping system of the MASCIS Impactor is critical for consistent injury. Different clamp positions can change injury severity. Clamping T8 and T11 spinous processes stabilizes the spinal column during impact and keeps the spinal cords straight and horizontal. When we clamped the spinal column at T7, 24-hour lesion volume was less and did not differ between the 12.5- and 25.0-mm contusions. The clamps must placed on T8 and T11 vertebral processes and the spinal cords should be horizontal. Animals with broken T8 vertebra should be excluded.

Dural breakage

In the central nervous system, the meninges are comprised of three membranes, including the pia, arachnoid and dura mater. Dura is the thickest outer layer of meninges that protects central nervous system. Once dura is broken, spinal cord might suffer bigger impact. Also, dura breakage may lead to lot of B cells and T cells invade into injury site and change inflammation after injury.

Most human injuries result from fracture and dislocation of spinal column. While penetrating wounds due to a bullet or knife cause dural openings, they are relatively rare. Dural breakage has not been previously reported in contusion injuries of other rat strains such as Long-Evens, Sprague-Dawley, or Wistar rats. However, we found a considerable number of dural breakage after impact and the percentage increased along with greater drop height and heavier rod weight (5 g vs. 10 g) used to contuse the spinal cord in F344 rats.

Our results suggest that dural tears led to greater tissue damage in the spinal cord at 24 hours after contusion, increased variability, and did not allow graded SCI. Thus, we suggest that dural integrity should be carefully observed after impact and rats with dural breakage be excluded from the study. We further found that keeping the ligamentum flavum intact helps avoid dural breakage.

2.4.3 F344 contusion model by MASICS Impactor

In contusion model, two critical factors influence impact parameters and injured severity: drop height and mass of falling weight. Drop height determines the impact velocity, which is crucial for contusion injury. The mass of the falling weight does not alter impact velocity according to Galileo's formula but does alter impact force and affect compression distance and compression time.

For F344 contusion model, our results suggest significant differences between 12.5- and 25.0-mm weight drop in all impact parameters. Also, we confirm that decreasing the mass of falling weight reduces compression distance (Cd) and time (Ct) but not impact velocity. Finally, variability of both 12.5- and 25.0-mm contusions was very small and it indicates consistent contusion injury in the F344 model.

Compression rate and kinetic energy

In MASCIS, compression rate correlated with locomotor recovery and spared white matter(*50*). However compression rate did not reflect 24-hour lesion volumes resulting from contusion with different rod weights in the F344 model. The higher impact velocity associated with higher drop height increased compression distance but reduced compression time, causing a notable difference in compression rate between 12.5- and 25.0-mm contusions. When we increased the mass of falling rod, compression distance and compression time both increased. Thus, the compression rate is highly correlated with lesion

volumes between 12.5 and 25.0 mm but failed to reflect the lesion volumes between different rod weights.

We calculated kinetic energy and average impact force and found the two parameters were linearly correlated with lesion volume. These two parameters were determined not only by impact velocity also included the mass of falling rod. Therefore kinetic energy and average impact force are better parameters than compression rate for predicting lesion volume, especially when different masses of falling weight were used for contusion.

2.4.4 Chronic change after SCI in F344 rats

Spared white matter/ Neurons

Injury initiates cellular responses in the spinal cord. Primary injury causes tissue damage, initiating responses that lead to cell death and hemorrhage,releasing free radicals, cytokines, and chemokines that cause secondary injuries involving vascular and cellular mechanisms. The vascular response includes edema, ischemia and inflammation. Cellular mechanisms include macrophage and neutrophil infiltration, gliosis, and stem cell proliferation. The secondary injuries lead to central hemorrhagic necrosis and vascular changes that contribute further white and gray matter loss. In this study, we measured white matter damage and neuronal loss at 8 weeks after injury.

Contusion injury causes severe damage of gray matter in F344 rats. At the contusion epicenter, no neurons survived the 12.5- and 25.0-mm contusions. Neurons were absent ± 0.5 mm from the epicenter of 12.5-mm weight drop and ±1.5 mm from the epicenter of 25.0-mm weight drop. Total neural counts showed that 12.5-mm weight drop had significantly more spared neurons than the rats injure with 25.0-mm weight drop.

Graded white matter damage was also apparent after 12.5- and 25.0-mm contusions in F344 rats. At contusion epicenter, both 12.5-mm and 25.0-mm weight drops showed very small spared white matter in the ventral region. The surviving rim of white matter was very thin at the epicenter after a 12.5-mm and virtually absent after 25.0-mm weight drops. At ± 3 mm from the contusion epicenter, spinal cords contused with a 12.5 mm showed more spared white matter than spinal cords contused with 25 mm.

Rostral to the injury site, the dorsal column usually has greater damage in the gracile fasciculus. The gracile fasciculus is a bundle of ascending fibers which carries proprioceptive information from the mid thoracic and lumbosacral segments. Contusion injury disconnects these axons from their cell bodies located in the dorsal root ganglia below the injury site. Below the injury, the white matter loss was present in both dorsal median and dorsolateral columns. The dorsomedial and dorsolateral regions contain descending axons, including corticospinal and rubrospinal tracts from the motor cortex and the red nuclei respectively. After SCI, the spinal tracts are separated from their cells of origin

and undergo Wallerian degeneration.

Recovery

The Basso-Beattie-Bresnahan BBB locomotor score is the most popular test of locomotor function in SCI models. The testing is based on analysis of movements of three hindlimb joints, sweeping, weight support, coordination between forelimb and hindlimb, paws, tail and trunk position. The BBB scale is designed for contusion injury model, based on timing of recovery of different post-injury behaviors. The later a behavior recovers, the higher score it receives. The BBB score correlates linearly with lesion volume and injury severity.

In F344 contusion model, BBB scores reflected injury severity and white matter sparing. BBB scores differed significantly between 12.5- and 25.0-mm weight drop contusions. White matter sparing and body weight changes correlated linearly with BBB scores.

2.4.5 *MASCIS vs. F344 rat model*

MASCIS standardized the weight drop spinal cord contusion model in Long-Evans hooded rats and demonstrated that the Impactor produced consistent contusion injuries. The model specified anesthesia, surgical, and animal care for the model. It provided accurate measurements of contusion parameters, lesion volumes, and locomotor recovery after contusion. In this study, we modified the contusion model for F344 rats. Based on contusion parameters, lesion volumes, hindlimb function and long-term white matter sparing

and neuronal loss, we demonstrated that the MASCIS Impactor produces graded and consistent spinal cord injuries in F344 rats. However, we had to modify the F344 contusion model in several ways.

First, we choose 100 ±1 days F344 rats instead of 77 ±1 days in the standard MASCIS contusion model. Even though we used 100-day old F344 rats, their body and spinal cord sizes are still smaller than 77-day old Sprague-Dawley rats. Also F344 rats had a higher risk of dural breakage after contusion.

Despite differences in body weight and spinal cord size, impact parameters were similar between rat strains. For example, impact velocity, compression distance, and compression rates in F344 rats were comparable with those in Long-Evans hooded and Sprague-Dawley rats. However, lesion volumes were larger in F344 rats than Sprague-Dawley and Long Evan's hooded rats (*15*). Also, locomotor recovery in the F344 rat was less than in Sprague-Dawley and Long-Evans hooded rats(*11*). After 12.5-mm weight drop, Long-Evans hooded rats recovered BBB of 14 points (*11*) while F344 rats had BBB of 12 points. With 25.0-mm contusion, Long-Evans hooded rats recovered to BBB scores of 9 points (*11*) while F344 rats reached to BBB of 6 points. MASCIS Impactor produced more severe contusion injury in F344 rats model.

CHAPTER 3 F344 CONTUSION MODEL FOR CELL TRANSPLANTATION

3.1 Introduction

3.1.1 Cell therapy

Cell therapy is a treatment in which living cells are injected into recipients. After transplantation, grafted cells could replace damage cells or tissues and repair deficit functions. Also cells might improve healing process by releasing beneficial growth factors, cytokines, and chemokines. Regardless of mechanisms the cells must survive in the host to repair tissue and deliver beneficial factors.

Autologous transplantation means self-transplantation, i.e. the donor and recipient are the same individual. The grafted cells won't be rejected by the host immune system and will survive without immunosuppression. Allogeneic transplantation means transplantation from one individual to another from the same species. Unless the donor and recipient are closely related and have matched human leukocyte antigens (HLA), the allogeneic transplants should trigger host immune response to reject the allograft. In allogeneic transplantation, grafted cells can survive if the donor and transplants are HLA-matched or the recipient immune system is suppressed with immunosuppressive drugs or cells.

Transplantation studies that use tissue or cells from non-immune matched allogeneic individuals of the same species or from other species (xenotransplantation) require either an immune-deficient host or

immunosuppression. Immunosuppression may change not only the immune system in the host but affect the behavior of both the host and grafted cells.

A majority of human transplants involve autologous or HLA-matched cells and tissues. Thus, there is a need for an animal model to mimic autologous or immune-matched transplants without immunosuppression. Thus we wanted to establish a rat model, which can eliminate interference from immunosuppressant drugs and allow us to evaluate the therapeutic effect of grafted cells without immunosuppression.

3.1.2 F344 model allows cell transplantation without immunosuppression

F344 rat is an inbred albino strain, developed by M. R. Curtis at Columbia University in 1920 (*20*). Inbred Fischer rats are isogenic, homozygous, and express uniform and stable phenotypes. Isogenicity allows grafted F344 cells transplanted into other F344 rats without immunosuppression (*24, 25, 31, 51*).

Our group developed a F344 rat strain expressing the green fluorescent protein (GFP) by repeatedly backcrossing of eGFP Sprague-Dawley males to wild-type F344 females for over 20 generations. The GFP F344 strain is more than 99% congenic to wild-type F344 rats and is dominated by F344 rats. In earlier study, Marano et al. (*53*) demonstrated that GFP F344 rats are immune-compatible with F344 rats by transplanting ovaries from young GFP F344 rats into wild-type F344 rats and showing that transplanted rats can give birth to GFP

rat pups (*31*). The eGFP cells are very bright and can be readily visualized and identified after transplantation.

3.1.3 Olfactory ensheathing glial (OEG) cells

After establishing and validating the F344 rat spinal contusion model, we planned to transplant GFP cells from GFP F344 rats to wild-type F344 hosts after SCI. Specifically, we were interested in studying the effects of olfactory ensheathing glia (OEG), a cell type reported to stimulate spinal cord regeneration and improve locomotor recovery (*54-80*) in rats after SCI. In almost all studies published to date, the transplanted OEG cells were from allogeneic individuals. In animals that are not treated with immunosuppressants such as cyclosporine, the cells usually do not survive longer than 2-4 weeks.

OEG cells are a type of macroglia that are born in the olfactory mucosa and migrate in the olfactory nerve to the olfactory bulb. The olfactory nerve is the only structure in the central nervous system (CNS) that continually regenerates throughout adult life. OEG cells play a key role in axonal growth and guidance of newly formed olfactory axons (*81*). OEG cells provide a growth permissive environment for growing axons by secreting several neurotrophins such as BDNF, GDNF and NGF (*82, 83*) and express cell adhesion molecules such as N-CAM (*84-86*) and ECM-molecules such as laminin (*87*) which are also growth-promoting substrates for axons. OEG cells have been tested to treat SCI in several animal models (*88*). Previously, our lab transplanted Sprague-Dawley

OEG cells into Sprague-Dawley hosts. However, the grafted cells do not survive without immunosuppression. Therefore we want to use the same type of cell to compare the cell survival in Sprague-Dawley and F344 rats.

3.2 Method

3.2.1 Spinal contusion model

I anesthetized pathogen-free 100-day old F344 rats with isoflurane (5% induction and 2% maintenance), cut the hair on the back with an electric shaver, and cleaned the skin on the back with betadine and alcohol wipes. After using the surgical blade to make a midline incision of the skin by surgical scalpel with No. 15 blade, I bluntly dissected and separated muscles attached on T7 to T12 vertebras by long surgical scissors to expose rat's spinal column. I then exposed the T13 spinal cords with a laminectomy, removing half of T9 and all of T10 spinal lamina using curved microrongeurs, and clamped the dorsal processes of T8 and T11 to stabilize and suspend spinal column. A 10-gram rod was dropped from 12.5-mm onto T13 spinal cord. After the contusion, subcutaneous fat was placed on the dural surface to retard adhesion of dura to surrounding tissues. The skin is closed with stainless steel clips.

3.2.2 Animal care

The spinal-injured F344 rats received 7 days of prophylactic antibiotics (cefazolin 50 mg/kg) and daily bladder expression after SCI. If urine became cloudy or hemorrhagic, the rats would be quarantined and started on a fluoroquinolone antibiotic (enrofloxacin 2.5 mg/kg/day) for 10 days. The rats were examined daily for autophagia. At the first sign of skin irritation in dermatomes below the injury site, the rat was started on daily acetaminophen (oral 65 mg/kg/day "Baby's Tylenol, Johnson & Johnson). If autophagia progresses to expose muscle or internal organs, the rat would be euthanized

3.2.3 Primary OEG culture

I cultured the OEG cells from GFP F344 rats. First, I anesthetized the rat pups by exposing them to 5% isoflurane and decapitation. I rapidly dissected out the olfactory bulbs, immediately placed them in 4°C Hank's buffered salt solution (HBSS), peeled meninges and olfactory nerve layer (ONL) off with fine forceps, and diced the tissue into small fragments. After centrifuging and re-suspending three times, I homogenized the small tissue fragments by repeated passage through the tip of a 1 ml pipette, washed the tissue through 70um nylon mesh, and then plated the cells on uncoated tissue culture dishes (Falcon) overnight to eliminate fibroblasts. Non-adherent cells were transferred to coated tissue culture flask, incubated for 5-7 days, and then used p75 immunopanning to purify the cells (*69, 89, 90*)

Briefly, I coated a petri dish coated with goat-anti-mouse immunoglobulin G (IgG,1:100, Jackson ImmunoResearch Laboratories) overnight at 4°C and then coated the dish with I192 hybridoma supernatant which contains anti-p75 antibodies (1:10, gift from Dr. Eugene M. Johnson) for 2 hours at 4°C, then washed the culture dish thrice with PBS solution. I added 500,000 dissociated OEG cells to the dish for 1 hour at 4°C, washed unattached cells out with PBS, scraped off the attached cells, and grew them in DMEM-F12 media (Invitrogen) with 10% fetal bovine serum (FBS, Invitrogen) for 2 weeks to obtain OEG cells for transplantation.

3.2.4 Cell transplantation

Before transplantation, I detached and suspended the OEG cells in serum free DMEM-F12 medium so to achieve a suspension of about 100,000 cells/*μ*liter, and then aspirated the cells into a Hamilton syringe. Shortly after the injury, we used a micromanipulator to insert the micropipette tip about 1 mm deep into the midline and injected 2 *μ*l of the cell suspension or media into spinal cord above and below the impact site.

3.2.5 Locomotor assessment

Sean O'Leary and I used the BBB score to assess locomotor recovery in the rats weekly (*17*). We scored the rats over a 4-minute period to come up with a 0-21 point BBB score for each side and for both sides. We used Consensus

scoring approach for BBB assessments. TABLE 1 summarizes the criteria for the each BBB category.

3.2.6 Euthanasia, perfusion and fixation

At 8 and 16 weeks after injury, Sean O'Leary and I anesthetized the rats with sodium pentobarbital (65 mg/kg, i.p.) and perfused transcardially with saline followed with 4% paraformaldehyde fixative solution. The spinal cords were dissected out of the spinal column, inspected with an epifluorescence dissecting microscope (Zeiss Stemi SV11), immersed overnight in 4% paraformaldehyde, and then transferred to a 30% sucrose buffer solution for 24 hours. Then spinal cord sections were cut with a cryostat machine (Hacker Instruments & Industries, Bright OPF5000) at 30μm thickness and mounted on slides.

3.2.7 *Immunochemistry*

Tissue sections or cultured cells on cover slips were washed with phosphate-buffered solution (PBS) and incubated in blocking solution containing 10% normal goat serum (Vector Laboratories) and 0.3% Triton X-100 (Fisher Scientifics) in PBS for an hour. The samples were incubated with primary antibodies for overnight at 4 degree. After washing by PBS three times, the samples were incubated with secondary antibodies at room temperature for 2 hours. Then I stained nuclei with Hoechst 33342 (1:1000 dilution, Sigma-Aldrich)

for 5 minutes and washed samples for five times by PBS. The samples were mounted by coverslips with mounting medium (AQUA-Mount, Thermo Scientific). The primary antibodies included polyclonal anti-p75NTR (1:200 dilution, MILLIPORE), monoclonal anti-S100 (1:100 dilution, Sigma), monoclonal anti-ED1 (1:800 dilution, Serotec) and polyclonal anti-GFAP (1:200 dilution, DAKO). The secondary antibodies included goat-anti-mouse Alexa Fluor 555, 647 (1:1000 dilution, Invitrogen) and goat-anti-rabbit Alexa Fluor 555, 647 (1:1000 dilution, Invitrogen). All the primary and secondary antibodies were diluted by blocking solution.

3.2.8 Microscopy.

I photographed fixed unstained whole-mount spinal cords with a Zeiss Stemi SV11 epifluorescent dissection microscope equipped with a PhotoMatrix CoolSnap-Pro digital camera. I used a Zeiss LSM510 confocal microscope for high-resolution images and deconvolved images (Huygens, Bitplane AG) to reduce light scatter.

3.2.9 Statistics

We used repeated measures ANOVA to assess BBB scores between control and OEG groups over time. To compare the gender effect on impact parameters and lesion volumes, we also used ANOVA. We used StatView to run

the ANOVA and repeated measures ANOVA. Results were expressed as mean ± standard errors of means (SEM)

3.3 Results

3.3.1 Primary OEG cell culture

We have developed an efficient procedure to grow high percentage of pure OEG cells from neonatal olfactory bulb (Figure 18). After culturing of cells from olfactory bulb, I then used the immunopanning to increase the purity of OEG cells (as described on pp.46-47). About 95% of primary cultured OEGs expressed the low-affinity NGF receptor p75 (Figure 18C), also most of OEGs expressed S100 (Figure 18D) which is general marker for OEG. Three different morphology have been observed in primary OEG cultures which are bipolar, multipolar and flat forms. The three different morphologies also have been observed by previous study in our lab and other studies (*55, 85, 91*).

3.3.2 OEG cells survival and migration in vivo

After establishing the contusion model in F344 rats, we cultured OEG (95% p75 and S100 positive) from neonatal olfactory bulb of GFP F344 rats. A total of 2 *μ*l of the cell suspension (OEG group: 100,000 cells per *μ*l) or media (Control group) were injected into the spinal cord above and below the impact

site shortly after a 12.5-mm weight (10 g) drop contusion injury. The interval of two injection sites was about 8 mm.

By 8 weeks, the OEGs graft with green fluorescent could be seen in fixed whole mounted spinal cord by using epifluorescence dissection microscope (Figure 19A). Most of cells stayed in the injection site but some of cells migrated toward to the injury epicenter. By 16 weeks, we found grafted GFP-OEGs still survived in the host and gathered toward to the injury epicenter (Figure 19B).

3.3.3 p75 expression

By 8 weeks after transplantation, we found majority of GFP-OEGs were p75 negative (Figure 20). Most of p75 positive cells were located in the injury epicenter. We assumed these cells are endogenous Schwann cells, which migrated from dorsal root into the injury site. We also found the endogenous p75 positive cells were limited in the injury site in control group (Figure 20 A, C). With OEGs transplantation, the endogenous p75 positive cells seems been appealed by grafted OEGs and migrated along implanted OEGs (Figure 20 B, D-F).

3.3.4 Recovery

To determine whether the OEG transplantation promoted functional recovery, we evaluated hindlimb function with BBB scores (*17*) every week after injury for 8 weeks. Figure 21 shows F344 rats in control and OEG groups had no hindlimb (HL) movement at day 2 after injury (BBB = 0 in control group; BBB = 0

in OEG group). At 3 weeks post-injury, rats in both groups had occasional weight-supported plantar steps but no FL-HL coordination (BBB = 11 in control group; BBB = 11 in OEG group). Before 6 weeks, the HL function in control and OEG groups were similar. By 6 weeks, the rats in control group showed frequent to consistent weight-supported plantar steps and occasional FL-HL coordination (BBB = 12) while the OEG group showed frequent to consistent weight supported plantar steps and frequent FL-HL coordination (BBB = 14). At 8 weeks OEG group showed BBB scores of 14 while the control group showed BBB of 12. Repeated measures ANOVA indicated no significant difference between control and OEG groups for overall BBB scores ($F=1.834$, $p=0.187$, $n=17$ in control; $n=11$ in OEG). However, t-test showed significant difference between control and OEG groups at 6 and 8 weeks (6wk: $p=0.0249$; 8wk: $p=0.0218$).

We then analyzed locomotor performance by splitting males and females to determine the gender effect. Figure 22 shows very distinct locomotor activities between female and male F344 rats. Control female F344 rats had similar pattern of locomotor activity after SCI with OEG group (Figure 22A). At 3 weeks post-injury, both groups had occasional weight-supported plantar steps and FL-HL coordination (BBB = 11 in control; BBB = 11 in OEG). By 8 weeks, female F344 rats in control group recovered to BBB scores of 13 while the OEG group recovered to BBB scores of 14. Repeated measures ANOVA indicated that in female F344 rats, no significant difference was showed between control and OEG groups ($F=0.16$, $p=0.696$, $n=9$ in control group; $n=6$ in OEG group).

The male F344 rats in control and OEG groups had similar BBB scores at first four weeks (Figure 22B). By 5 weeks, the control group reached to BBB scores of 11 and the OEG group had BBB scores of 14. The locomotor activity in OEG group gradually improved during 5 to 8 weeks. By 8 weeks, the male OEG group recovered to BBB scores of 15 while the control male rats still maintained at BBB scores of 11. Repeated measures ANOVA showed significant difference between control and OEG groups in male F344 rats ($F=14.048$, $p=0.0032$, $n=8$ in control group; $n=5$ in OEG group).

Figure 23A shows the locomotor behavior in different treatment groups (control and OEG) and different genders. Repeated measures ANOVA showed no difference between genders and treatments but interactive effect between gender and treatment was significant (Figure 23B).

3.3.5 Gender difference

The locomotor activity differed significantly between control male and female F344 rats after SCI. The untreated control female rats recovered to 13 points while control males reached to BBB of 11 points. To rule out possible explanations of this gender difference, we compared spinal cord anatomy, cord size, and cell volume fraction between male and female F344 rats. Even though male rats were >100g heavier than females, repeated measures ANOVA showed that the spinal cord size and CVF were similar between male and female rats (as described in Chapter 2 on pp.18-19). Repeated measures ANOVA also indicated

the contusion parameters including the impact velocity, compression distance, compression rate and lesion volumes showed no difference between male and female F344 rats (Males: n=6 in 12.5-mm, n=6 in 25.0-mm; Females: n=6 in 12.5-mm, n=7 in 25.0-mm) (Figure 23).

3.4 **Discussion**

3.4.1 F344 contusion model for cell transplantation

Many investigators (*24-29*) have shown that organ and cells transplants from F344 to F344 rats survive long times in without immunosuppression. In our studies, we confirmed that immune compatibility for cell transplants into the spinal cord do not change after SCI. All the transplanted OEG cells survive in the host at least 16 weeks.

3.4.2 p75 expression

When the OEG cells are cultured and isolated for transplantation, all of them express GFP and 95% cells expressed p75. Previous studies in our laboratory indicated OEG cells lose p75 expression when they ensheath axons in vitro and in vivo. At 8 weeks after transplantation, most of the GFP OEG cells are p75 negative, suggesting that many of the cells are myelinating axons.

Many p75 positive cells clustered at the injury epicenter and these p75 positive cells did not migrate far from the injury site. Many of non-GFP p75+ cells

may be host Schwann cells entering the spinal cord through the dorsal roots. These p75+ cells were likely endogenous Schwann cells which migrated from dorsal roots into the injured spinal cord. Previous studies showed the astrocytes produce N-cadherin ephrins and aggrecan, which inhibit Schwann cell migration (*92-94*). OEG cells promote migration of Schwann cells by secreting nerve growth factor (*95, 96*).

3.4.3 Functional Recovery

Many laboratories have transplanted OEG into brain (*97-99*), peripheral nerves (*100-106*), and spinal cord, finding that the cells improve recovery, regeneration (*54-80*) and remyelination (*107-114*). However, some studies found no regeneration or recovery (*74, 115-123*). In 2007, Franssen and his colleagues (*88*) reviewed studies of OEG transplantation in SCI models. This review selected 54 papers: 41 studies showed positive effects and 13 showed no or limited effects. In our study, we cultured and obtained 95% pure OEG cells from neonatal olfactory bulb. Then we transplanted OEG cells above and below the impact site right after contusion injury. The results showed significant functional improvement by 8 weeks after OEG transplantation but only in male rats. Control untreated female F344 rats recovered as well as OEG transplantation group.

3.4.4 Gender effect

SCI has significantly different effects on male and female humans. Jackson, et al. (*124*) gathered demographic profiles of traumatic spinal cord injured patients from 1972 to 2003 in the United States. They collected total 30532 cases and reported the male and female ratio stay stable at 4:1 over three decades. Also Sipski et al. (*125*) reported men tend to show more severe injury and less recovery than women. However, two clinical studies showed no gender difference on functional recovery after SCI (*126, 127*).

The gender issue has not been well addressed in animal SCI studies. Many investigators prefer using single gender for experiments. Only some studies have compared biochemical, anatomical and functional outcomes of male and female animals. A few papers reported significant differences (*128, 129*) while others did not (*130-133*). None of the other studies, however, have taken the same care to ensure that the injuries are the same or to use age-matched animals. When these factors are carefully controlled, gender differences are not present in outbred rat strains, such as Sprague-Dawley and Long-Evans hooded rats. In F344 contusion model, we found a significant gender effect on SCI. After a 12.5-mm weight drop, female F344 rats recovered to BBB of 14 while males only recovered to BBB of 11.

We proposed several hypotheses concerning the mechanism of the gender effect:

1. Different anatomy of spinal segments under T9/T10 vertebra.

2. Different size of spinal cords.
3. Different metabolism.
4. Sex hormones (estrogen/testosterone)
5. Different immune response

Anatomical differences between genders would explain differences in injury outcomes. To test the hypotheses, we compared anatomical positions of the impact site, cord size and cell volume fraction, impact parameters, and 24-hour lesion volumes between male and female rats. Anatomical locations of impact site, impact parameters, and 24-hour lesion volumes did not differ significantly between male and female F344 rats. We conclude that the 12.5- and 25.0-mm contusions caused similar primary and secondary injuries in male and female F344 rats.

Differences in metabolism may lead to differences in free radical production after SCI and affect secondary tissue injury. A previous study (*134*) had reported that peroxide production by hepatic mitochondria is 40% higher in male than female Wistar rats. Also, brain mitochondria in male rats produced over 80% more peroxides than in females. Therefore, we hypothesized male F344 rats generate more free radical than females after SCI.

Sex hormones such as estrogen, progesterone may affect the injury response and repair after CNS injury. In 2014, Elkabes and Nicot (*135*) summarized the effects of estrogen and progesterone on SCI. Estrogen

treatment had neuroprotective effects and reduced the number of apoptotic cells (*136-139*), increased white matter sparing (*138, 140-143*) and improved functional recovery after SCI (*136, 138, 139, 142, 143*) . A few studies mentioned beneficial effects of progesterone after SCI (*133, 144*). Most investigators used male rats for SCI and gave extra estrogen or progesterone to the animals by intravenous or intraperitoneal injection. Although these studies do not mimic estrogen or progesterone levels in females, hormonal therapies may influence outcomes between male and female rats.

The immune responses are different between sexes. In 2014, McCombe and Greer (*145*) reported that females showed greater percentage of lymphocytes, IgM levels, allograft rejection, in vitro response to mitogens, ability to combat infection, response to vaccination, CD4/CD8 ration and Th1 response. Autoimmune diseases also appear to affect females more than males (*146, 147*). The immune responses to injury appeared to be different between genders (*148*) and this might result in more or less inflammatory reaction after SCI.

CHPATER 4 THE EFFECT OF CYCLOSPORIN-A ON LOCOMOTOR RECOVERY AFTER SCI

4.1 Introduction

4.1.1 Cyclosporin-A as a immunosuppressant drug

History and medical use

In 1969, Hans Peter Frey and his wife (*149*) collected the soil samples contained the fungus, *Tolypocladium inflatum*, in Norway. In 1971, a scientist at Sandoz (now Novartis), Jean-Francois Borel, found a compound from *Tolypocladium inflatum,* which altered the behavior of immune cells grown in vitro. In 1972, Hartmann F. Stähelin (*150*), a Swiss pharmacologist at Sandoz, used the new screening process and found immunosuppressive effect of cyclosporin-A (CsA). Later, Dreyfuss, et al. (*151*) determined the structure and cellular effects of CsA in 1975.

In 1976, Borel, et al. (*152, 153*) found CsA prevented immune rejection of skin grafts and prevented graft-versus-host-disease (GVHD) after bone marrow transplants in animal models (*154*). In 1978, Calne, et al. (*155*) at the University of Cambridge used CsA to treat patients who were receiving renal allografts. They (*156*) subsequently used CsA in 34 patients who received kidney, pancreas or liver transplantation. In 1983, FDA approved CsA for preventing graft rejection in people.

CsA had significantly less side effects than cytostatic immunosuppressant drugs such as methotrexate azathioprine and corticosteroids (*157*), CsA does not cause myelotoxicity and does not affect proliferation of hematopoietic stem cells (*158*).

Cyclosporine mechanisms

In immune cells, calcium ion (Ca^{2+}) plays an important role as an intracellular messenger. Ca^{2+} ions bind to calmodulin and the calcium-activated calmodulin will bind to calceinurin (*159*). Calcineurin is a protein phosphatase composed by two subunits, a catalytic subunit (CnA) and regulatory subunit (CnB). When inactive, an inhibitory domain covers catalytic unit CnA. Calmodulin binding of CnA will release the inhibitory domain and activate phosphatase activity. Calcineurin dephosphorylates and activates nuclear factor of activated T-cells (NFAT) and other nuclear factors (*160*). NFAT is a transcriptional regulator that translocates into nucleus and induce gene expression (*161*). In immunocompetent lymphocytes, especially T-lymphocytes, NFAT activates genes that initiate immune response related cytokines including interleukin 2 (IL-2), interleukin 4 (IL-4) (*162*).

Cyclosporine binds to a cytosolic protein called cyclophilin (*163*). The complex of cyclosporine and cyclophilin blocks the phosphatase activity of calcineurin by binding to its catalytic subunit, CnA (*164*). Once CnA is blocked,

calcineurin fails to dephosphorylate and activate NFAT and consequently inhibits expressions of inflammatory cytokines (*164-166*).

4.1.2 CsA as a immune manipulator and inflammation inhibitor

CsA is a widely used immune suppressant after organ or tissue transplantation (*167*). CsA is effective for preventing immune rejection of many types of tissues, including bone marrow, skeletal muscles, lung, cornea, skin, heart, kidney and liver in patients (*167, 168*). CsA significantly reduces immune reactions and improves survival of grafted tissues or organs. In 1998, Borel et al. (*169*) collected data about cyclosporine effects on patients with transplantation. Before CsA, overall 1-year graft survival rates were about 60%. After CsA was used, graft survival increased to about 80%. In patients with liver transplantation, 5-year survival rate increased from 20% to 60% after CsA introduced to clinic. Also, the patients with heart transplantation show 5-year survival of 70% with CsA treatment compared to nearly zero before. Heart-lung and lung transplants had never been successful without CsA treatment. After CsA became available, 1-year survival from heart and lung transplants increased to 65%. CsA treatment also maintained about 80% grafted pancreas and kidney survival at first year. CsA thus is very effective in preventing rejection of transplanted organs and reducing GVHD after bone marrow transplantation.

4.1.3 Neuroprotection

Although CsA was considered an immune suppressant, several investigators reported in 1991 that CsA is neuroprotective in liver transplant patients. Shortly afterward, Lopez, et al. (*170*) found that the immunosuppressant calcineurin inhibitor, FK506 or tacrolimus may be effective in reducing the consequences of global ischemic brain injury, suggesting that the effect of CsA is due to calcineurin inhibition. In 1992, Shiga, et al.(*171*) reported that CsA protects against ischemia-reperfusion injuries in the brain. Dawson, et al. (*172, 173*) showed that calcineurin inhibitors are beneficial for ischemia and other NMDA receptor-mediated excitotoxicity by blocking calcineurin-induced cNOS activation. In 1995, Wakita et al. (*174*) reported the protective effect of CsA in chronic cerebral hypoperfusion rats and that CsA reduces CD4 and CD8 lymphocyte infiltration and microglia/macrophage activation.

CsA protects CNS from injury through several possible mechanisms. The first type of mechanisms is calcineurin-dependent. By blocking calcineurin activation, CsA prevents activation of transcription factor NFAT in immune cells such as T-cells (*162*), microglia (*175*) and macrophages (*176*). NFAT plays an important role for transcription of pro-inflammatory cytokines such as tumor necrosis factor (TNF)-alpha (*177-180*). Thus, CsA should ameliorate inflammatory reactions by blocking NFAT activation.

CsA also blocks calcineurin effects nitric oxide synthase (NOS). NOS produces nitric oxide (NO). Normally, NO is a intracellular messenger that is activated by neurotransmitter receptor activation (*181*). After injury in CNS, glutamate release induces NOS and NO production and high level of NO causes neurotoxin (*182*). CsA reduces NOS and NO production after injury (*183, 184*). CsA also inhibits apoptosis by blocking activation of the pro-apoptotic Bcl-2 protein, BAD, which is activated by calcineurin. When activated, BAD translocates into mitochondria and initiates cytochrome c release and apoptotic cascade. CsA blocks translocation of BAD and apoptosis by inactivating calcineurin (*185*).

The second type of mechanisms is calcineurin-independent. These include mitochondrial protection by inhibiting the mitochondrial permeability transition pore (MPTP) (*186*) and promotion of brain-derived neurotrophic factor(BDNF) release after injury (*187*).

The ability of CsA to protect neurons and prevent cell death has been tested extensively in brain injury models. In animals, CsA reduces microglia/macrophage activation, axonal injury (*188-190*), and the total area of brain injury (*191-193*) after stroke. CsA also preserves mitochondrial integrity and suppresses cytochrome C releasing after ischemia (*194, 195*). CsA has been used in clinical trials of brain injury and stroke since 2006 (*196-198*), mostly phase II trails of traumatic brain injury (TBI). Large-scale phase III trials to evaluate efficacy of CsA in brain injury are still in progress.

In SCI models, CsA reduces lipid peroxidation (*199, 200*) and inhibits expression of NOS (*183, 184*). CsA increases red nuclei neurons survival after SCI (*18*). However, the efficacy of CsA for SCI is still controversial. First, most of the studies showed no significant tissue sparing after CsA treatment of SCI (*18, 201-203*). Secondly, while some studies showed behavioral recovery (*18, 204*), other studies showed no or limited recovery (*201-203, 205*).

4.1.4 Drug administration

In the clinic, intravenous (iv) and oral administrations are the most common routes of administration for CsA. In animals, intraperitoneal (ip) and oral injections are more commonly used. Some studies combined i.p. and oral administrations for long-term treatment. For examples, animals received i.p. injection shortly after injury and then had osmotic pumps implanted for continuous CsA delivery or received the drug orally.

The route of administration affects drug absorption, distribution and consequently effects of CsA as a neuroprotective therapy. In 1999, Yoshimoto, et al. (*206*) found that iv injection of CsA does not reduce cerebral infarct volumes but intracarotid injection reduces infarct volume from 40% to 10%. This may be due to higher CsA concentrations in target tissue when given intra-arterially compared to intravenously.

Route of administration alters CsA bioavailability. For example the bioavailability from oral administration is much lower than iv injection because of

incomplete absorption from digestive system. Drug distribution is also affected by the binding with molecules. For example, CsA is a lipophilic molecule and CsA distribution depends on biological carriers such as lipoprotein (*207*). Tight blinding between lipoprotein and CsA also changes drug availability in different tissues. Except the liver and kidney, which are the main organs for CsA metabolism and elimination, CsA tends to accumulate in fat tissue (*208*). Also, erythrocytes take up CsA and when CsA binding in erythrocytes saturates, more unbound CsA can enter into tissues (*209*). Several studies have described the pharmacokinetic of CsA (*208-211*), None have clearly described the optimal neuroprotective dose in blood or target tissues such as brain or spinal cord.

4.1.5 Alteration of CsA pharmacodynamics after SCI

SCI alters metabolic and physiological function that influence drug absorption, distribution, metabolism, and elimination. For example, SCI markedly reduces absorption by the gastrointestinal (GI) tract and dramatically affects bioavailability of orally administered CsA. Delayed gastric emptying and decreased GI motility dramatically affect drug absorption. However, drug absorption through intramuscular or i.p. administrations should not change after SCI (*212*).

After absorption, CsA enters into the blood stream and distributes throughout the body. SCI may affect this distribution. For example, SCI may change regional blood flow, capillary permeability and blood brain barrier which

cause different drug distribution in the CNS. SCI also changes blood plasma components and this may lead to different physicochemical binding of the drug. For example, after SCI, plasma albumin may be decreased and more unbound drug may enter tissues (*213*).

SCI also affects drug metabolism and elimination. CsA metabolism takes place mainly in hepatic enzyme system, called cytochrome P450. The cytochrome P450 superfamily oxidizes drug molecules and this process requires considerable hepatic blood flow. After SCI, hepatic blood flow is reduced and it slows drug metabolism and maintains high drug concentration in body. Previous studies (*213, 214*) have reported the bioavailability of several drugs, including phenacetin and methylprednisolone, which are both dominated by hepatic metabolism, increase after SCI. Drug metabolites can be eliminated through several pathways. The most important one is renal elimination. SCI impairs renal function and generally increases the half-life of drug metabolites due to slower renal clearance (*215*).

SCI alters CsA pharmacokinetics. Ibarra, et al. (*216*) have reported SCI has complex effect on CsA distribution depending on time and the routes of administration. During the acute state after SCI, CsA bioavailability through i.p. injection increases 5 fold compared to uninjured animals but returns to normal in chronic stage. SCI has opposite effects on oral administration of CsA. During the acute stage of SCI, oral CsA bioavailability dramatically decreases due to impaired absorption.

4.1.6 Adverse effects of CsA

Although CsA is toxic to rats, this toxicity is dose-dependent. CsA immunosuppression increases the risk of infection and malignancy. High dose CsA causes neurotoxicity, hepatotoxicity, nephrotoxicity, and hypertension (*217-225*). The therapeutic range of CsA must be carefully maintained between the minimum effective dose (MED) and the maximum tolerated dose (MTD).

4.2 Method

4.2.1 Animal, contusion and care

Pathogen-free 100-day old F344 rats were anesthetized with isoflurane (5% induction and 2% maintenance) and shaved. After cleaning the skin with betadine and alcohol wipes, I exposed the T13 spinal cord with a laminectomy removing half of T9 and all of T10 lamina. The rats were clamped at the dorsal vertebral processes of T8 and T11 and placed on a sponge covered with sterile wrap. I then used the MASCIS Impactor to drop a 10-gram rod 12.5 mm onto the dural surface of the T13 spinal cord. Subcutaneous fat was placed on the dural surface to retard adhesion of dura to surrounding tissues. The skin was closed with stainless steel clips.

The rats received 7 days of prophylactic antibiotics (cefazolin 50 mg/kg) and daily bladder expression after SCI. If the urine became cloudy or hemorrhagic after a week, the rats were quarantined and started on a fluoroquinolone antibiotic (enrofloxacin 2.5 mg/kg/day) for 10 days. The rats

were examined daily for autophagia. At the first sign of skin irritation in dermatomes below the injury site, the rats were started on daily acetaminophen (oral 65 mg/kg/day "Baby's Tylenol, Johnson & Johnson). If the autophagia progressed to expose muscle or organs, the rat was euthanized. The rats are euthanized at scheduled times (2 week or 16 weeks after injury) by pentobarbital (65 mg/kg i.p.) and either decapitated or perfused with fixative (4% paraformaldehyde).

4.2.2 Preparation and injection of CsA.

We purchased the medical use CsA (Sandimmune Injection) from NOVARTIS. Each mL contains 50 mg cyclosporine, 650 mg polyoxyethylated caster oil, 32.9% alcohol and qs nitrogen. The Sandimmune Injection can be diluted further with 0.9% Sodium Chloride before use.

We prepared 5 mg/ml CsA solution by diluting the 5 ml sterile ampul, which contained 250 mg CsA (Sandimmune Injection, NOVARTIS) with 45 ml sterile saline. Then we weighted rats every week and injected 2 mg/kg CsA into F344 rats and 10 mg/kg CsA to Sprague-Dawley rats subcutaneously right after contusion injury and then every morning after SCI.

4.2.3 External jugular vein catheterization and blood sample collection

In pharmacokinetics, overall uptake and elimination of a drug reach a dynamic equilibrium called steady state. Before reaching steady state, the

concentration of a drug is still changing. We waited 2 weeks after injecting 2 mg/kg/day CsA subcutaneously and collected blood samples to determine CsA levels at steady state.

To obtain repeated, low-stress blood samples from rats within 24 hours, I collected blood samples from external jugular vein catheters. First, the rats were anesthetized by isoflurane (5% for induction and 2% for maintenance). To insert the external jugular catheter, I made a 2-cm incision on the right shoulder just before the clavicle and exposed the external jugular vein. Next, I used forceps to make tissue pocket under the jugular vein and placed three parallel silk sutures under the vein. I then pulled up the suture close to the rostral end so to stop blood flow. Next, I placed a loose loop suture close to the caudal end and clamped the suture with a hemostat. Then I cut the vein with microsissors and inserted a PE50 catheter into the vein through the venotomy and tightened all three sutures, using the knot in the caudal site to secure the catheter inside the jugular vein and two other knots to anchor the catheter. Then I used 22 1/2 G needle to withdraw and flush back to make sure the catheter was unobstructed. I filled the catheter with lock solution (heparinized glycerol 500 IU/ml) and used bone wax to seal the end of the catheter.

The jugular vein catheterization allowed us to collect blood samples several time a day. We injected CsA subcutaneously after SCI and collected blood samples from JVC. First I removed the bone wax form catheter and withdrew lock solution. After obtaining 150 μl of blood, I slowly flushed catheter

with 150 μl sterile saline, filled it with lock solution, and sealed it by bone wax again. The whole blood samples were mixed with heparin and stored in a -20˚C freezer.

4.2.4 Sample preparation and ELISA

Blood samples were collected at 8 time points after CsA sc injection for 2 weeks. All the blood samples were well mixed with heparin and stored in -20 °c before use. I used the CsA ELISA kit from Abnova to quantify the CsA levels in rat bloods. I diluted the whole blood samples with PBS at a (1:1) ratio. Then I added 50 μl standard solutions, blank solutions and samples to 96 wells. After co-incubated with 50 μl Reagent A for 1 hour at 37 degree, I washed the well three times by wash buffer. Then I added 100 μl Reagent B for 45 minutes at 37 degree and washed it 5 times by wash buffer. Next I added 90 μl Substrate solution at 37 degree and 50 μl Stop solution 30 minutes after. Then I used a BioTekx800 Absorbance Microplate Reader to read the plate at 450 nm.

4.2.5 Calculation of area under the curve (AUC) and average cyclosporin-A concentration

After obtained the CsA concentrations from 8 time points, I first calculated the area under the curve (AUC), which represents the total drug exposure over time by trapezoidal rule. The trapezoidal rule works by approximating the region

under the graph of the function f(x) as a trapezoid and calculating its area between two points by the equation:

$$\int_a^b f(x)dx \approx (b-a)\left[\frac{f(a)+f(b)}{2}\right]$$

In our studies, I collected blood samples at 0-hr, 2-hr, 4-hr, 6-hr, 8-hr, 10-hr, 12-hr, and 24-hr after injection and then I calculated the AUC between 0h to 24h by following equation:

$$\begin{aligned}\int_{0h}^{24h} f(x)dx \approx{}& (2-0)\left[\frac{f(0)+f(2)}{2}\right]+(4-2)\left[\frac{f(2)+f(4)}{2}\right]\\ &+(6-4)\left[\frac{f(4)+f(6)}{2}\right]+(8-6)\left[\frac{f(6)+f(8)}{2}\right]\\ &+(10-8)\left[\frac{f(8)+f(10)}{2}\right]+(12-10)\left[\frac{f(10)+f(12)}{2}\right]+(24\\ &-12)\left[\frac{f(12)+f(24)}{2}\right]\end{aligned}$$

To calculate the average concentration over a time interval, I used the equation: $AUC/_t$.

4.2.6 Locomotor assessment

Sean O'Leary and I used the standard BBB score (*17*) to assess locomotor recovery in the rats weekly. We scored the rats over a 4-minute period using the 0-21 point BBB score for each side of the body and assigned a consensus BBB score for both sides.

4.2.7 Rubrospinal tract (RST) tracing and histology

To trace rubrospinal axons at 15 weeks after injury, I anesthetized the F344 rats with isoflurane and injected 1 μl of 2.5 % Fluorogold (Fluorochrome) in 0.9% saline into dorsal spinal cord under T12 lamina below the injury site. After one week, Sean O'Leary and I euthanized the rats, perfused them with 4% paraformaldehyde, removed the brain, cryoprotected the brain with 30% sucrose solutions, cut the midbrain into 30 μm sections, and selected 36 sections containing the red nucleus. I stained the sections with fluororecent Nissl stain (1:300 ThermoFischer Scientific) as a conterstain to identify the location of red nuclei. Using confocal microscopy, I only counted the large well-stained rubrospinal neurons with whole body labeled by fluorogold. The number of labeled neurons in each section is the average number the left and right red nuclei. The number of labeled cells recorded for each brain is the sum of cells counted in every other section.

4.2.8 Statistics

We used repeated measures ANOVA to assess differences of CsA concentrations between rats with different injuries and from different strains. We also used the repeated measures ANOVA to analyze the locomotor activity and weight changes over time after SCI. To compare the Fluorogold (FG) labeled cell counts, we used t-test to compare the control and CsA treatment and we used the ANOVA to analyze the gender effect in this result and did post-hoc testing

(Scheffe's test). To assess the correlation between the BBB vs. weight changes and BBB vs. cell counts in red nuclei, we did the linear regression. We use StatView to run the ANOVA, repeated measures ANOVA, linear regression and t-test. Results were expressed as mean± standard error of means (SEM).

4.3 Results

4.3.1 Maximum tolerated dose of CsA in spinal-injured F344 Rats

According to previous studies in our laboratory, a dose of 10 mg/kg/day CsA is necessary to prevent immune rejection of grafted OEG cells in Sprague-Dawley rats. We chose the same dose to treat F344 rats right after SCI. However, we had to stop the initial experiments after 1 week because all F344 rats died within two days after CsA injection regardless of gender. The high mortality rate was due to complex interaction between SCI and high dose CsA administration. The 10 mg/kg/day subcutaneous injection was lethal to spinal-injured F344 rats but uninjured F344 rats survived under the same treatment.

We tested several CsA doses in F344 rats after SCI including 10 mg/kg, 5 mg/kg and 2.5 mg/kg. Lower doses allowed F344 rats to survive longer after SCI. However, even at the lowest tested dose of 2.5 mg/kg/day CsA, the rats appeared sick and some didn't survive beyond a week. We eventually determined that the highest dose of CsA tolerated by F344 rats was 2 mg/kg/day.

4.3.2 Effective immunosuppressive dose in F344 rats

CsA concentration at steady state in F344 and Sprague-Dawley rats

We then carried out experiments to determine whether 2 mg/kg/day showed effective immunosuppression in F344 rats. Previous study proved the 10 mg/kg daily sc injection of CsA is the effective dose in Sprague-Dawley rats. We wanted to determine if the 2 mg/kg/day sc injection in F344 rats can reach to the same effective level in blood. We also wanted to compare the CsA concentrations in uninjured and SCI rats. We then gave daily subcutaneous 2 mg/kg doses of CsA to uninjured or SCI F344 rats and injected 10 mg/kg/day CsA to uninjured or SCI Sprague-Dawley rats over two weeks to allow CsA in blood levels reaching to steady state. At 2 weeks, I performed the external jugular vein catheterization and collected blood samples for eight time points over 24 hours to measure average CsA concentration.

. Figure 25 shows CsA concentrations over 24 hours at steady state. The CsA in blood level were multi-compartmental distribution after subcutaneous injection. The CsA concentrations were under toxic level (400ng/ml) (*226*) for most of time points in both Sprague-Dawley and F344 rats in uninjured and SCI groups. Except one F344 rat in uninjured group showed CsA concentration was higher but close to 400 ng/ml (Figure 25D). CsA concentration maintained in between 200 to 400 ng/ml for most of time points.

After determined the CsA concentrations, I then calculated the area under the curve (AUC) and average CsA concentration (as descried in the Methods pp.70-71). The AUC were 5954.58 ± 833.62 ng/ml•h and 5729.13 ± 481.53 ng/ml•h respectively in uninjured and injured Sprague-Dawley rats. In Fischer 344 rats, the AUC were 7019.73 ± 922.61 ng/ml•h and 6140.71 ± 334.11 ng/ml•h individually in uninjured and injured groups.

By equation AUC/t, I then calculated the average CsA concentrations (Figure 25E). Sprague-Dawley rats had an average CsA level of 248.11 ± 36.82 ng/ml in sham group and an average level of 238.71 ± 20.06 ng/ml in 12.5-mm group. In F344 rats, the average CsA concentrations were 292.49 ± 38.42 ng/ml in sham group and 255.86 ± 13.92 ng/ml in 12.5-mm group. Repeated measures ANOVA showed no significant difference between strains (F=0.992, p=0.3406) and injury (F=0.555, p= 0.4719, SD: n=4 in Sham; n=3 in 12.5-mm, F344: n=4 in sham; n=4 in 12.5-mm).

The result suggested 10 mg/kg/day CsA in Sprague-Dawley and 2 mg/kg/day CsA in F344 were produced equivalent CsA levels in blood. Also the SCI showed no effect on CsA level at 2 weeks after injury.

OEG cells from Sprague-Dawley survive for 8 weeks with 2 mg/kg/day CsA injection

Daily injections of 2 mg/kg CsA into F344 rats yielded similar steady state and blood CsA levels as Sprague-Dawley rats treated with daily 10 mg/kg/day

CsA. We thus went ahead to investigate whether daily 2 mg/kg would effectively suppress the immune system in F344 rats to allow long-term survival of Sprague-Dawley OEG cells. I transplanted OEG cells isolated from Sprague-Dawley GFP pups into F344 spinal cord after 12.5-mm weight drop injuries. Note that this is a cross-strain transplant and the cells should be rejected since Sprague-Dawley cells are not immune-compatible with F344 rats. Our results showed that daily 2 mg/kg subcutaneous administration allowed grafted cells to survival at least 8 weeks (Figure 26).

4.3.3 Recovery

After confirming that the proper dose of CsA in F344 model is 2 mg/kg/day, we wanted to determine if this dose show any effect on SCI. We injected 2 mg/kg/day CsA subcutaneously starting shortly after SCI (12.5-mm weight drop) and then daily for 6 weeks. We kept the F344 rats for 13 weeks to assess locomotor performance, body weight changes, and rubrospinal tract tracing.

BBB scores

We evaluated locomotor performance of each rat every week, using Basso-Beattie-Bresnahan (BBB) locomotor scores (*16, 17*) (Figure 27). Both control and CsA-treated groups showed no hindlimb (HL) movement at day 2 after injury (BBB=0 in control group; BBB= 0 in CsA group). After 1 week, the

F344 rats with CsA injection started to show extensive movements of two joints and slight movement of another joint (BBB= 6) while the control untreated spinal-injured F344 rats showed extensive movements of two joints (BBB= 3). At 3 weeks, the CsA group already showed frequent-to-consistent weight-supported plantar steps and occasionally forelimb-hindlimb (FL-HL) coordination (BBB = 12) while the control showed sweeping with no weight support (BBB = 8). At 6 weeks, CsA group reached to BBB of 14 while control stayed in BBB of 10. From 6 to 13 weeks, CsA group kept improving and reached to BBB of 14 while control group showed very limit improvement and kept in BBB of 10. Repeated measures ANOVA indicated significant differences between control and CsA groups ($F=8.205$, $p=0.0096$, $n=11$ in both groups).

We also analyzed data by splitting gender. In the F344 rat model, female rats in both control and CsA groups showed better locomotor activities than male rats. Female F344 rats recovered to BBB of 12 and increased to BBB of 15 with CsA injection (Figure 28A). In male F344 rats, control only recovered to BBB of 8 and CsA group recovered to BBB of 12 (Figure 28B). No significant difference was shown between control and CsA groups in both genders (Male: $F=3.875$, $p=0.0511$, $n=6$ in control; $n=5$ in CsA; Female: $F=5.057$, $p=0.08$, $n=5$ in control; $n=6$ in CsA). It might due to the total number of rats in each group was decreased.

Figure 29 shows the locomotor behavior in different treatments (control and CsA) and different genders. Repeated measures ANOVA revealed

significant differences between genders (F=7.529, p=0.0133) and treatments (F=8.925, p=0.0079) but no significant interactive effect was shown between gender and treatment (F=0.224, p=0.642, n=5 in female control, n=6 in male control, n=6 in female CsA, n=5 in male CsA).

Body weight changes

Given the difference of growth curve between male and female F344 rats, we compared the weight changes of male and female F344 rats after SCI (Figure 28).

At the first week after injury, F344 females showed weight loss of 22.8 ± 2.177 g and 23.167 ± 2.167 g individually in control and CsA groups (Figure 30A). Female rats in both control and CsA groups started to gain weight since second week after injury. By 13 weeks, females respectively gained a total of 32.8 ± 6.77g and 35.834 ± 6.72 in control and CsA group, about 2.7 g per week in both groups. Repeated measures ANOVA showed no difference in weight changes between control and CsA females F344 rats (F=0.414, p=0.536,n=5 in control; n=6 in CsA).

By 1 week after 12.5-mm contusion, male F344 rats lost 50.67 ± 5.23 and 52.6 ± 3.61 g respectively in control and CsA groups (Figure 30B). From second week after SCI, male F344 rats in both control and CsA-treated groups started to gain weight. In the control group, males increase 65.57 ± 13.59 g by 13 weeks after SCI, gaining approximately 5g per weeks. CsA treated male F344 rats

increased a total of 123.2 ± 16.33 g by 13 weeks, gain about 9 g per week. Repeat measures ANOVA showed significant differences between control and CsA groups (F=8.413, p=0.0176, n=6 in control; n=5 in CsA).

Correlation between hindlimb function and weight changes

Regression analysis (Figure 30C) showed that behavioral recovery correlated linearly with weight changes with correlation coefficient of 0.647 in male F344 rats ($p<0.001$). The regression line had y-intercept of 8.467 ± 0.277 and slope of 0.074 ± 0.007. In female F344 rats, the correlation coefficient was 0.700 ($p<0.001$) with y-intercept of 11.837 ± 0.273 and the slope of 0.244 ± 0.02.

Preserved Rubrospinal Tract axons and labeled neurons in red nuclei

To assess the rubrospinal tract (RST), we injected 1 μl of 2.5% fluorogold (FG) dye into spinal cord under the T12 lamina 1 week before euthanasia. Rubrospinal axons that cross the injury site should pick up dye and transport the dye back the cells and the number labeled neurons in red nuclei should reflect the number of axons crossing the injury site. After perfusion, I cut the brain tissue into 30 μm and stained selected samples with green fluorescent Nissl stain as a conterstain.

Figure 31A shows clear structure of red nucleus and oculomotor nucleus in midbrain with fluorescent Nissl stain. FG-labeled neurons located in red nuclei and expressed red fluorescent in Figure 31B. Figure 31C and D are the pictures

which showed FG-labeled neurons respectively in control male and female F344 rats. Figure 31E and F are the pictures which showed FG-labeled neurons respectively in CsA male and female F344 rats.

At 15 weeks after a 12.5-mm weight drop, the control F344 rats had 102.33 ± 19.32 FG-labeled RST neurons. After subcutaneous injection of 2 mg/kg/day CsA for 6 weeks, the CsA treated rats had 157.188 ± 15.63 RST neurons labeled by FG. T-test indicated a significant difference between control and CsA treatment ($p=0.0464$, n=9 in control; n=8 in CsA) (Figure 32A).

Male and female F344 rats had different locomotor activities. Male F344 rats had 76.6 ± 24.21 and 138.17 ± 32.89 fluorogold labeled RST neurons in the control and CsA-treated groups respectively. Female F344 rats had 134.5 ± 25.35 labeled-neurons in control group and 168.6 ± 16.52 labeled neurons in CsA group. ANOVA suggested no significant difference of retrogradely labeled RST neuronal counts between males and females ($F=3.287$, $p=0.093$, Control: n=4 in female; n=5 in male, CsA n=5 in female; n=3 in male), the difference was close to significance and may have been significantly difference if the experiments included more animals (Figure 32B).

Regression analysis indicated that BBB scores correlated linearly with the number of labeled neurons in red nuclei (Figure 32C). The correlation coefficient was 0.726 ($p=0.0015$). The y-intercept of regression line was 8.337 ± 3.909 and slope was 9.887 ± 2.415.

4.4 Discussion

4.4.1 Why is the CsA level in F344 higher than Sprague-Dawley?

Hepatic enzymes dominate the clearance of CsA. CsA is metabolized and biotransformed by hepatic enzymes to 25 metabolites including three primary metabolites (the monohydroxylated metabolites M1 and M17, N-demethylated metabolite M21) and other secondary metabolites (*227*).

In our study, we found that blood CsA concentrations were much higher in F344 rats than Sprague-Dawley rats when given the same CsA regimen. The mechanism of the higher CsA levels is unclear but it might due to lack or deficiency of hepatic P450 3A enzymes, which are necessary for CsA metabolism, and possibly less hepatic blood flow in F344 rats.

Hepatotoxicity

Another factor might affect CsA level is toxic effects of CsA treatment on the liver. High doses of CsA damage the liver and kidney, and cause hypertension of neurological damage. Because a majority of CsA is metabolized in liver, hepatotoxicity may reduce metabolism of CsA.

The degree of CsA-induced hepatotoxicity differs among rat strains. In 1986, Augustine et al. (*228*) reported that F344 rats were more sensitive to CsA-induced hepatotoxicity. They gave CsA orally (25 mg/kg for 14 days) to three strains of laboratory rats, i.e. Sprague-Dawley, Wistar, and F344 rats. CsA treatment significantly reduced mircrosomal proteins and cytochrome p450 in

liver and impaired hepatic drug metabolism in all three strains. However, F344 rats had more impairment of hepatic metabolism than Sprague-Dawley or Wistar rats. After CsA treatment, F344 rats lost 27% activity of NADPH-Cytochrome c reductase, 70% activity of ETM N-demethylase, and 47% activity of ANL hydroxylase in the liver. Also F344 rats had 31.6 mg/g microsomal protein, which was less than the other two strains (~35 mg/g in Sprague-Dawley or Wistars). After CsA treatment for 14 days, microsomal protein decreased to 24 mg/g in F344 rats while Sprague-Dawley and Wistar rats still had about 30 mg/g microsomal protein in liver.

Although Augustine, et al. (*228*) showed strain-related differences of CsA-induced hepatotoxicity, they did not measure CsA metabolism among strains. CsA treatment for 14 days reduced liver P450 but the reduction of liver enzymes did not differ among the three rat strains and the measurements did not distinguish various forms of cytochrome P450 family. To clarify the mechanism for strains-related CsA effect, expression of cytochrome P450 specifically related to cyclosporine-metabolism must be identified.

4.4.2 Effective dose

In clinical use, the usual adult dose for organ transplant is 2 to 5 mg/kg/day iv infusion once or divided twice daily or 8 to 12 mg/kg/day orally once or divided twice daily. The therapeutic range is between 200-400 ng/ml in blood level (*226*). CsA concentrations lower than 200 ng/ml are associated with higher

risk of graft-versus-host-disease (GVHD) and higher level than 400 ng/ml may trigger toxic effect especially on renal and hepatic function.

In the animal model, the range of CsA dose is between 5 to 30 mg/kg daily. The drug administrations are various depending on the purpose of studies. For pharmacological study, they tend to treat CsA by iv infusion in order to obtain pharmacokinetic metrics. For other studies related to immunosuppression or neuroprotection, researchers prefer to administrate CsA orally or ip injection for long-term treatment.

Most studies about immunosuppression or neuroprotection do not monitor CsA concentration. The effective dose is usually determined from graft survival or tissue sparing. For example, many laboratories use 10 mg/kg/day of CsA because this dose is necessary and sufficient to prevent immune rejection of transplanted cells.

Our results suggest that CsA pharmacokinetics differ among rat strains and care should be taken to titrate the CsA dose for optimum immunosuppression and minimum toxicity. For example, subcutaneously injected 10 mg/kg/day CsA dose was obviously toxic to F344 rats and none of the animals survived more than 3 days after SCI. The maximum tolerated dose is fivefold less at 2 mg/kg/day. Daily injections of 2 mg/kg CsA resulted in blood CsA concentrations of 255 ng/ml which is located in the therapeutic range (200 ~ 400 ng/kg) (*226*). Blood CsA levels in F344 rats corresponded to blood CsA levels in Sprague-Dawley treated with 10 mg/kg/day of CsA. Grafted Sprague-Dawley

OEG cells survived in F344 host at least for 8 weeks with 2 mg/kg CsA daily sc injection.

4.4.3 SCI effect on CsA pharmacokinetics in F344 rats

SCI alters pharmacokinetics of CsA in the acute stage of injury. Ibarra et al. (*216*) found increased bioavailability of ip injected CsA and AUC is 5 times higher in rats at 24 hours after SCI compared to uninjured rats.

In our study, 100% of F344 rats died within two days after SCI when treated with CsA 10 mg/kg/day. Uninjured F344 survived at least 1 week after receiving the same 10 mg/kg/day dose of CsA but nevertheless died after 1 week. We conclude that SCI increased CsA bioavailability at acute stage and CsA accumulated to lethal levels by two days after injury. The SCI effect on CsA bioavailability seems to decrease after 2 weeks. Blood CsA levels did not differ significantly between injured and uninjured animals at 2 weeks after CsA treatment.

4.4.4 Cyclosporin-A effect on SCI

Twelve studies (Table 3.) have reported CsA effects on SCI in rats. These studies showed that CsA inhibited lipid peroxidation formation (*200, 229*), nitric oxide synthase expression (*183, 184*), preserved myelination (*204*), and improved the number of retrogradely labeled RST neurons (*18*). However, several studies showed no change in tissue sparing after SCI (*18, 184, 201-203,*

229, 230). Eight studies assessed behavior changes after SCI with CsA treatment: 3 studies reported significantly functional improvement with CsA (*18, 204, 229*) but 5 studies showed no or limited functional recovery (*201-203, 205, 230*).

The variable therapeutic effects may be due to differences in SCI models, rat strains, and different routes and doses of CsA. Twelve published studies on the subject used several SCI models including contusion, compression, lateral funiculotomy, hemisection, and transection and three rat strains, including Wistar, Sprague-Dawley, and F344 rats. CsA was given intraperitoneally, subcutaneously, or orally. The doses ranged from 2.5 mg/kg/day to 20 mg/kg/day. It is not surprising that there is such diversity of results from these experiments.

Rat strains, injury model, CsA administration and dose affect CsA bioavailability and concentration in the brain and spinal cords. Therefore, the CsA concentration should be monitored in blood level and spinal cord to compare therapeutic effects of CsA. All studies of CsA treatment on SCI did not monitor CsA concentrations in blood or tissue.

Our study indicated that 2 mg/kg/day of CsA injected subcutaneously into F344 rats effectively suppressed the immune system and significantly improved in hindlimb function after SCI. We monitored blood CsA concentration and found the levels to be around 255 ng/ml in F344 treated for 2 weeks with 2 mg/kg/day.

Sprague-Dawley rats need approximately 5 times higher doses (10 mg/kg/day) to reach to similar concentration in blood level.

CHAPTER 5 CONCLUSION

5.1 Contusion model for cell transplantation

Most commonly used laboratory rat strains are outbred and will reject cells from other rats of the same strain unless they are immune incompetent or immunosuppressed. The F344 strain is an isogenic inbred strain that allows transplanted cells to survive without immunosuppression. The F344 contusion model is therefore important for cell transplantation studies. Most cells transplanted into humans fall into three categories: autologous, HLA-matched, or allogeneic. The first two categories usually do not require any or just short-term immunosuppression while the last usually requires long-term immunosuppression with drugs such as CsA. However, as our data shows, immunosuppressant drugs such as CsA not only prevent immune rejection but appear to affect the injury process and change the behaviors or therapeutic effects of transplanted cells. Our group developed a F344 strain expressing green fluorescent protein (GFP). We confirmed that cells isolated from GFP F344 rats can be transplanted into wild-type F344 rats without immune rejection. The development of the GFP F344 rat and a contusion model using F344 rats allow convenient transplantation of cells from GFP F344 rats to regular F344 rats without immunosuppression.

5.2 F344 Contusion model by MASCIS Impactor

MASCIS standardized the weight drop spinal cord contusion model in Long-Evans hooded and Sprague-Dawley rats and demonstrated that the Impactor produced consistent contusion injuries when a 10 g weight is dropped 12.5, 25, and 50 mm onto spinal cord exposed by a T9-10 laminectomy in 77±1 days old rats. F344 rats are significantly smaller than Long-Evans and Sprague-Dawley rats. At 77 days old, female F344 rats are too small to be held reliably with the spinal clamps and contusions tended to break the dura, increasing the variability of injury. We therefore standardized the contusion model to 100±1 day old F344 rats and found that If we did not remove the ligmentum flavum, which lies on the dural surface of the spinal cord exposed by a T9-10 laminectomy, contusion with a 10 gram weight did not break the dura.

With these changes of the model, the MASCIS Impactor produces graded and consistent contusion parameters and spinal cord injuries in F344 rats. Contusion parameters in 100±1 day-old F344 rats are similar to those in 77±1 day-old Long-Evans hooded and Sprague-Dawley rats but lesion volumes are larger (*15*) and locomotor recovery in F344 rat is less than Sprague-Dawley and Long-Evans hooded rats (*11*).

5.3 Gender difference

Four out of five spinal-injured people are males (*124*). The mechanisms underlying this large gender gap are unknown. Some

investigators have speculated that more males are spinal-injured because of their tendency to engage risky behavior that lead to more spinal cord injuries. However, such arguments are difficult to prove.

The gender issue has not been well addressed in animal models. Many investigators use either males or females but not both for experiments. Few studies (*128-133*) have compared spinal cord injuries between male and female rodents. Previous studies in our lab using outbred rat strains such as Sprague-Dawley and Long-Evans hooded rats showed no gender difference after SCI. F344 is the first rat strain that has shown a significant gender difference in our laboratory. In the two sets of experiments, female F344 rats recovered significantly better than male rats without any treatment. Also male and female F344 rats responded differently to treatments. In male F344 rats, OEG transplantation and CsA treatment promoted functional recovery after SCI. However only CsA treatment significantly improved locomotor scores in female F344 rats. F344 contusion model provides an excellent opportunity to investigate mechanisms of gender differences. Moreover, the F344 contusion model can be used to assess differences of treatment effects between genders.

Our results suggested that a gender difference is present in F344 rats and that animal studies should include balanced genders. Most of SCI publications ignored gender issue and studies that use single gender or unbalanced gender may have obscured the gender-dependent treatment

effect. Stratification and including sufficient numbers of males and females is the key to detecting gender differences.

In the discussion of Chapter 3, we proposed five hypotheses concerning potential mechanisms of gender gap, including mechanical, anatomical, metabolic, hormonal, and immune differences. Careful comparison of impact parameters and spinal cord anatomy revealed no mechanical or anatomical differences between male and female F344 rats. Differences in metabolism between male and female F344 rats may contribute to greater tissue damage in male spinal cords. Previous studies (*134*) reported that peroxide production in liver and brain is higher in male rats than females, suggested that males may have greater secondary injury than females. We measured cytochrome C levels in livers and spinal cords of male and female F344 rats, as well as malondialdehyde levels in the spinal cords. We found no difference in cytochrome C or malondialdehyde levels in livers and spinal cords of male and female F344 rats. Also we found no difference of 24-hour lesion volumes in spinal cords of male and female F344 rats, suggesting that increased lipid peroxidation and greater secondary tissue damage is not responsible for the gender difference. What ever contributed to the better recovery in the female rats probably occurred after 24 hour.

Several previous studies reported that sex hormones, especially estrogen, have neuroprotective effects including prevention of apoptosis (*136-139*) and sparing of white matter (*138, 140-143*). Estrogen also promotes endogenous remyelination (*231*) and angiogenesis (*232*). Several studies (*136, 138, 139, 142, 143*) have reported that administrating estrogen improves functional recovery after SCI. However, the role of sex hormones in gender effect is controversial. Some investigators used male rats or female rats with ovariectomy and gave estrogen by iv or ip injection. In these studies, estrogen concentrations were maintained at much higher levels than normal physiological estrogen levels in female rats. Estrogen is usually low except during estrus, which occurs every 5 days in rats. While exogenously administered estrogen may be neuroprotective, both the dosing and timing of existing do not explain the gender difference in our study. To clarify the role of sex hormones in gender differences, more studies need to be done. For example, a more convincing experiment would be to show that antagonists of estrogen abolish the gender difference in F344 rats.

Differences in immune response to SCI may explain the different recovery in male and female F344 rats. Our preliminary data suggest increased injury-induced peripheral blood neutrophil response in male F344 rats may be responsible for their slower and less effective locomotor recovery. Neutrophils are the first peripheral leukocytes to infiltrate into spinal cord between 24-48 hours after injury. Neutrophils secrete pro-inflammatory cytokines, proteases, and free radicals (*233*). Less neutrophil accumulation in spinal cord results in lower

oxidative stress and apoptosis and improves functional recovery after SCI (*234-237*).

We believe the most likely explanation of the gender difference is the different immune response of male and female F344 rats after SCI. SCI induces changes in peripheral white blood cell counts. Our preliminary data showed that SCI causes a higher percentage of neutrophils in white blood cell counts of male F344 peripheral blood compared to those of female F344 rats. However, we need to confirm that male F344 rats have higher total neutrophil counts rather than just greater percentages of neutrophils. . Also, we must confirm higher numbers of infiltrated neutrophils in injured male spinal cords. Finally, to show cause and effect, we need to show that reducing the male neutrophil response so that it is similar to female neutrophil response will eliminate the gender difference. Several methods are available to reduce neutrophils, including using an antibody (*238*) to deplete neutrophils.

5.4 OEG transplantation

Many laboratories have transplanted OEG into spinal cord injured animals and find that the cells improve recovery, facilitate regeneration (*54-80*) and increase remyelination (*107-114*). However, some investigators found no regeneration or recovery (*74, 115-123*). In 2007, Franssen and his colleagues reviewed studies of OEG transplantation in SCI models (*88*). They selected 54 papers: 41 studies showed positive effects and 13 showed no or limited effects. .

Several conditions may have changed efficacy of OEG cells i.e. different source of OEG cells, purity, transplant timing and location. Our findings now suggest another important factor, gender. OEG transplantation improved recovery only in male F344 rats and not female F344 rats. Control untreated female F344 rats recovered as well as OEG transplantation group.

OEG transplantation significantly improved functional recovery in male rats at 6 weeks after SCI. Possible mechanisms of the therapeutic effect of OEG transplantation include neural plasticity, regeneration and remyelination (*88*). OEG cells support axon growth by secreting neurotrophins such as BDNF, GDNF and NGF(*82, 83*). OEG also express cell adhesion molecules such as N-CAM and L1 (*84-86*) and ECM-molecules such as laminin (*87*) that can attract and guild axonal growth. Finally, OEG cells myelinate axons (*107-114*), observed by Kai Liu in our laboratory as well (unpublished studies).

5.5 CsA effect on locomotor recovery

CsA treatment significantly improved locomotor recovery after contusion injury in both male and female F344 rats. CsA therapy is likely to be neuroprotective rather than regenerative because recovery occurred within 2-3 weeks of starting CsA treatment, too fast for regeneration, which should take 6 or more weeks. Several laboratories have reported the CsA has neuroprotective effects on injured rat spinal cords, including inhibition of lipid peroxidation (*229,*

239) and improved mitochondrial function (*18, 184, 240*), improved neurologic (*241*) and locomotor recovery (*202, 242*), reduced lesion size (*230*), increased remyelination (*243*), improved mean arterial pressure after SCI (*244*), and reduced neuronal loss after intraspinal quisqualate injections (*245*) and hypoxic injury (*240*). Other researchers have reported neuroprotective effects of CsA on brain injury models (*246, 247*) and *in vitro* models of neural injury (*248*). However, some investigators did not find such effects in traumatic (*249-252*) and ischemic rat SCI models (*253*). Also, at least one clinical trial of CsA in TBI did not show any benefit (*198*).

The variability of CsA results reported in the literature may have been due to different doses and routes of CsA administration. In this study, we found that CsA bioavailability differed amongst rat strains. We suggest that blood CsA levels are monitored to confirm that the dose is in therapeutic dose range and under toxic range.

Our results suggest that F344 rats are much more sensitive to CsA than Sprague-Dawley or Long-Evans hooded rats. The latter two strains of rats usually require 10 mg/kg of CsA to suppress the immune system. F344 rats require only 2 mg/kg/day sc yielding an average blood CsA concentration of 255 ng/ml, within the CsA therapeutic range. A 2 mg/kg/day of CsA effectively suppressed the immune system and significantly improved in hind limb function after SCI in F344 rats. Higher doses are toxic to F344 rats.

We could not determine whether higher doses were more neuroprotective for SCI due to toxicity of CsA for other organs in F344 rats. However we should be able to test higher CsA concentrations by injecting CsA intrathecally or directly into spinal cords. We also gave the CsA treatment starting immediately after injury and then daily for 6 weeks. We therefore do not know whether CsA treatment would improve recovery when started later or for shorter periods after SCI. Finally, CsA improved hindlimb function on both male and female F344 rats, even though control female rats recovered better than control males. These results suggest that CsA not only has beneficial effect on both genders but also on both mild and severe SCI.

CsA may protect the spinal cord through multiple mechanisms. These include inhibition of nitric oxide (NO) synthetase and reduction of lipid peroxidation after SCI (*183, 184*). Also, CsA inhibits apoptosis by upregulating expression of anti- apoptotic protein Bcl-2 (*254*) and preserves mitochondrial function by inhibiting permeability transition pore formation (*255*). CsA may also reduce secondary injury by reducing inflammation after SCI. Spinal cord contusion elicits a strong inflammatory and immune responses, including increased peripheral immune cells and infiltrations of neutrophils, monocytes, and lymphocytes into the spinal cord. In addition, injury also activates resident microglia (*256, 257*). CsA inhibits calcineurin, a phosphatase that regulates cell migration (*258*), cytokine and chemokine release (*259, 260*), as well as inflammation and immune response to injury (*261, 262*). Calceinurin inhibitors

such as CsA or FK506 reduce immune cell infiltration (*263, 264*), as well as pro-inflammatory (*265-267*).

CsA may also contribute to neuroprotection by reducing the number of neutrophils that infiltrate the spinal cord. Neutrophils enter the injured spinal cord from peripheral blood and produce pro-inflammatory cytokine, proteases, free radicals, which can aggravate inflammation and increase cell death through both necrotic or apoptotic mechanisms. Previous studies (*234-237*) showed that less neutrophil accumulation in spinal cord results in less oxidative stress and apoptosis and improves functional recovery after SCI. CsA significantly reduces neutrophil counts in blood and diminishes neutrophil infiltration in liver ischemia and reperfusion injury in human patients (*263*). CsA treatment causes severe neutropenia, reducing neutrophil count to < 500 in blood compared to normal levels of 1500 to 8000 neutrophils per μliter (*268*).

CsA also reduces infiltration of macrophages. In recent years, scientists have shown that macrophages can alter their phenotype and function depending on their environment. Two main phenotypes have been reported have been described: M1 and M2. M1 macrophages are present at acutely injured spinal cord and facilitate inflammation by producing pro-inflammatory cytokines, reactive oxygen species (ROS) and NO. M2 macrophage contributes to wound healing and tissue repair by producing anti-inflammatory factors. Previous study (*204*) showed that CsA inhibits infiltration of activated macrophages/microglia (CD68+) in murine spinal cords after SCI.

CsA reduces pro-inflammatory cytokines, including TNF-alpha, IL-1, and IL-6, released by immune cells. These cytokines stimulate more inflammatory responses that can contribute to secondary injury. Schwab and Klusman (*269*) reported a mixture of IL-1 beta, IL-6 and TNF alpha increased macrophages activation and tissue loss at injured spinal cord. Administration of neutralizing antibody or antagonist against pro-inflammatory cytokines reduces apoptotic cells (*270*) and promotes functional recovery (*271*) after SCI.

Calcineurin regulates pro-inflammatory responses in microglia (*272*) and astrocytes (*273*). Previous studies showed calcineurin inhibitors such as CsA or FK506 reduce production of pro-inflammatory cytokine by LPS-stimulated macrophages *in vitro* and *in vivo* (*265*), microglia in Alzheimer's mice model (*274*), human macrophage (*266*), stimulated B and T lymphocytes (*275*). Therefore, CsA treatment protects the spinal cord by reducing production of pro-inflammatory cytokines after SCI.

In order to test the above hypotheses, we plan to measure the numbers of immune cells and the level of pro-inflammatory cytokines in peripheral blood and spinal cord before and after SCI. We will collect the blood samples before injury and contuse F344 T13 spinal cords by MASCIS impactor, inject saline or 2 mg/kg CsA subcutaneously daily into F344 rats, collect peripheral blood samples at 12h, 24h and 72h after injury, count neutrophils and macrophages, and measure pro-inflammatory cytokines including TNF, IL-1, IL-6, and IFN-γ by ELISA and lipid peroxidation by thiobarbiturate acid (TBA) test. For spinal cord tissues, we will

euthanize and perfuse F344 rats at 12h, 24h and 72h after SCI and use the immunohistology to determine the numbers of neutrophils and M1 macrophages. We will also collect fresh spinal cords after euthanasia and quantify pro-inflammatory cytokines by ELISA kit and lipid peroxidation by TBA test.

5.6 Summary

The contusion model in F344 rats unexpectedly turns out to be useful for studying several aspects of SCI that cannot be studied in other rat models. First, the F344 model allows study and testing of cells from other F344 rats without using immunosuppressants, as well as the study of immunosuppressant drugs on transplanted cells from other F344 rats. Secondly, we found significant differences of recovery in male and female F344 rats after SCI and different therapeutic effects of treatments. This model allows study for the mechanisms of gender differences and differences of treatment effects in male and female rats. Finally, CsA has a robust neuroprotective effect on both male and female F344 rats. It is interesting that this effect may be due to reduction on peripheral cellular immune response to SCI.

TABLES & FIGURES

Table 1. Basso, Beattie, and Bresnahan Locomotor Rating Scale (*17*)

0	No observable hind limb (HL) movement.
1	Slight movement of one or two joints, usually the hip and/or knee.
2	Extensive movement of one joint or extensive movement of one joint and slight movement of one other joint.
3	Extensive movement of two joints.
4	Slight movement of all three joints of the HL.
5	Slight movement of two joints and extensive movement of the third.
6	Extensive movement of two joints and slight movement of the third.
7	Extensive movement of all three joints of the HL.
8	Sweeping with no weight support or plantar placement of the paw with no weight support.
9	Plantar placement of the paw with weight support in stance only (i.e., when stationary) or occasional, frequent, or consistent weight supported dorsal stepping and no plantar stepping.
10	Occasional weight supported plantar steps, no forelimb (FL)-HL coordination.
11	Frequent to consistent weight supported plantar steps and no FL-HL coordination.
12	Frequent to consistent weight supported plantar steps and occasional FL-HL coordination.
13	Frequent to consistent weight supported plantar steps and frequent FL-HL coordination.
14	Consistent weight supported plantar steps, consistent FL-HL coordination; and predominant paw position during locomotion is rotated (internally or externally) when it makes initial contact with the surface as well as just before it is lifted off at the end of stance or frequent plantar stepping, consistent FL-HL coordination, and occasional dorsal stepping.
15	Consistent plantar stepping and consistent FL-HL coordination; and no toe clearance or occasional toe clearance during forward limb advancement; predominant paw position is parallel to the body at initial contact.
16	Consistent plantar stepping and consistent FL-HL coordination during gait; and toe clearance occurs frequently during forward limb advancement; predominant paw position is parallel at initial contact and rotated at lift off.
17	Consistent plantar stepping and consistent FL-HL coordination during gait; and toe clearance occurs frequently during forward limb advancement; predominant paw position is parallel at initial contact and lift off.
18	Consistent plantar stepping and consistent FL-HL coordination during gait; and toe clearance occurs consistently during forward limb advancement; predominant paw position is parallel at initial contact and rotated at lift off.
19	Consistent plantar stepping and consistent FL-HL coordination during gait; and toe clearance occurs consistently during forward limb advancement; predominant paw position is parallel at initial contact and lift off; and tail is down part or all of the time.
20	Consistent plantar stepping and consistent coordinated gait; consistent toe clearance; predominant paw position is parallel at initial contact and lift off; tail consistently up; and trunk instability.
21	Consistent plantar stepping and coordinated gait, consistent toe clearance, predominant paw position is parallel throughout stance, consistent trunk stability, tail consistently up.

Originally published in Journal of Neurotrauma, Volume 12, Number 1, 1995.

Table 2. Percentage(%) of dural breakage after SCI in F344 rats

	5-g	10-g
12.5 mm	27.3%	35.7%
25 mm	36.8%	43.5%

Table 3. Cyclosporin-A effect on SCI

Reference Authors/ Year	Rat strain/sex	SCI model	Administration	Functional recovery	Reported effects of CsA on SCI
Diaz-Ruiz, Rios et al. 1999 (*229*)	Wistar/F	T8/9 contusion	2.5 mg/kg/12hr ip injection	Tarlov's from 2 to 2.5	1. CsA Inhibited lipid peroxidation from 150 to 60 F.U./mg 2. Results showed no difference on spared tissue between control and CsA groups
Diaz-Ruiz, Rios et al. 2000 (*200*)	Wistar/F	T9 contusion (Allen 10cm)	2.5 mg/kg/12hr ip injection	No data	CsA treatment reduced lipid peroxidation from 150 to 50 F.U./mg
Rabchevsky, Fugaccia et al. 2001 (*201*)	SD/F	T9 contusion (NYU 12.5 mm)	A bolus 20 mg/kg ip + 2.5 mg/kg/day ip injection for 7 days	No functional recovery	CsA treatment did not change tissue sparing by 6 weeks after injury.
Ibarra, Correa et al. 2003 (*18*)	F344/F	1. T9 compression 2. T9 contusion (NYU 50 mm)	1. Oral 5mg/kg + 2.5 mg/kg/12hr ip injection for 3 days 2. 2.5 mg/kg/12hr ip injection for 72 h	1. Grid walking from 0.6 to 0.8 2. BBB from 4 to 6	1. More labeled red nuclei cells were seen in CsA group compared to control group. 2. CsA treatment did not increase spared tissue..
Diaz-Ruiz, Vergara et al. 2004 (*183*)	Wistar/F	T9 contusion (Allen 10cm)	2.5 mg/kg/12h ip injection	No data	1. CsA inhibited the expression of nitric oxide synthase.
Diaz-Ruiz, Vergara et al. 2005 (*184*)	Wistar/F	T9 contusion (Allen 10cm)	2.5 mg/kg/12h ip injection	No data	1. CsA inhibited the expression of nNOS and eNOS.
Hayashi, Shumsky et al. 2005 (*276*)	SD/F	Lateral funiculotomy	1.10mg/kg sc for 17 days 2. 10mg/kg sc for 3 days + oral 50 μg/ml in water	No data	1. CsA increased survival of grafted fibroblasts. 2. No tissue sparing was shown between control and CsA group. 3. CsA enhanced host axon growth into graft site.

Ibarra, Hernandez et al. 2007 (*205*)	SD/F	Transection	A bolus 2.5 mg/kg/12h ip injection +5 mg/kg/12h oral administration	No functional recovery	CsA promoted axonal growth.
McMahon, Albermann et al. 2009 (*202*)	SD/F	T9 contusion (Horizon)	5 mg/kg/day sc injection	No functional recovery	1. CsA had no effect on tissue sparing. 2. After CsA treatment, more astrocytes, less NeuN and MBP were in spinal cord compared to control by 3 weeks. By 7 weeks astrocyte became much less in CsA group.
Lü, Wang et al. 2010 (*204*)	SD/F	T9 contusion (NYU 12.5-mm)	10 mg/kg sc injection	BBB from 11 to 14	1. CsA decreased CD3+ microglia, macrophage cells in spinal cord. . 2. CsA decreased lesion volumes at 7 weeks. 3. CsA increased spared neurons and myelin compared to control group.
Lonjon, Boniface et al. 2011 (*203*)	Wistar/M	Compression	10 mg/kg/day sc injection	No functional recovery	1. CsA treatment had effect on tissue sparing. 2. 10mg/kg CsA had deleterious effects on kidneys.
Roozbehi, Joghataie et al. 2012 (*230*)	SD/F	L1 hemisection	2.5 mg/kg/day ip injection	BBB from 12 to 14	CsA treatment did not reduce lesion size.

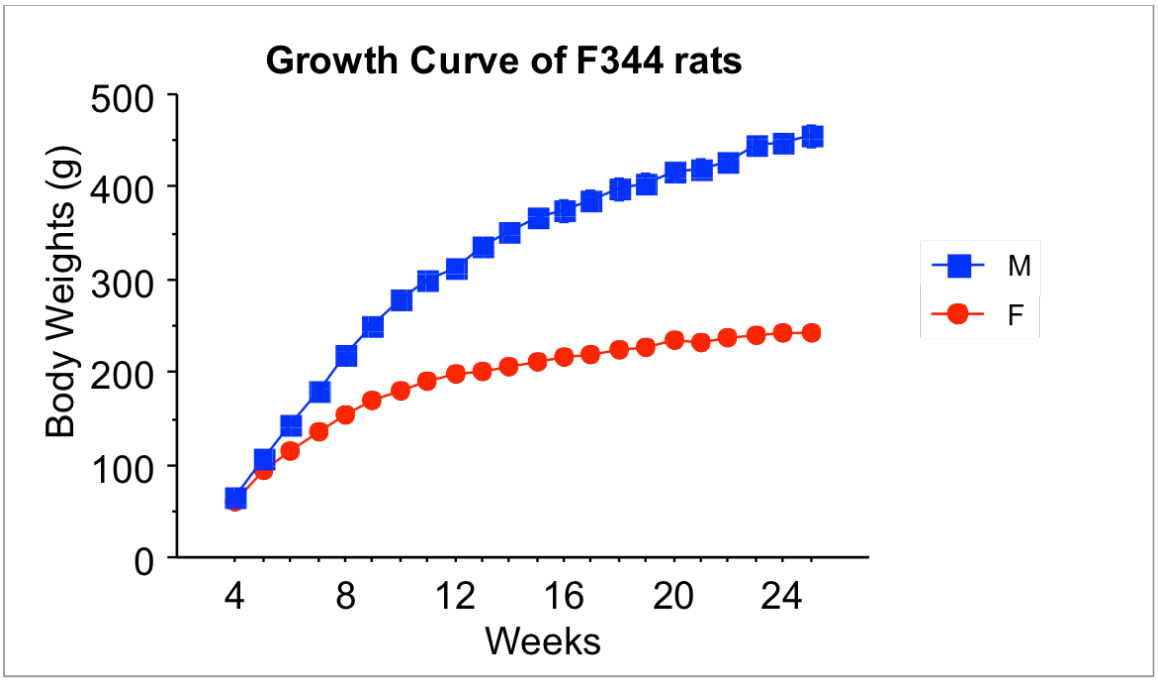

Figure 1. Growth curve of F344 rats.

Blue round dots indicate male F344 rats and red dots indicate female F344 rats.

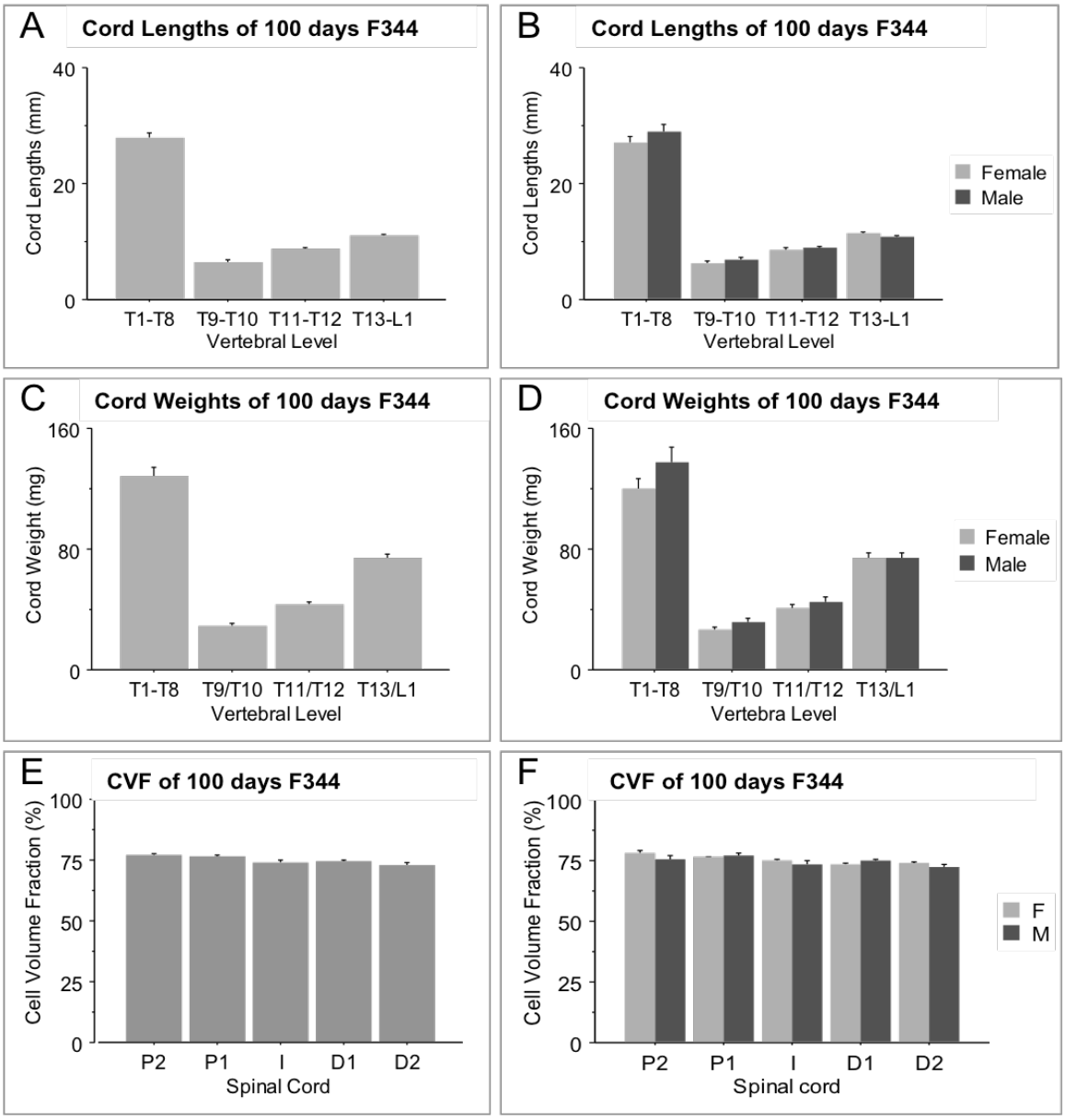

Figure 2. Spinal cord size of 100 days F344 rats.

A shows spinal cord length of F344. **B** shows spinal cord length split by gender. **C** shows the cord weight of F344. **D** shows cord weight split by gender. **E** shows cell volume fraction of F344. **F** shows cell volume fraction split by gender. Repeated measures ANOVA indicated cord length, weight and cell volume fractions were not significantly different between male and female F344 rats. n= 8 in **A,C,E;** n=4 in both groups in **B,D,F.** The error bars indicate standard errors of means (SEM).

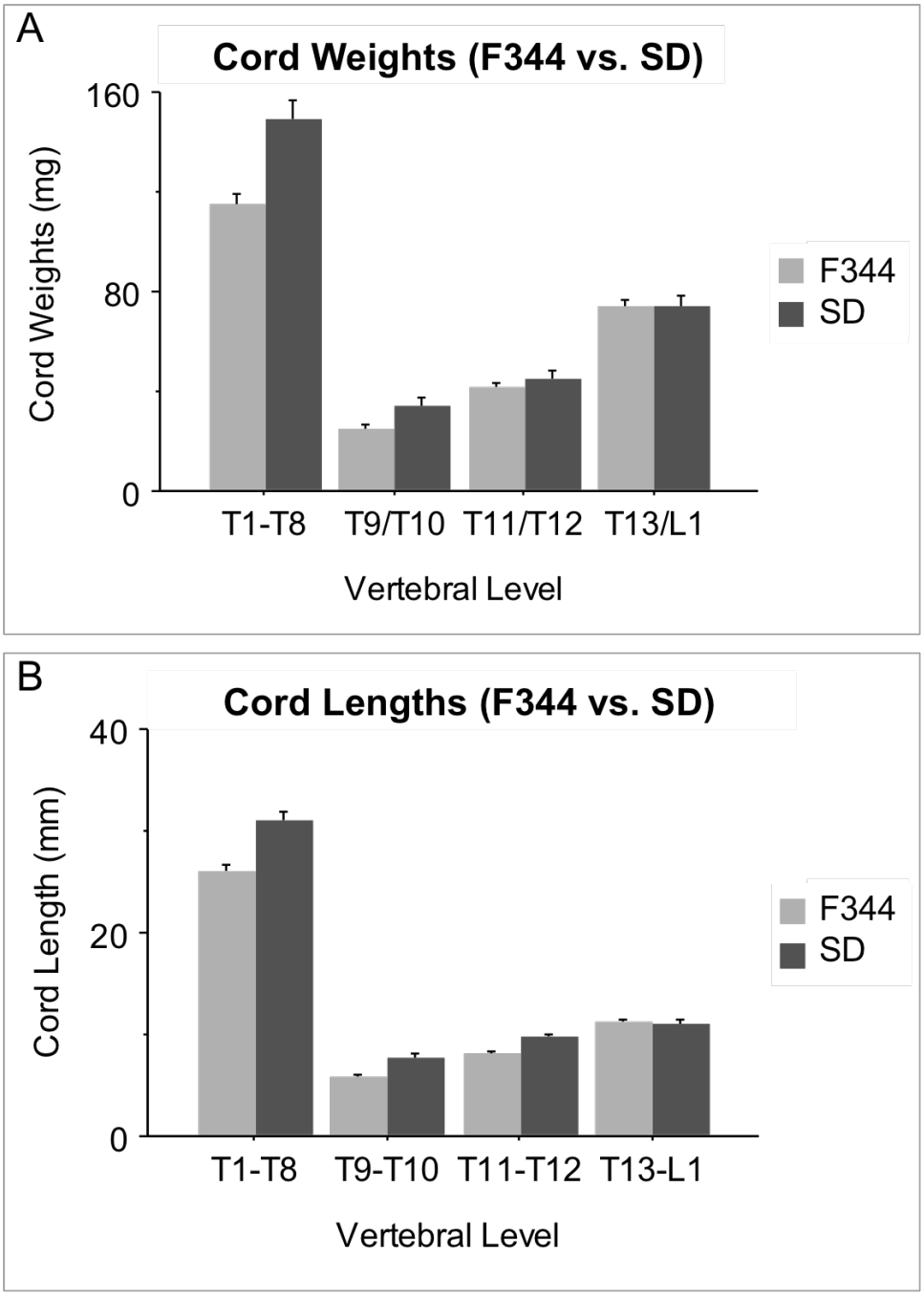

Figure 3. Comparison of cord weight and length between F344 and SD rats.

A shows spinal cord weight in 100 days F344 and 77 days SD rats. **B** shows spinal cord lengths in 100-day old F344 and 77-day old SD rats. Repeated measures ANOVA showed the cord length and weight significantly differed between F344 and SD rats. n=8 in F344; n=5 in SD. The error bars indicated standard errors of means (SEM).

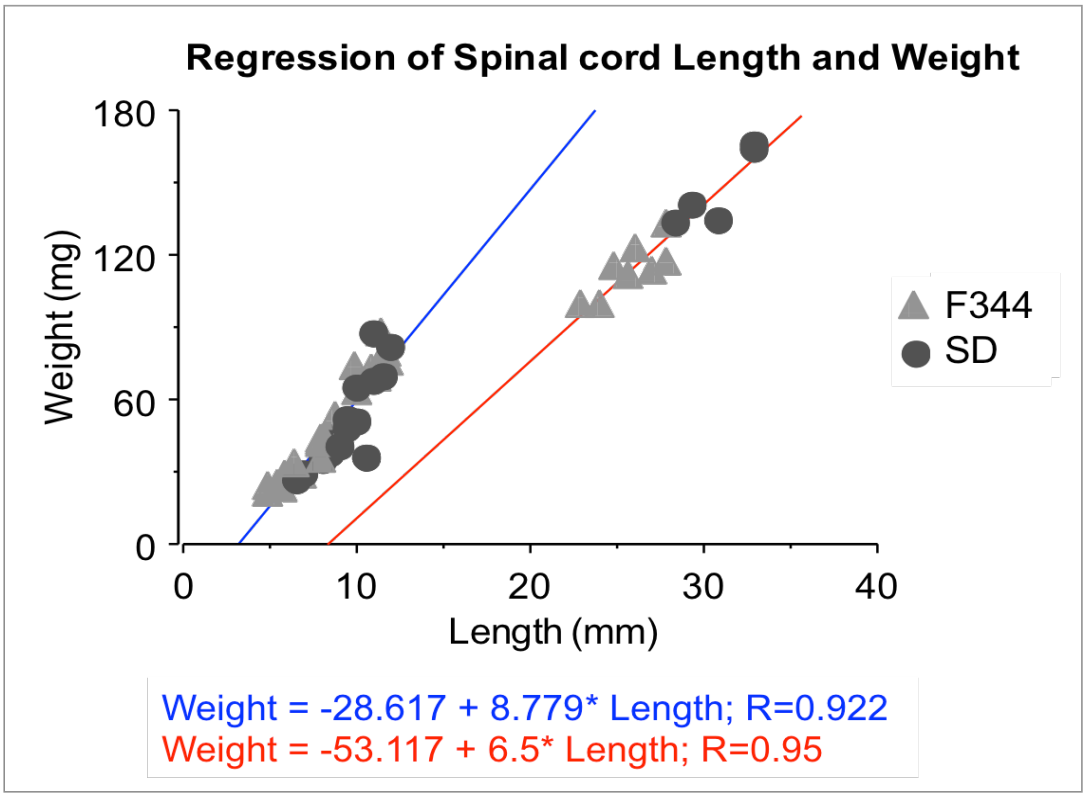

Figure 4. Correlation between spinal cord weight and length.

Triangles indicate F344 rats and dots indicate SD rats. SD and F344 groups have similar point distribution on the same regression lines. T1-T8 and rest of spinal cords including T9/T10, T11/T12, T13/L1 had separate distribution. Two linear regression lines represented different spinal segments. Red line shows the regression in T1-T8 group with correlation coefficient of 0.95 ($p<0.001$). Blue line shows the regression in T9/T10, T11/T12, T13/L1 groups with correlation coefficient of 0.922 ($p<0.001$).

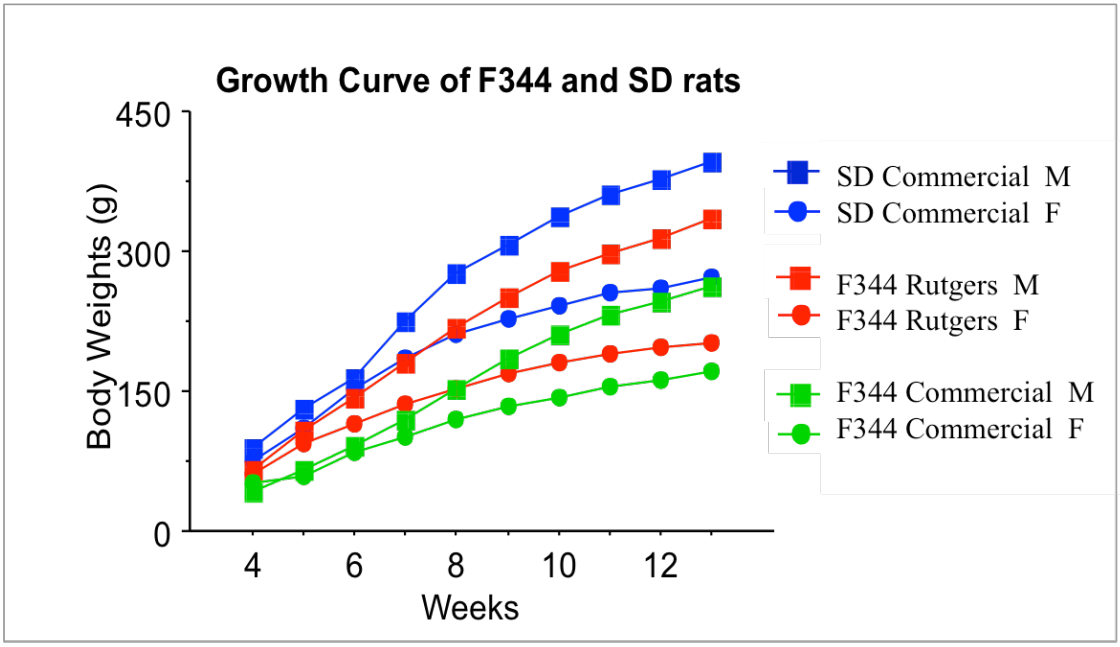

Figure 5. Growth curve of Sprague-Dawley and F344 rats

The blue points indicate SD rats from outside breeder. The red points indicate F344 rats from our local colony. The green points indicated F344 rats from outside breeder. Squares indicate male rats and round dot indicate female rats. The commercial data is from Harlan Laboratories.

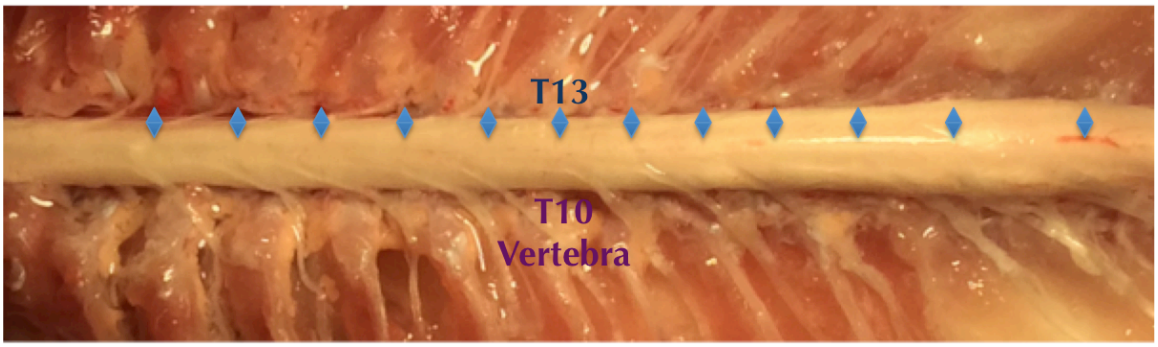

Figure 6. Anatomy of F344 rat's spinal cord

Spinal segments were determined by dorsal roots entry zone. T13 spinal segment is under T9/T10 vertebral interface in the F344 rat, which is identical with other outbred strains.

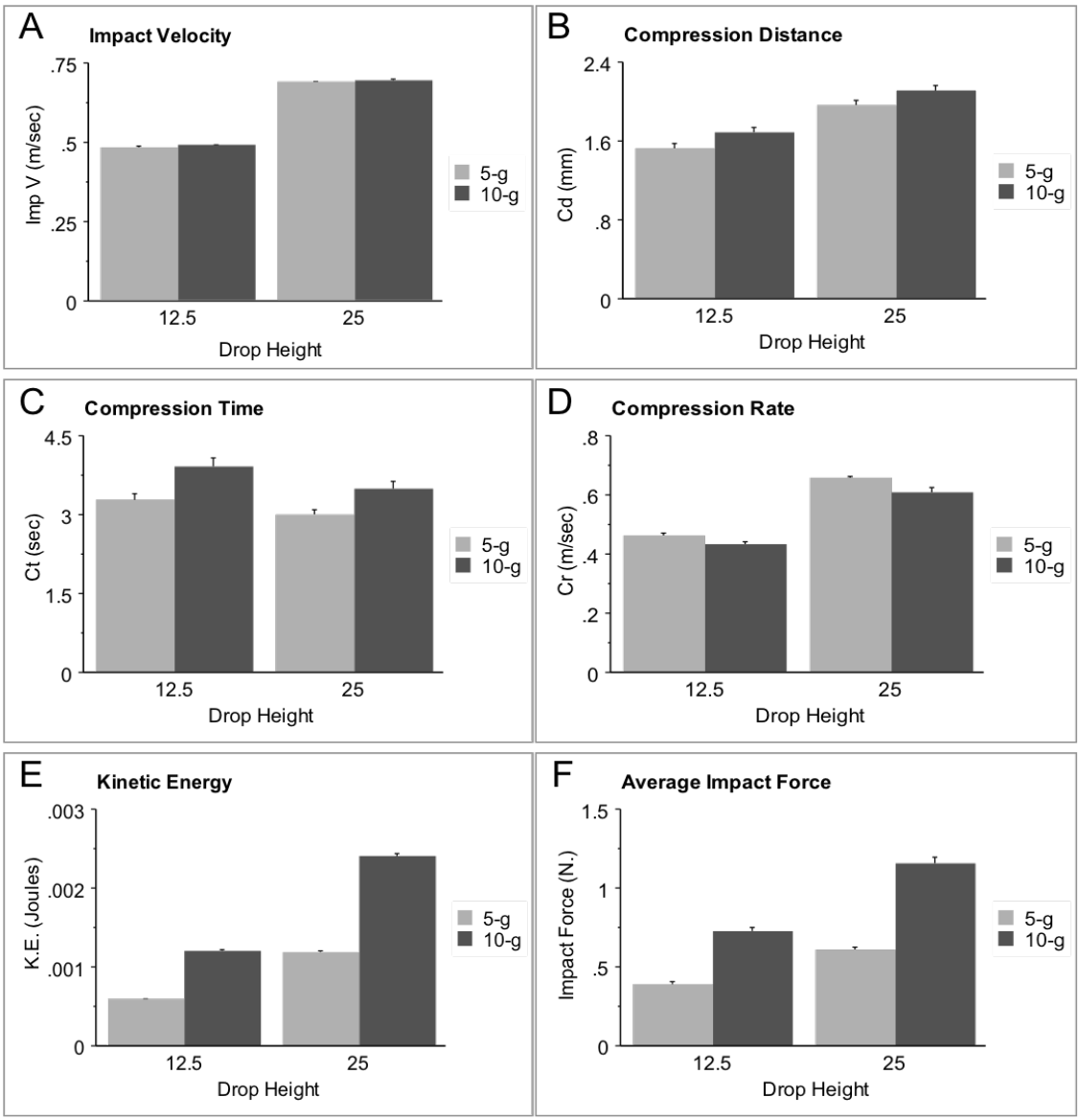

Figure 7. Impact parameters.

A shows impact velocity. **B** shows compression distance (Cd). **C** shows compression time (Ct). **D** shows compression rate (Cr). **E** shows kinetic energy. **F** shows average impact force. All the impact parameters except impact velocity were significant different between different rod weights and drop heights. The impact velocity was different between different drop heights but not with different drop weights. 5-g rod: n=8 in 12.5-mm group; n=9 in 25.0-mm group, 10-g rod: n=12 in 12.5-mm group; n=13 in 25.0-mm group. The error bars indicate standard errors of means (SEM).

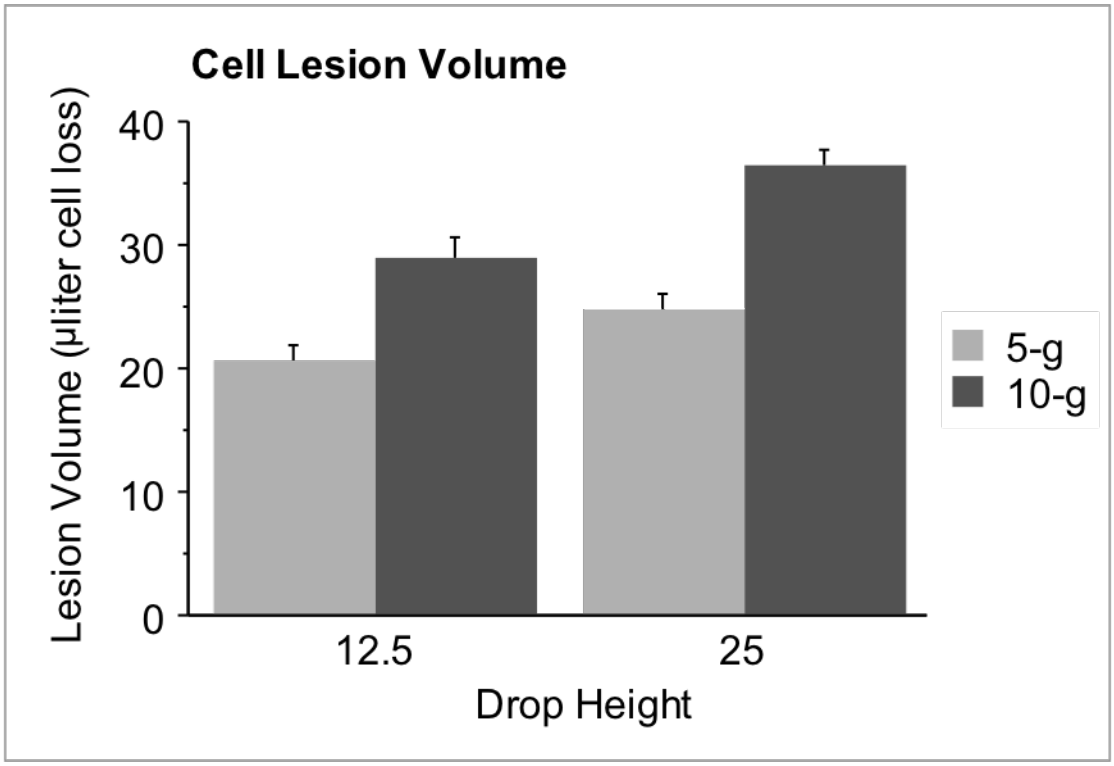

Figure 8. 24-hour lesion volumes.

We estimated primary tissue damage at 24 hours after injury by measurement of tissue sodium (Na) and potassium (K) concentration in extra- and intra- cellular compartments. ANOVA showed significant difference between 12.5- and 25.0-mm drop heights and also between 5-g and 10-g rod weights. 5-g rod: n=8 in 12.5-mm group; n=9 in 25.0-mm group, 10-g rod: n=12 in 12.5-mm group; n=13 in 25.0-mm group. The error bars indicate standard errors of means (SEM).

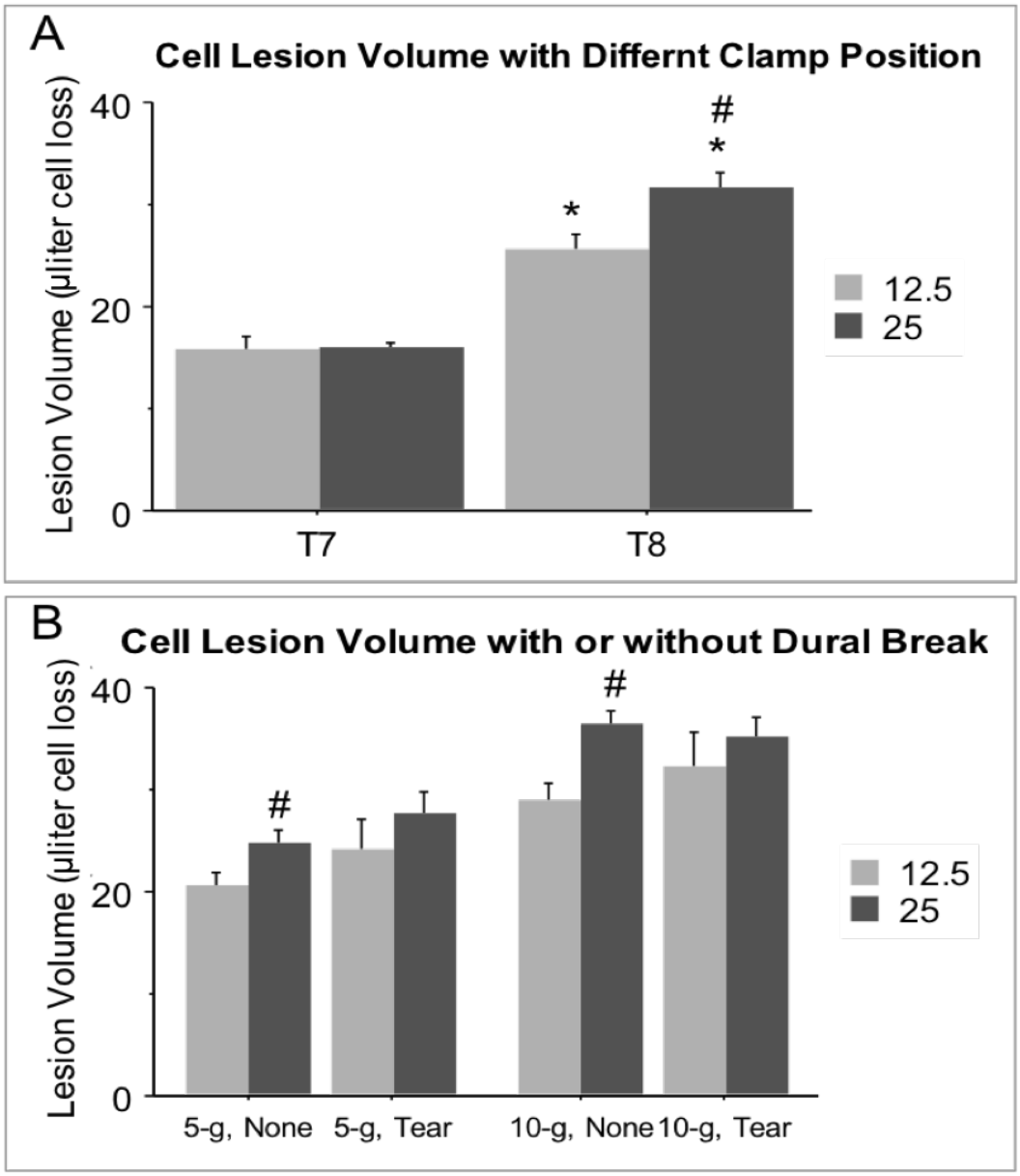

Figure 9. 24-hour lesion volumes with different clamp positions and dural breakage.

A shows mean lesion volume with clamp position at T7 and T8. The data was collected only from 5-g Impactor. T7 group had significantly less injuries than T8 group. Also, 12.5- and 25.0-mm contusions were not significantly different in T7 group. T7: n=5 in 12.5-mm group; n=3 in 25.0-mm group, T8: n=8 in 12.5-mm group; n=9 in 25.0-mm group. **B** shows lesion volumes with and

without dural breakage. Dural breakage did not increase the lesion volumes significantly but it caused non-graded injuries between 12.5- and 25.0-mm contusions. 5-g/None: n=8 in 12.5-mm; n=9 in 25-mm, 5-g/Tear: n=3 in 12.5-mm; n=7 in 25.0-mm, 10-g/None: n=12 in 12.5-mm; n=13 in 25.0-mm, 10-g/Tear: n=5 in 12.5-mm; n=10 in 25.0-mm. The error bars indicate standard errors of means (SEM). * indicates $p<0.05$ vs. T7, # indicates $p<0.05$ vs. 12.5-mm group.

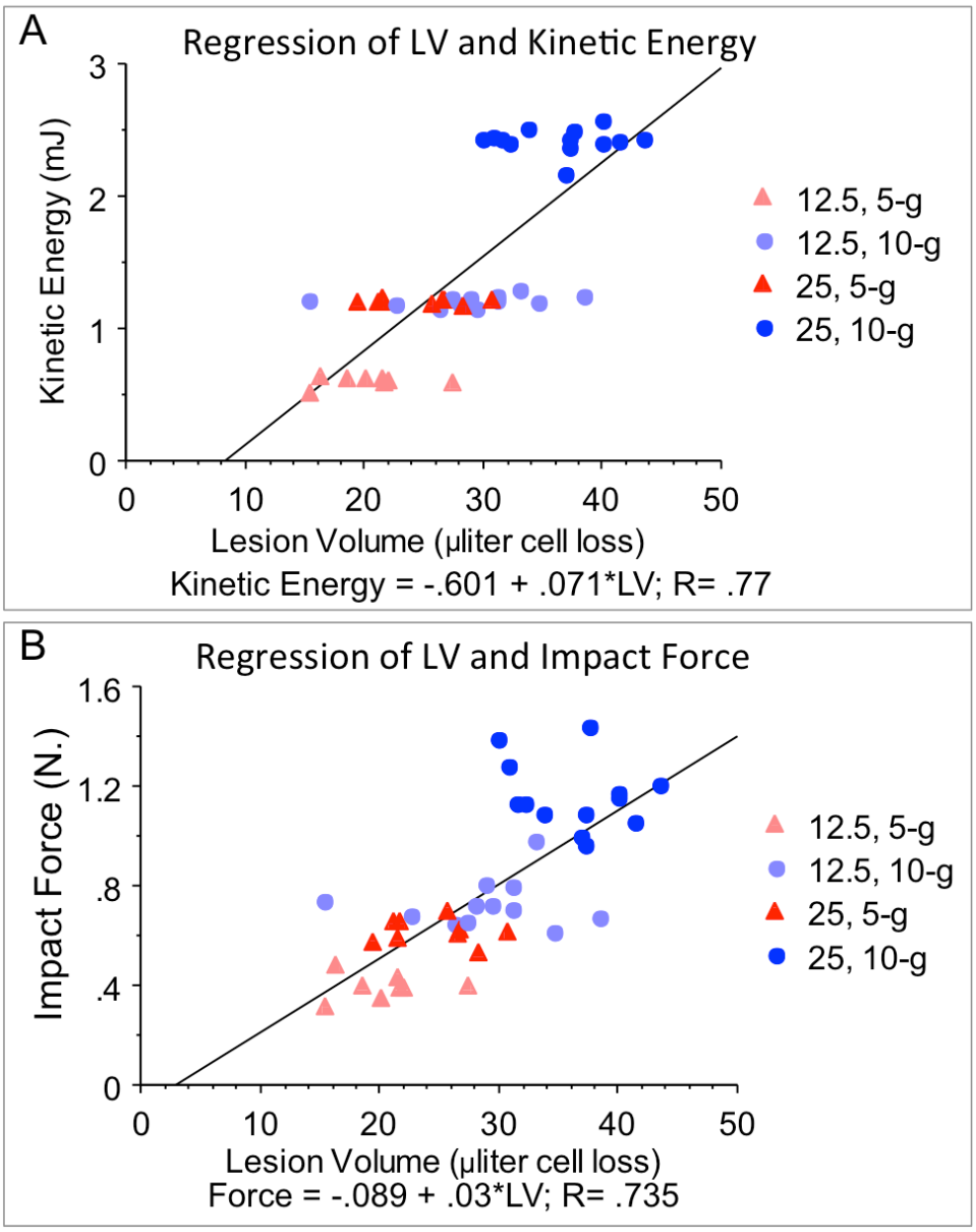

Figure 10. Correlation of lesion volumes vs. kinetic energy and impact force.

A shows regression plot between lesion volume and kinetic energy with a correlation coefficient of 0.77 ($p<0.001$). **B** shows regression plot of lesion volumes vs. average impact force with a correlation coefficient of 0.735 ($p<0.001$).

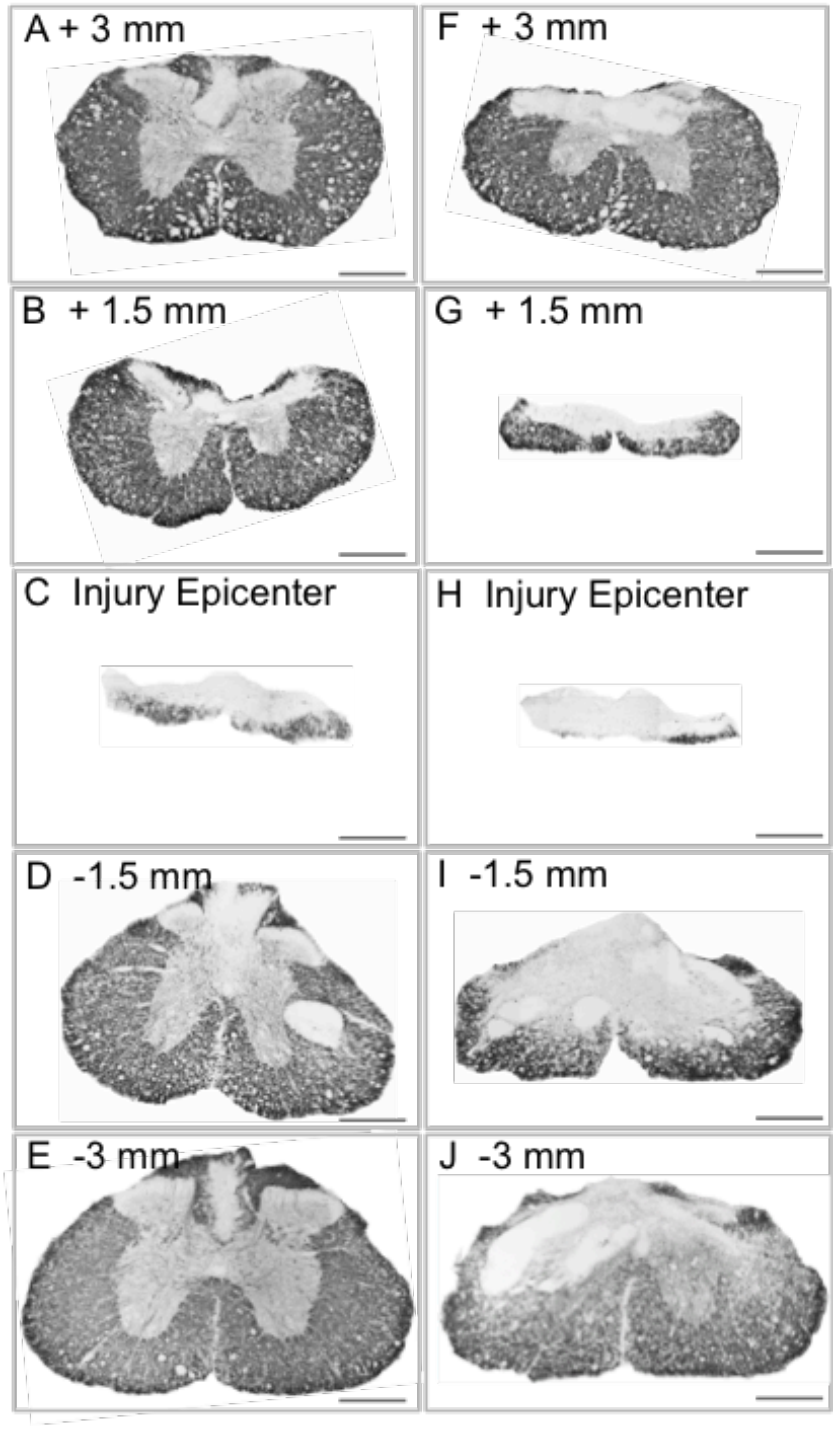

Figure 11. SMI-99 staining of white matter.

A-E show serial cross sections from rostral to caudal spinal cord in 12.5mm group. **F-J** show serial cross section from rostral to caudal spinal cord in 25mm group**.** Scale bar = 500 μm

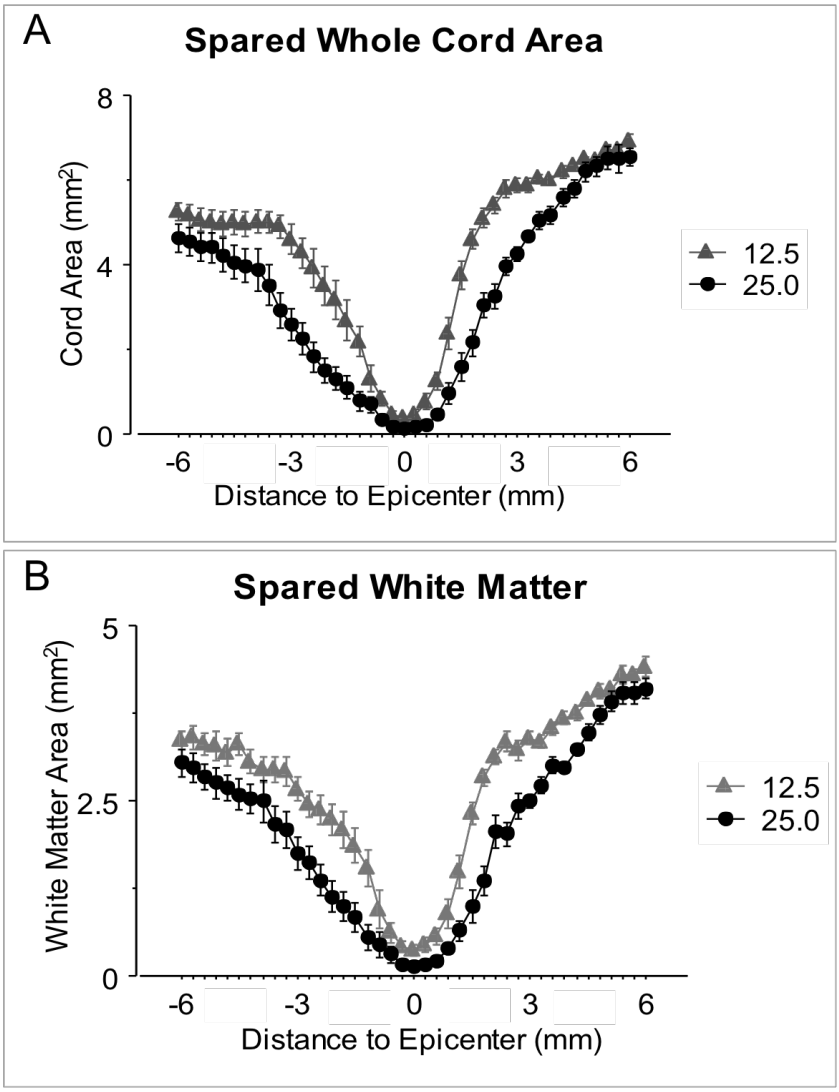

Figure 12. Spared whole cord and white matter.

A, Spared whole cord of ± 6 mm of the injury epicenter in 12.5-mm and 25-mm injury groups. **B,** Spared white matter of ± 6 mm of the injury epicenter in the 12.5-mm and 25-mm injury groups. The error bars indicate standard errors of means (SEM). Spared whole cord and with matter were significantly different between 12.5-mm and 25.0-mm groups. n=5 in12.5-mm; n=7 in 25.0-mm.

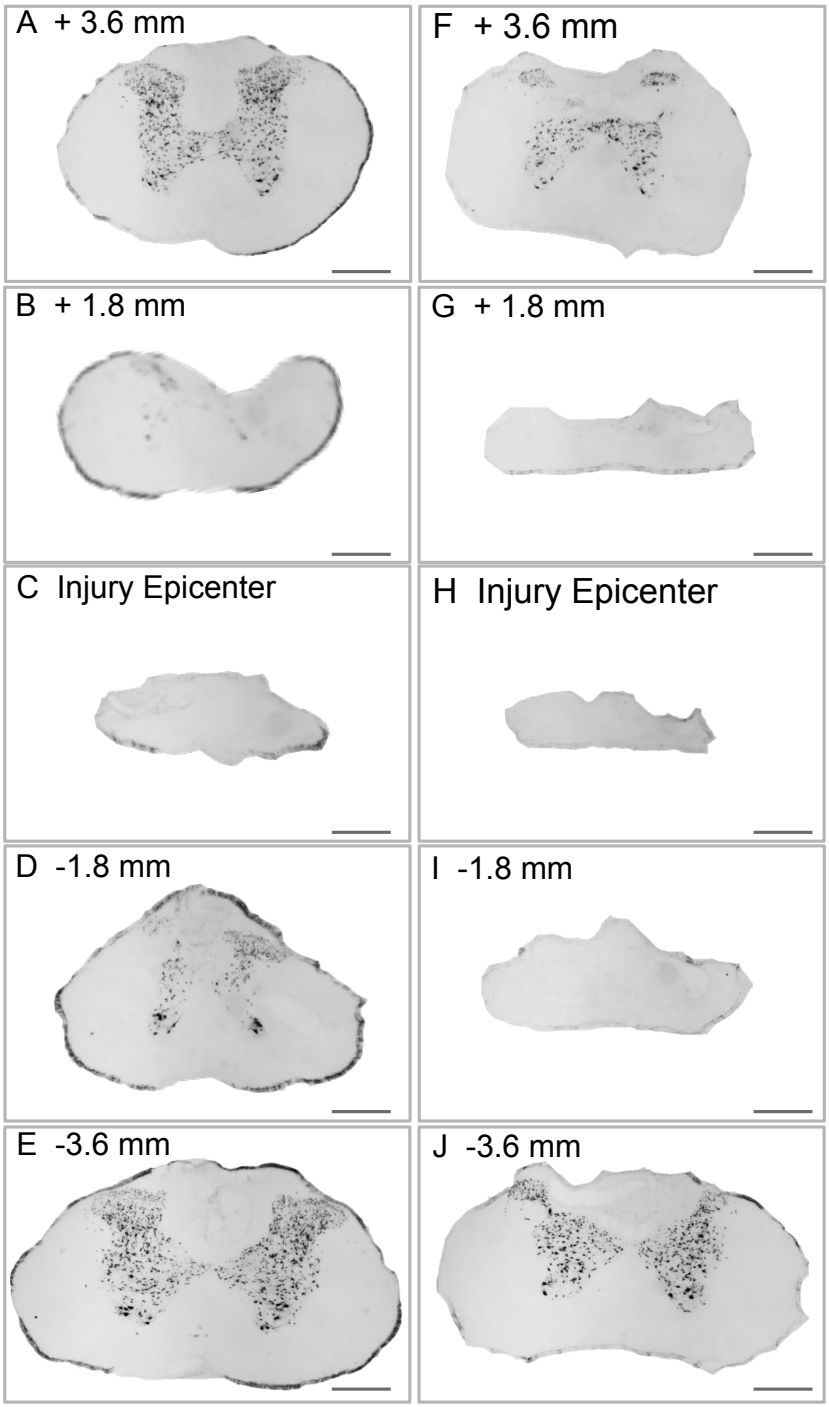

Figure 13. NeuN-stained neurons.

A-E show serial cross sections from rostral to caudal spinal cord in 12.5-mm group. **F-J** show serial cross section from rostral to caudal spinal cord in 25-mm group**.** Scale bar = 500 μm

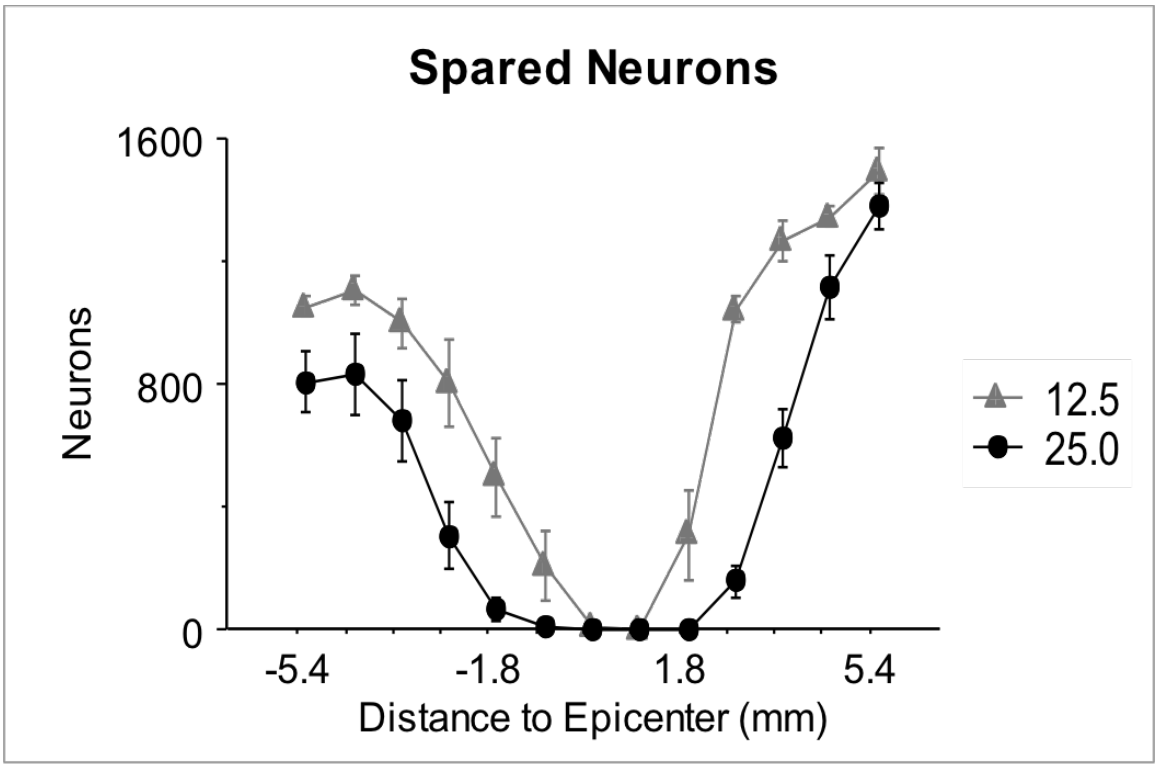

Figure 14. Counts of spared NeuN-stained neurons.

Graph of the numbers of spared neurons of ± 5.4 mm of the injury epicenter in 12.5-mm and 25.0-mm groups. Repeated measures ANOVA indicated significant difference between 12.5- and 25.0-mm groups. n=5 in12.5-mm; n=7 in 25.0-mm.The error bars indicate standard errors of means (SEM).

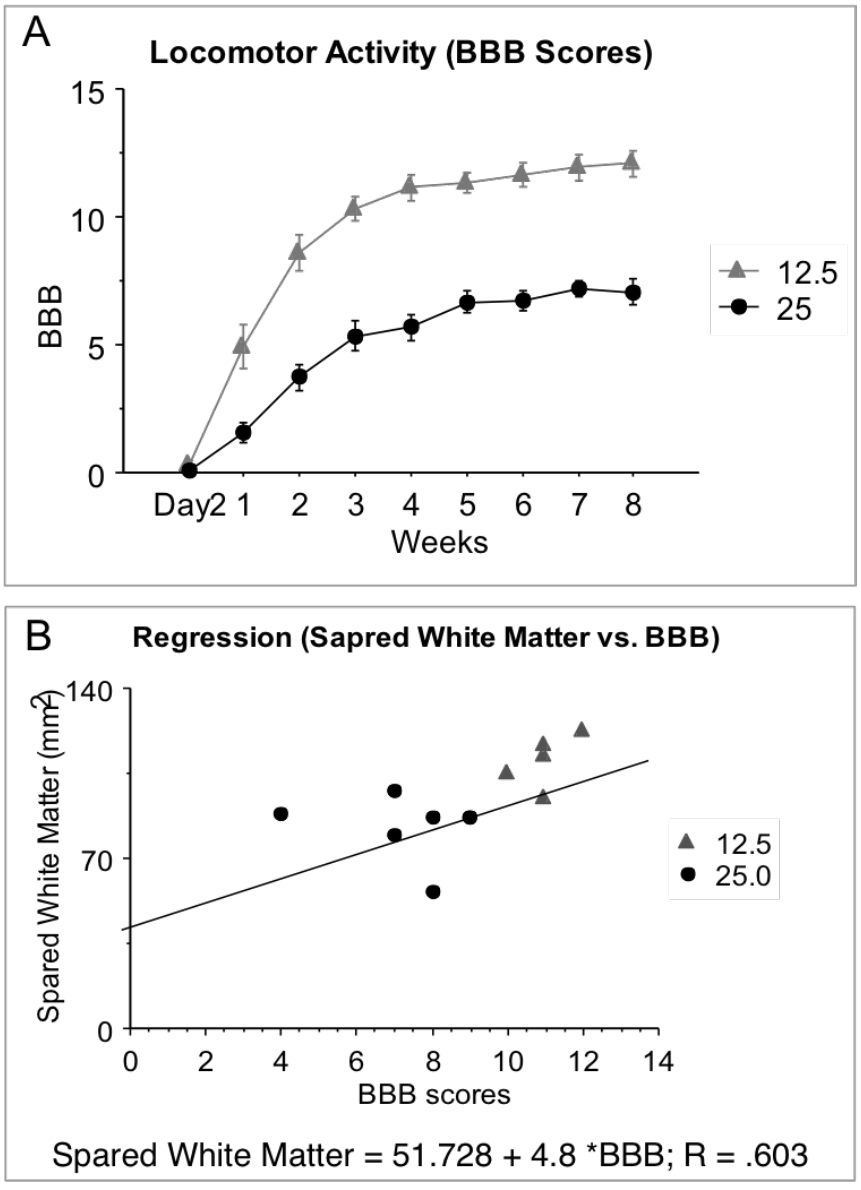

Figure 15. Locomotor behavior and correlation between BBB and spared white matter.

A shows locomotor performance every week until 8 weeks after SCI. BBB scores statistically differed between 12.5- and 25.0-mm groups. n=14 in 12.5-mm; n=15 in 25.0-mm. **B** shows the regression plot between spared white matter and BBB scores with a correlation coefficient of 0.603 (p=0.038). The error bars indicate standard errors of means (SEM)

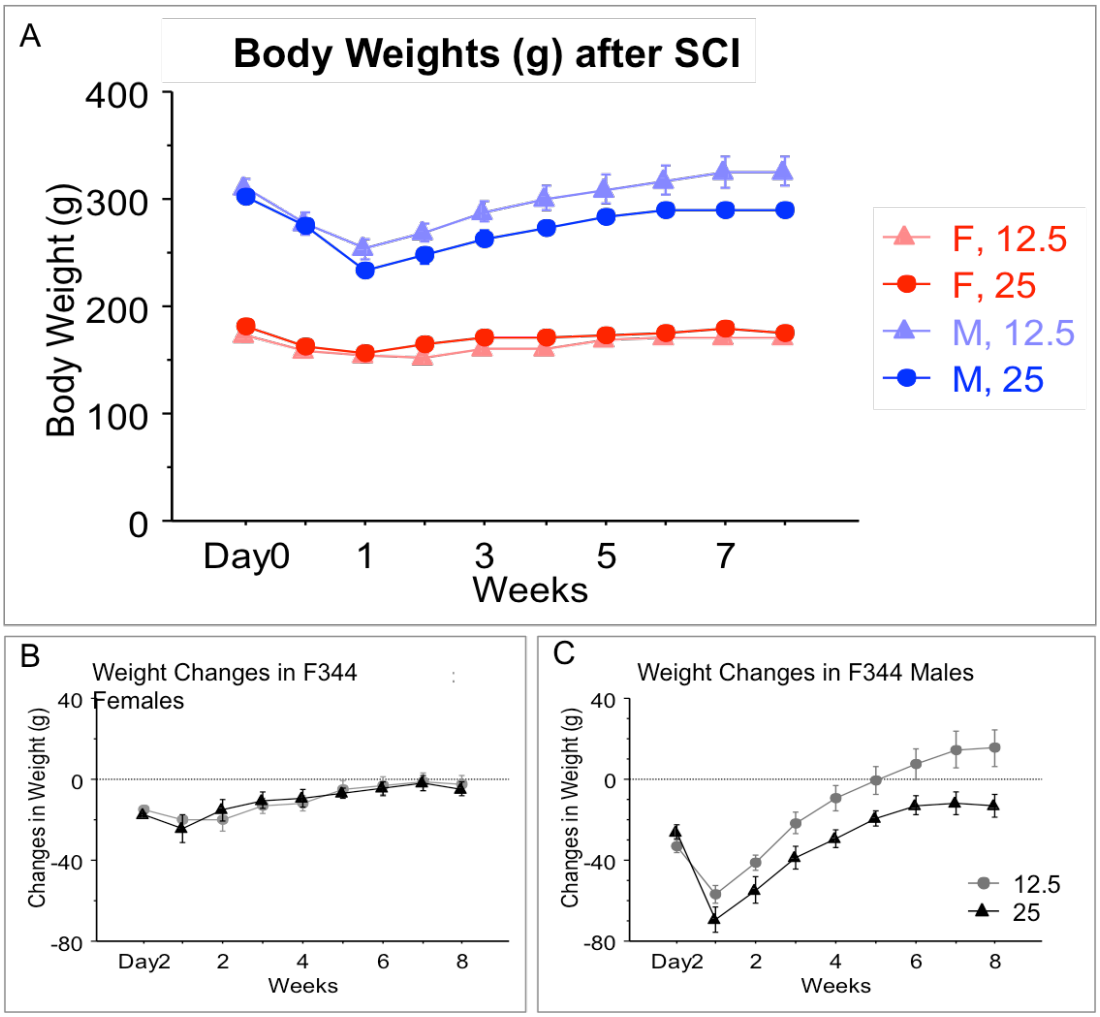

Figure 16. Body weights after SCI and weight changes over time.

A shows the mean body weight of spinal injured F344 rats. The triangles indicate 12.5-mm and dots indicate 25.0-mm group. Red and pink indicate Female rats and blue and light blue indicate male rats. Body weights were significantly different between male and female F344 rats. **B** shows the weight changes in female F344 rats after SCI. **C** shows weight changes in male F344 rats after SCI. Wight changes were significantly different between 12.5- and 25.0-mm groups in male F344 rats but not in female F344 rats. Female: n=8 in 12.5-mm; n=7 in 25.0-mm. Male: n=6 in 12.5-mm; n=8 in 25.0-mm. The error bars indicate standard errors of means (SEM).

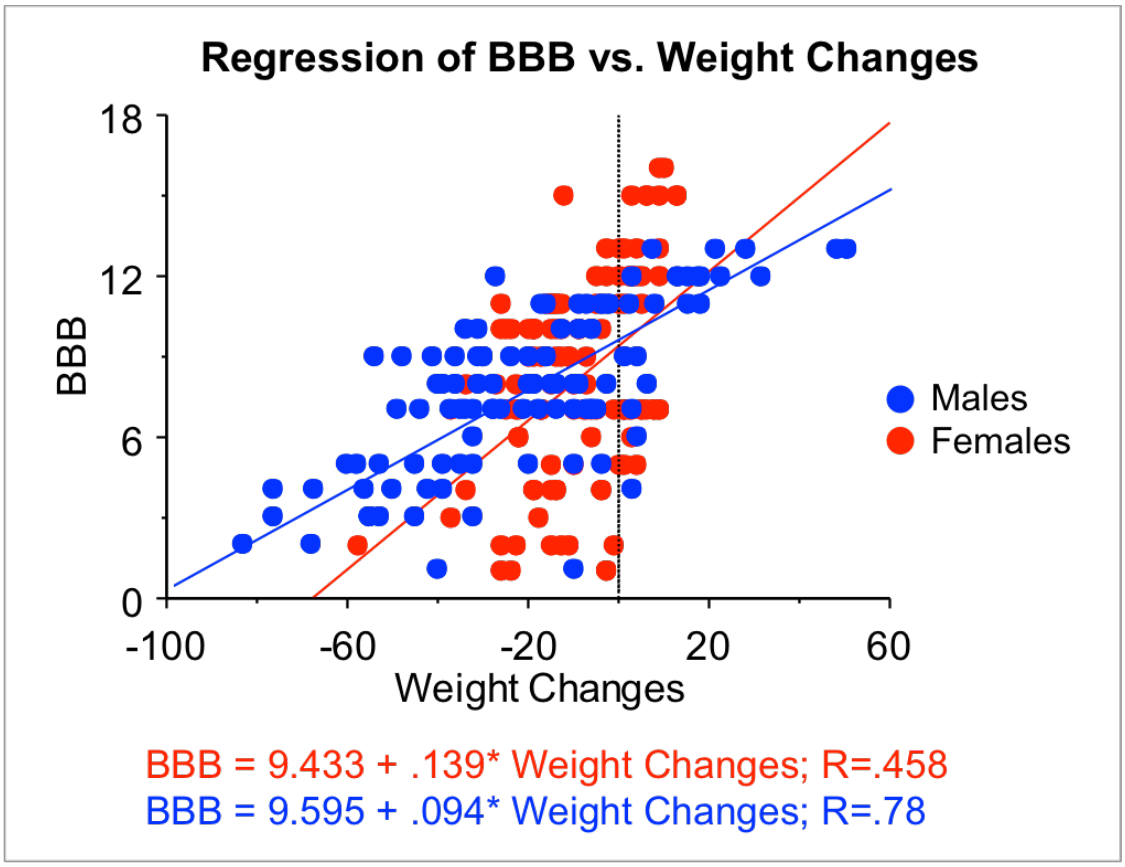

Figure 17. Correlation between BBB scores and weight changes.

Regression analysis showed the behavioral recovery correlated linearly with body weight changes (Female: $p<0.0001$, Male: $p<0.0001$). Blue regression line indicates male rats and red regression line indicates female rats

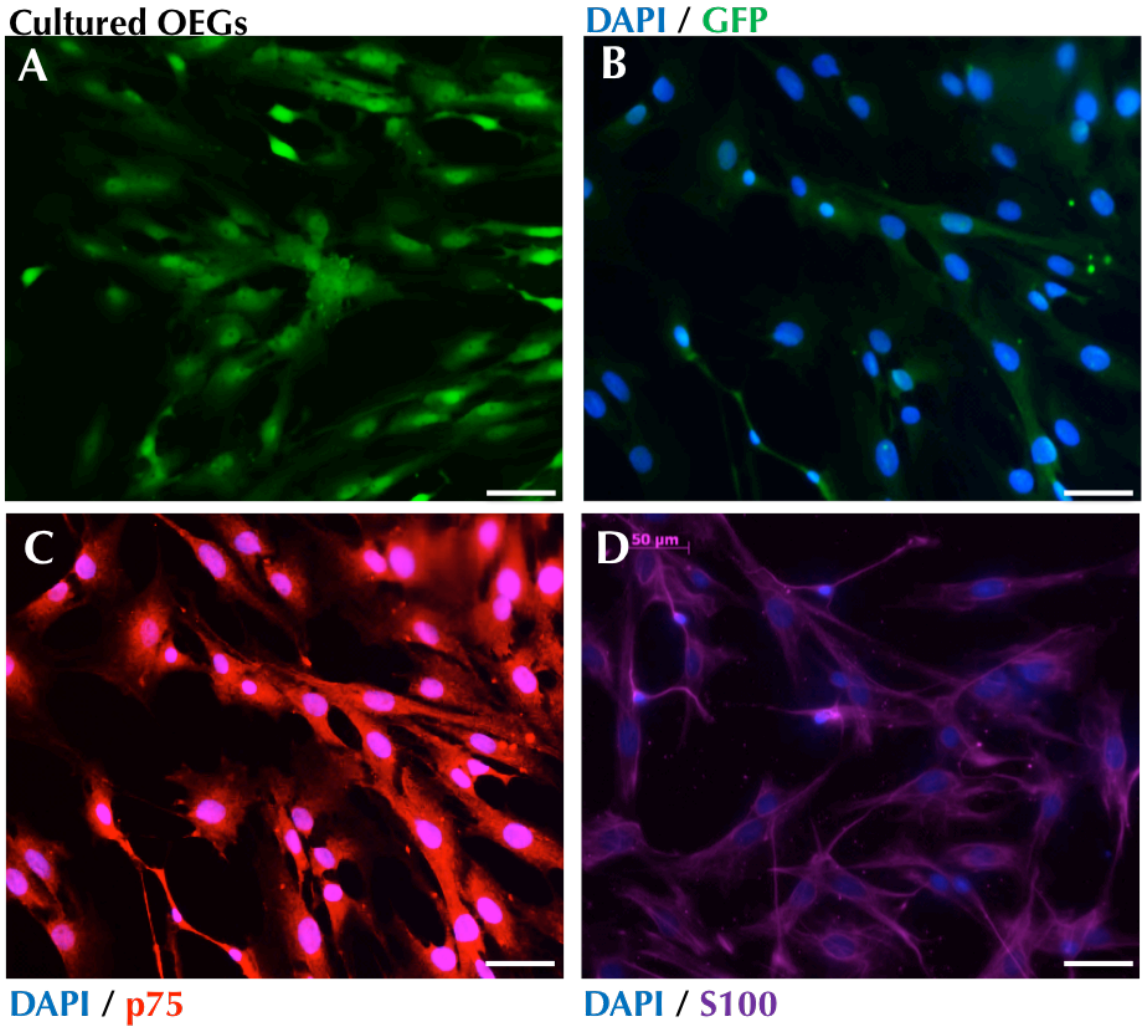

Figure 18. Primary olfactory ensheathing glial (OEG) cell culture

A, Living OEG cells show strong green fluorescence. **B**, Fixed OEG cells with nuclei stain (blue). **C**, Cultured OEG cells express p75 (red) in nuclei and cytoplasm. **D**, OEG also express S100 (purple) in cytoplasm. Bar = 50 μm

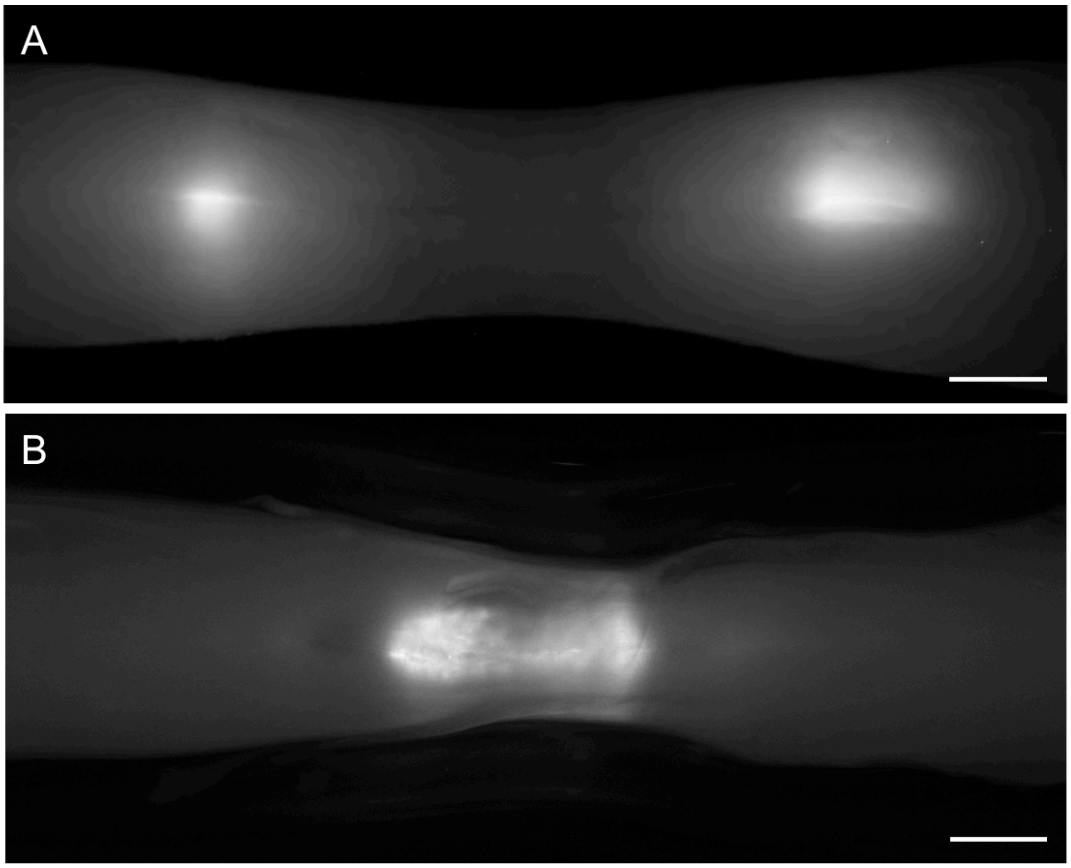

Figure 19. OEG survival in injured F344 spinal cords.

We transplanted OEG cells isolated from green fluorescent protein (GFP) F344-pups into wild-type F344 spinal cord after 12.5-mm weight drop injuries. By 8 weeks post injury, OEG still survived and GFP OEG grafts can be visualized in fixed whole mounted cord at 8 weeks (**A**) and 16 weeks (**B**), using an epifluorescent dissecting microscope. Rostral cord is to the left. Bar = 1 mm.

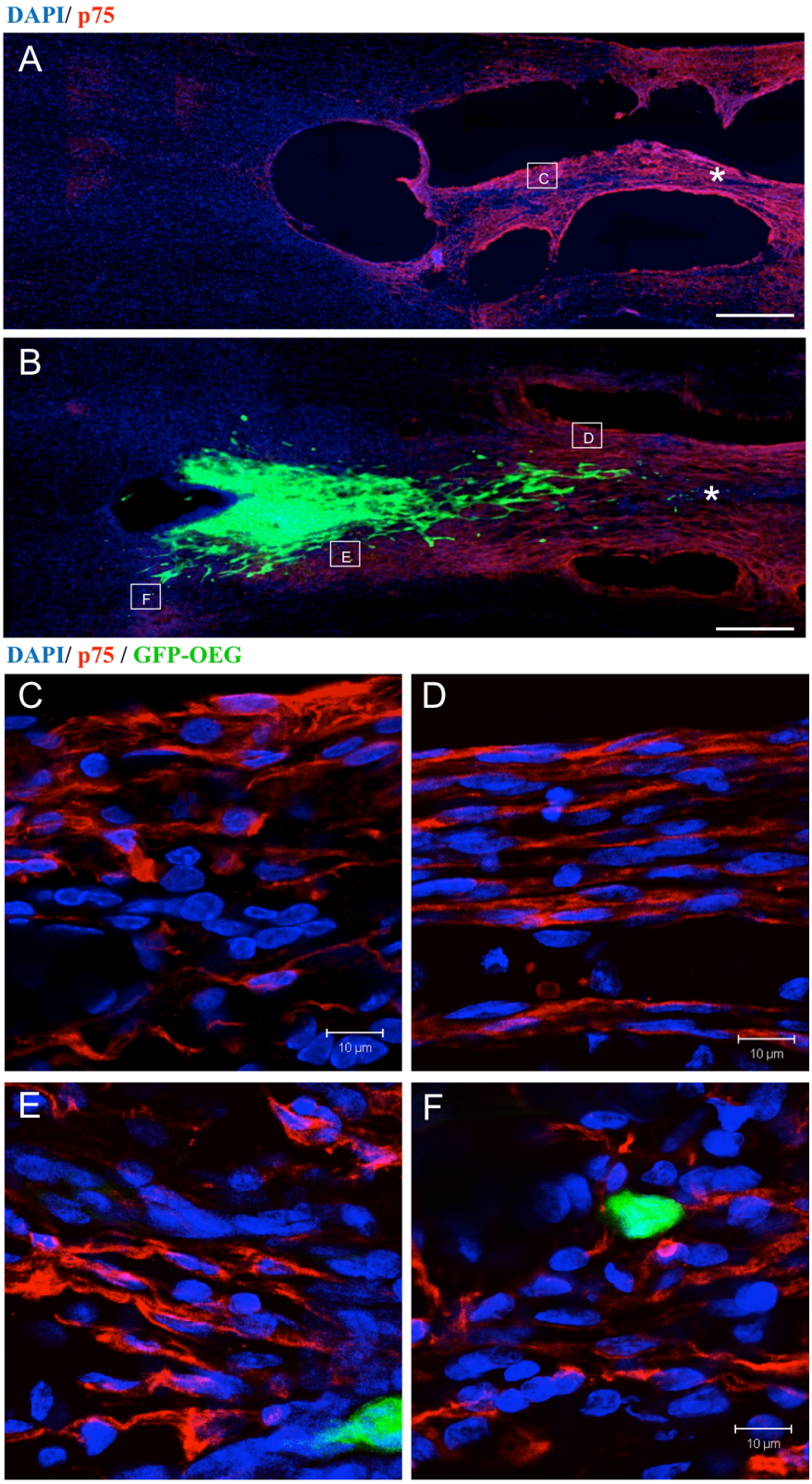

Figure 20. Endogenous Schwann cells invaded into the injured spinal cord.

A, In control rats (not transplanted) many p75 positive (red) endogenous Schwann cells are localized in the SCI site at 8 weeks. **B**, In OEG transplanted group, most of grafted OEG (green) were p75 negative. Many Schwann cells (red) are present at the injury site, where they appear to migrate toward grafted OEG (green). The asterisk (*) indicates epicenter of injury site. Bar = 0.5mm **(A, B**). **C.** A magnified image of panel **A**. **D, E, F** Magnified images of panel **B**. Bar = 10 μm **(C-F)**

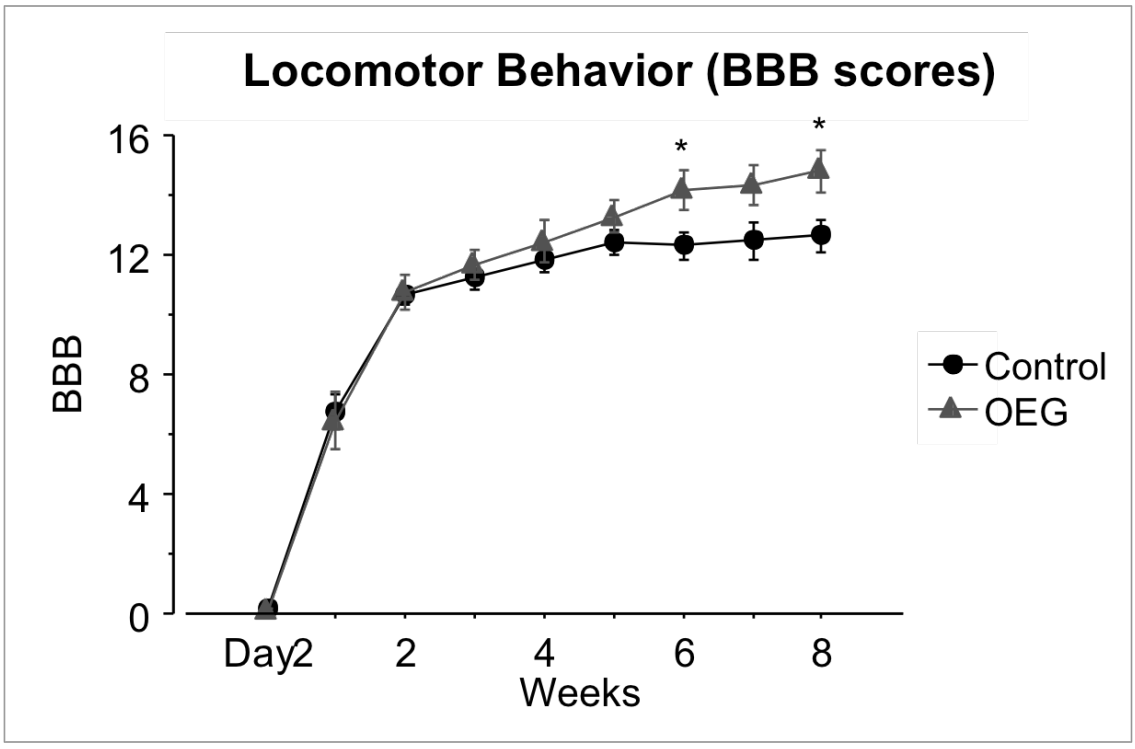

Figure 21. Locomotor behavior.

The figure shows BBB scores of rats with saline (Control) and OEG (OEG) transplants right after 12.5-mm weight drop injury. OEG group had significantly functional improvement in 6 weeks ($p=0.0249$) and 8 weeks ($p=0.0218$). n=17 in control; n=11 in OEG. The error bars indicate standard errors of means (SEM). * indicates $p<0.05$ vs. control.

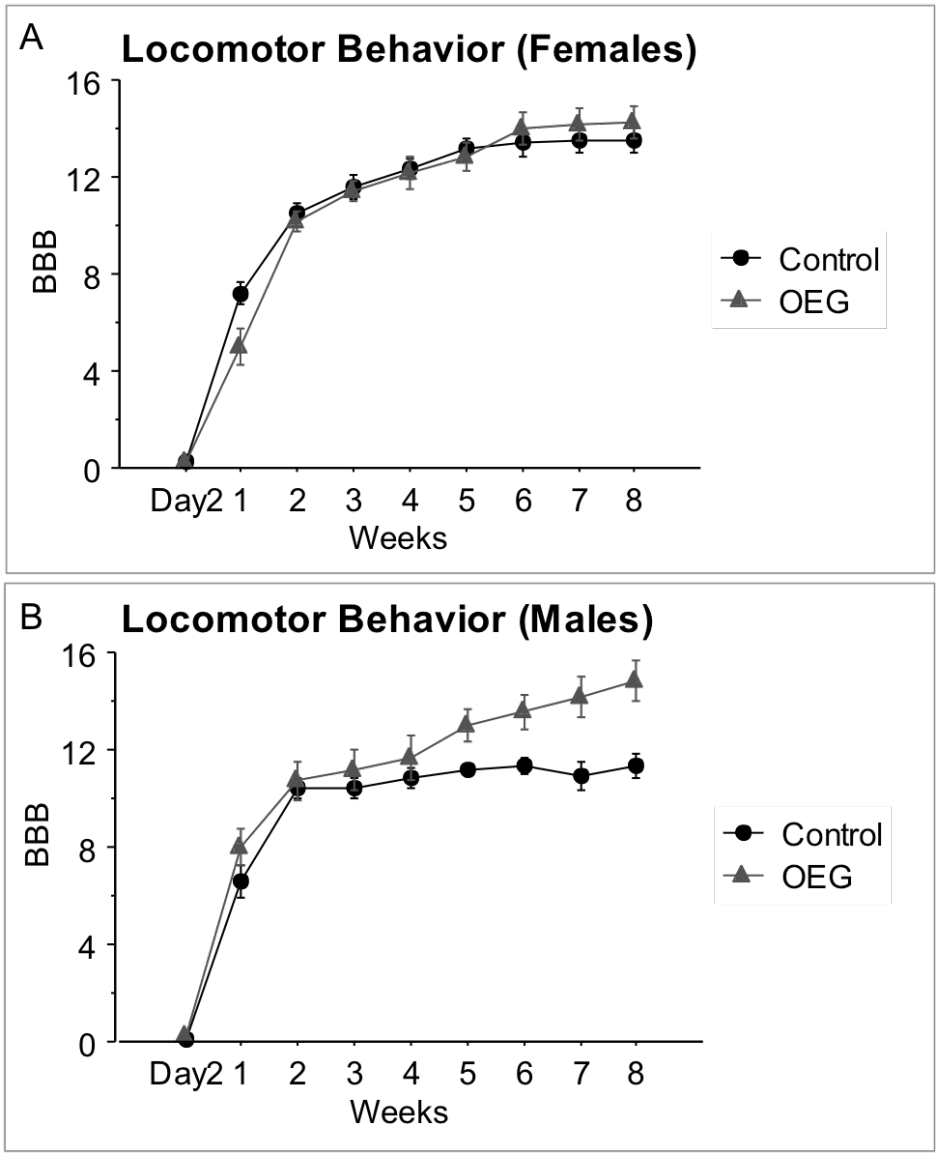

Figure 22. Locomotor behavior splitting by gender.

A shows the time course of BBB scores in female F344 rats. n=9 in control; n=6 in OEG. **B** shows the time course of BBB scores in male F344 rats. Repeated measures ANOVA showed significant difference between control and OEG treated group only in male F344 rats. n=8 in control; n=5 in OEG. The error bars indicate standard errors of means (SEM).

A

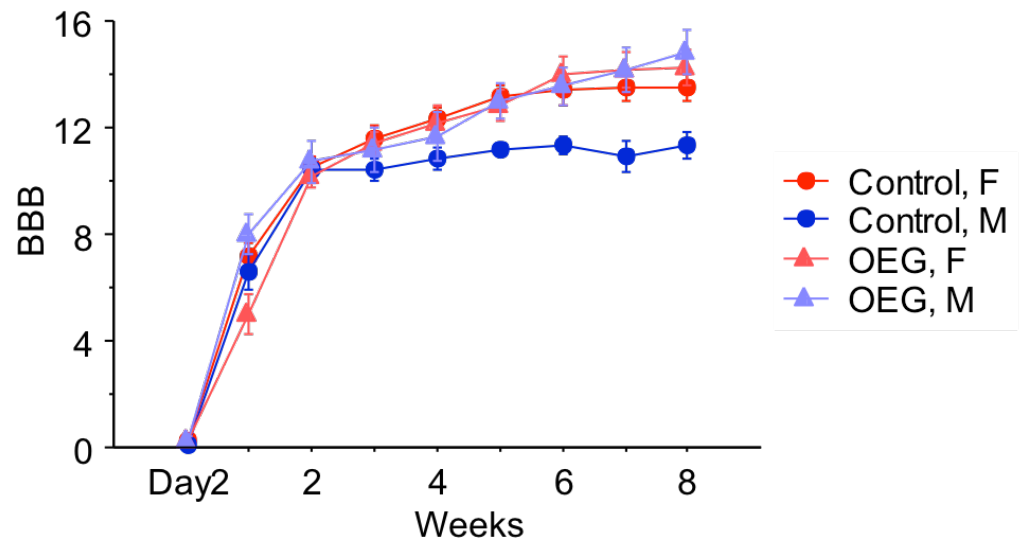

B

ANOVA table of locomotor behavior

	DF	Sum of Squares	Mean Square	F-Value	P-Value	Lambda	Power
Gender	1	0.973	0.973	0.048	0.8279	0.048	0.055
Cell	1	51.940	51.940	2.579	0.1214	2.579	0.323
Gender * Cell	1	102.351	102.351	5.083	0.0336	5.083	0.574
Subject(Group)	24	483.303	20.138				
Category for BBB	8	4174.675	521.834	372.240	<0.0001	2977.917	1.000
Category for BBB * Gender	8	37.569	4.696	3.350	0.0013	26.799	0.978
Category for BBB * Cell	8	46.480	5.810	4.144	0.0001	33.155	0.995
Category for BBB * Gender ...	8	30.234	3.779	2.696	0.0078	21.567	0.932
Category for BBB * Subject(...	192	269.160	1.402				

Figure 23. Locomotor behavior in different genders and treatments.

A, Graph shows the BBB scores in different treatment groups (Control and OEG) and different genders (M and F). Females: n=9 in control; n=6 in OEG, Males: n=8 in control; n=5 in OEG. **B,** ANOVA table of locomotor behavior. Repeated measures ANOVA showed no difference between genders and treatments but interactive effect between gender and treatment is significant.

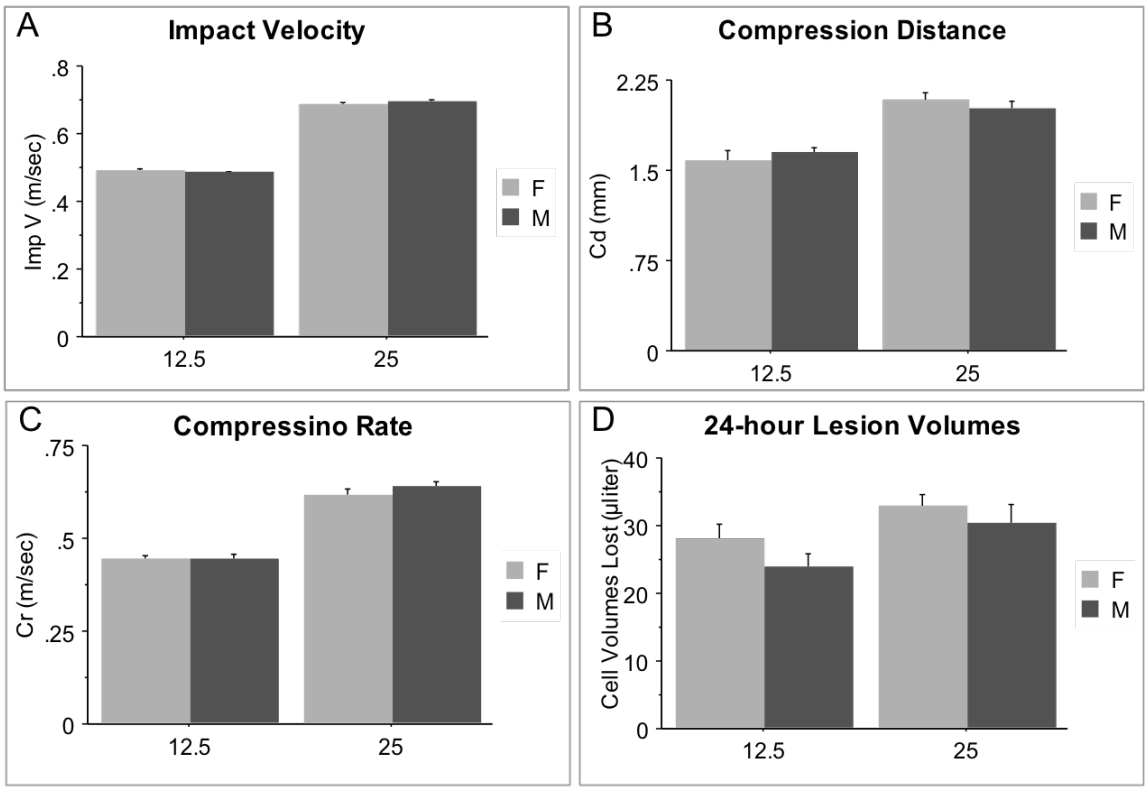

Figure 24. Contusion parameters spilt by gender.

The figures show contusion parameters including impact velocity (**A**), compression distance (**B**), compression rate (**C**), and 24-hr lesion volumes (**D**) splitting by gender. All contusion parameters were not significantly different between male and female F344 rats. 12.5-mm: n=6 in male; n=4 in female, 25.0-mm: n=6 in male; n=7 in female. The error bars indicate standard errors of means (SEM).

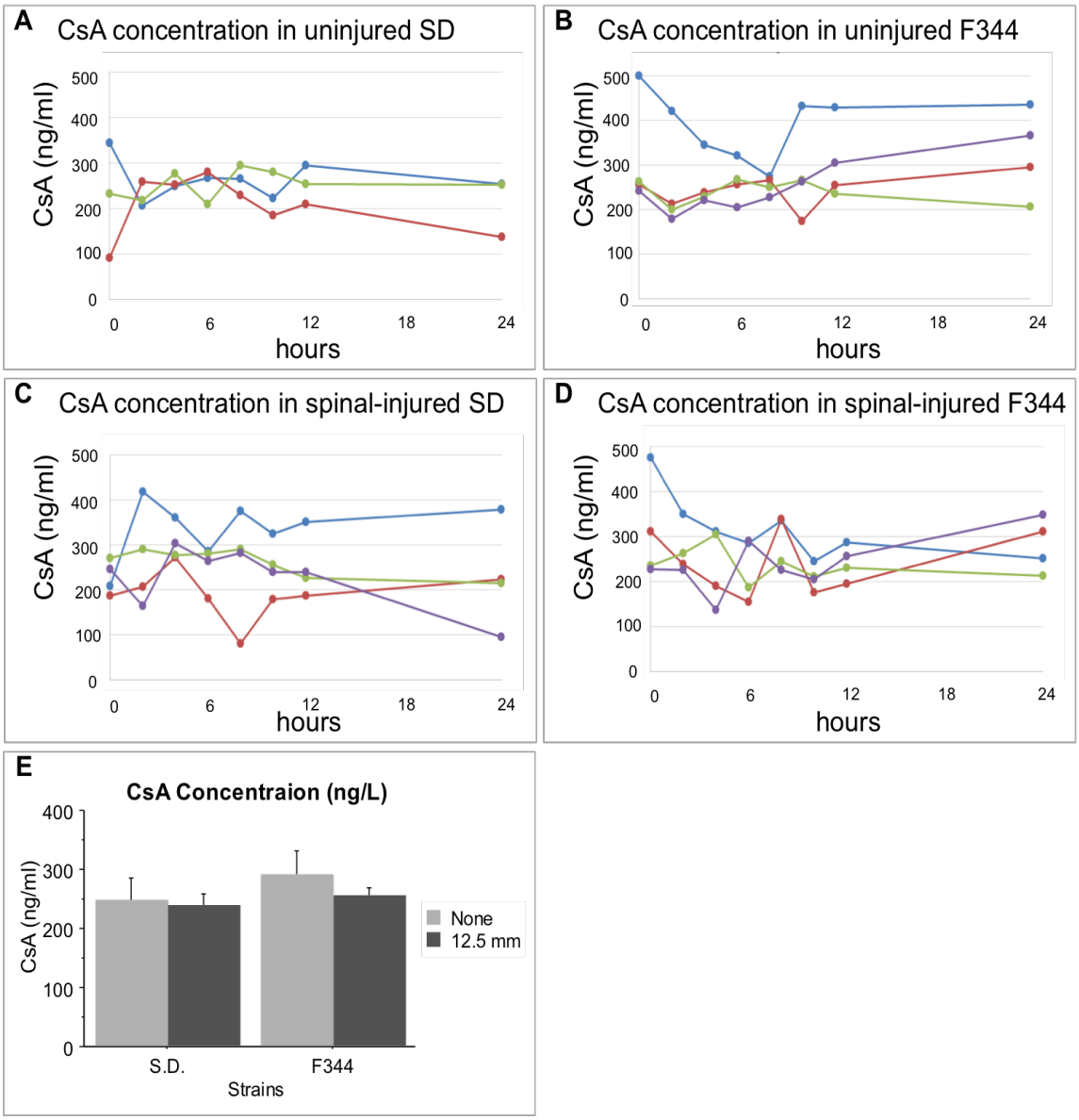

Figure 25. CsA concentration in blood level over 24 hours.

Blood samples were collected for eight time points over the span of 24-hr from uninjured (Sham) and spinal cord injured (12.5-mm) rats. SD rats were treated with 10 mg/kg/day CsA and F344 rats were injected 2 mg/kg/day CsA. In **A-D**, each line indicates CsA concentration over 24 hours in individual rats. **E** shows average CsA concentration at steady state. CsA concentrations were similar between SD and F344 rats regardless of SCI. SD: n=4 in sham; n=3 in 12.5-mm, F344: n=4 in sham; n=4 in 12.5-mm. The error bars indicate standard errors of means (SEM).

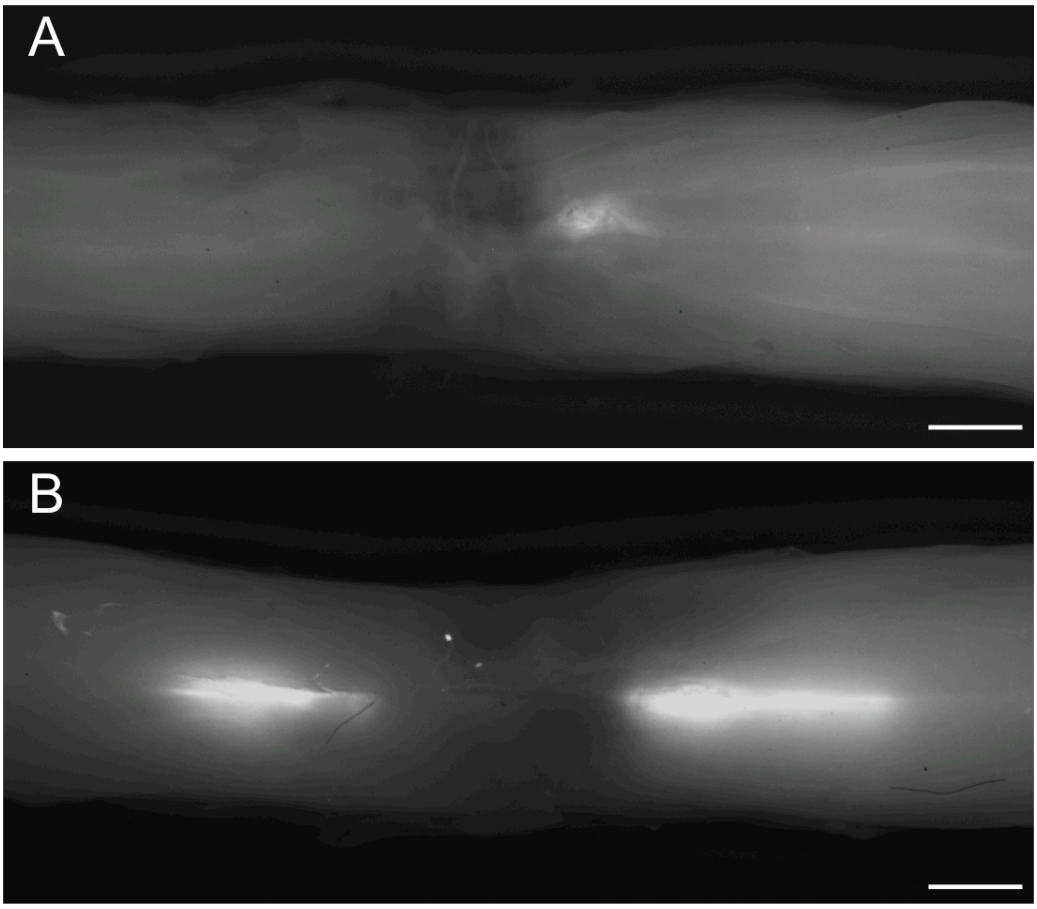

Figure 26. Sprague-Dawley OEG survival in F344 spinal cords.

OEG cells isolated from SD GFP-pups were transplanted into F344 spinal cord after 12.5-mm weight drop injuries. By 8 weeks post injury, OEG still survived in F344 rats with 2 mg/kg/day CsA injection. GFP OEG grafts can be visualized in fixed whole mounted cord by dorsal (**A**) and ventral sites (**B**), using an epifluorescent dissecting microscope. Rostral cord is to the left. Bar = 1 mm.

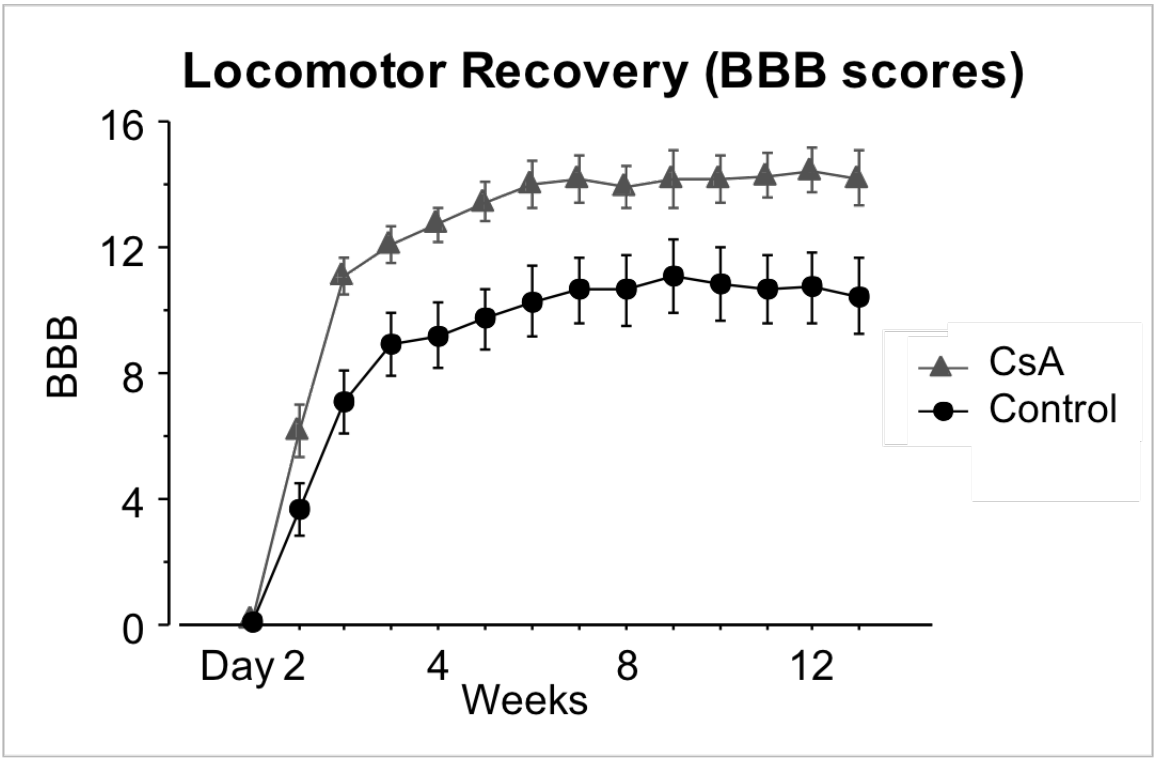

Figure 27. Locomotor behavior.

The figure demonstrates hindlimb activity from day 2 to 13 weeks post injury. Control group were injected saline daily until 6 weeks. CsA group were injected 2 mg/kg/day CsA for 6 weeks. BBB scores significant differed between control and CsA groups. n=11 in control; n=11 in CsA. The error bars indicate standard errors of means (SEM).

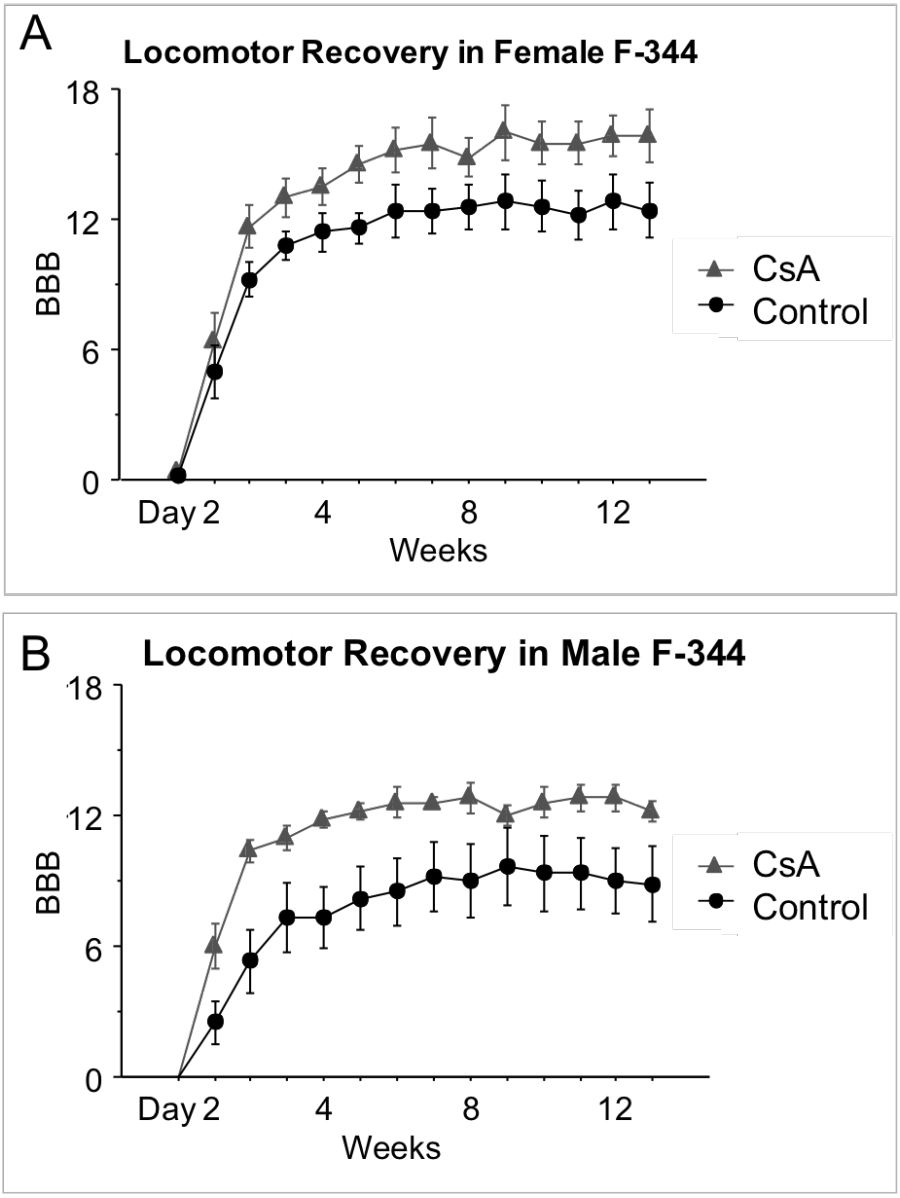

Figure 28. Locomotor behavior splitting by gender.

A shows the time course of BBB scores in females. n=5 in control; n=6 in CsA. **B** shows the time course of BBB scores in males. The F344 rats were injected saline (Control) or 2 mg/kg CsA (CsA) daily for 6 weeks. No significant difference was shown between control and CsA in both male and female F344 rats. n=6 in control; n=5 in CsA. The error bars indicate standard errors of means (SEM).

A

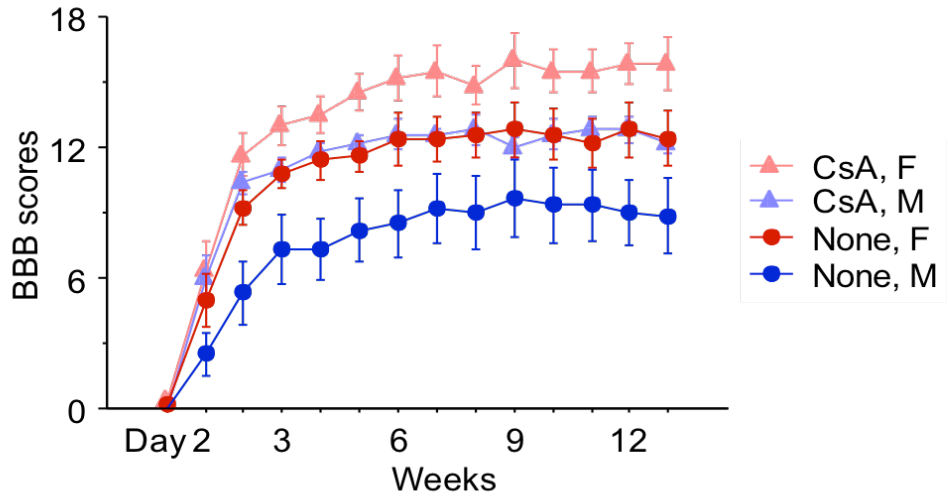

B

ANOVA table of locomotor behavior

	DF	Sum of Squares	Mean Square	F-Value	P-Value	Lambda	Power
gender	1	571.516	571.516	7.529	0.0133	7.529	0.744
Rx	1	677.490	677.490	8.925	0.0079	8.925	0.818
gender * Rx	1	16.971	16.971	0.224	0.6420	0.224	0.073
Subject(Group)	18	1366.357	75.909				
Weeks	13	3737.880	287.529	175.773	<0.0001	2285.053	1.000
Weeks * gender	13	56.136	4.318	2.640	0.0018	34.317	0.987
Weeks * Rx	13	57.980	4.460	2.727	0.0013	35.445	0.990
Weeks * gender * Rx	13	18.971	1.459	0.892	0.5621	11.597	0.537
Weeks * Subject(Group)	234	382.776	1.636				

Figure 29. Locomotor behavior in different genders and treatments.

A, Graph shows the BBB scores in different treatment groups (Control and CsA) and different genders (M and F). Female: n=5 in control, n=6 in CsA; Male: n=6 in control; n=5 CsA. **B,** ANOVA table of locomotor behavior. Repeated measures ANOVA showed significant difference between genders and treatments but no significant interactive effect between gender and treatment.

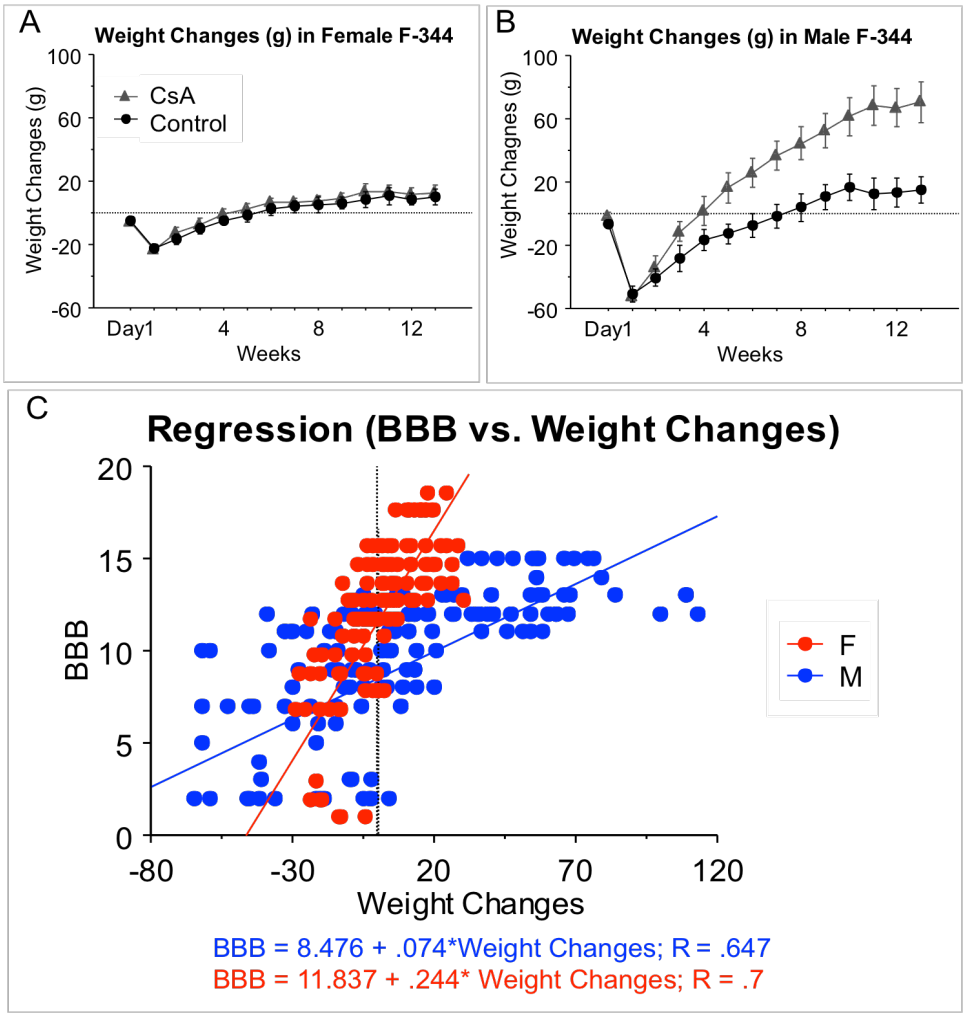

Figure 30. Weight changes and the correlation between weight changes and BBB scores.

A shows the weight changes in female F344 rats after SCI with saline (Control) or 2 mg/kg/day CsA (CsA) sc injection. n=5 in control; n=6 in CsA **B** shows weight changes in male F344 rats after SCI with saline (Control) or 2 mg/kg/day CsA (CsA) sc injection. n=6 in control; n=5 in CsA. The error bars indicate standard errors of means (SEM). Weight changes statistically differed between control and CsA groups in males but not in females. **C** shows regression plot of BBB scores vs. weight changes.

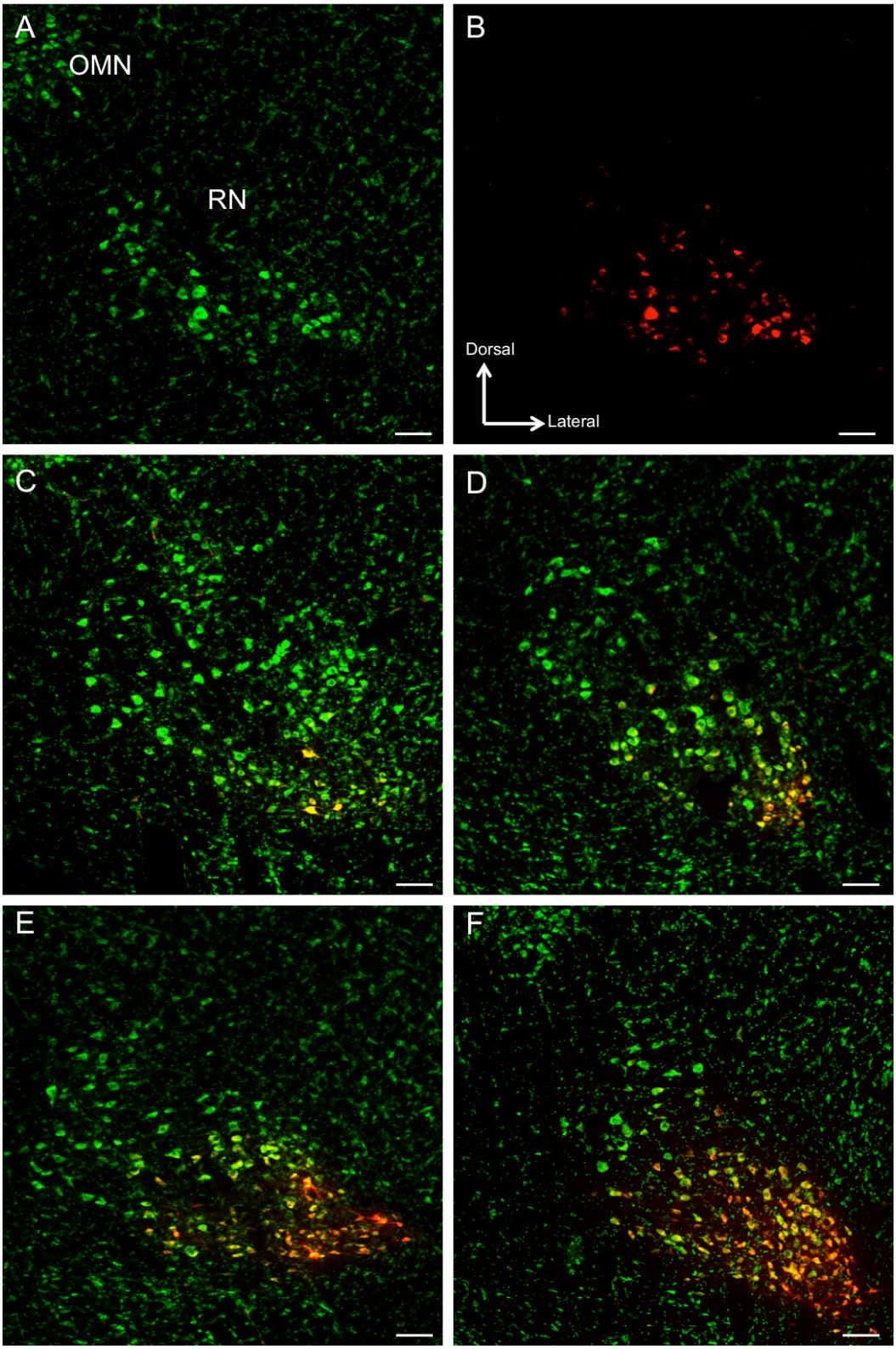

Figure 31. Fluorogold (FG)-labeled neurons in red nuclei.

A shows morphology of red nucleus and oculomotor nucleus in midbrain which was labeled by fluorescent Nissl stain. **B** shows fluorogold-labeled neurons in red nuclei. **C** shows FG-labeled neurons in male control group. **D** shows FG-labeled neurons in female control group. **E** shows FG-labeled neurons in male CsA group. **F** shows FG-labeled neurons in male CsA group. Bar=25 μm.

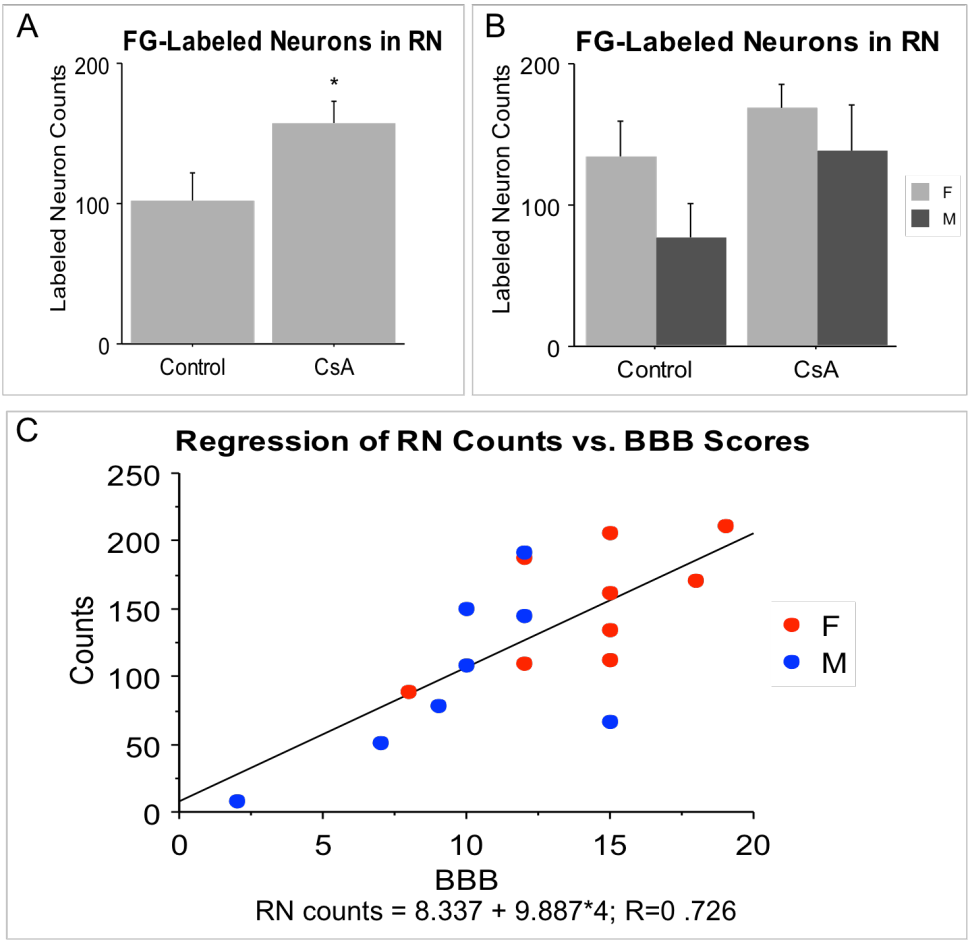

Figure 32. Total counts of FG-labeled neurons in red nuclei and the correlation between cell counts and BBB scores.

A, Graph of the numbers of FG-labeled neurons in control and CsA groups. CsA groups had statistically more FG-labeled neurons than control group. n=9 in control; n=8 in CsA. **B,** Graph of the numbers of FG-labeled neurons in control and CsA groups splitting by gender. For FG-labeled neurons, no significantly difference was shown between male and female F344 rats. Female: n=4 in control; n=5 in CsA, Male: n=5 in control; n=3 in CsA. **C** shows the regression plot between FG-labeled neurons and BBB scores with a correlation coefficient of 0.726 (p=0.0015). * indicates $p<0.05$ vs. control. The error bars indicate standard errors of means (SEM).

REFERENCES

1. S. L. Carlson, M. E. Parrish, J. E. Springer, K. Doty, L. Dossett, Acute inflammatory response in spinal cord following impact injury. *Experimental neurology* **151**, 77-88 (1998).
2. A. R. Blight, W. Young, Central axons in injured cat spinal cord recover electrophysiological function following remyelination by Schwann cells. *Journal of the neurological sciences* **91**, 15-34 (1989).
3. M. S. Beattie *et al.*, Endogenous repair after spinal cord contusion injuries in the rat. *Experimental neurology* **148**, 453-463 (1997).
4. L. Noble, J. R. Wrathall, Spinal cord contusion in the rat: morphometric analyses of alterations in the spinal cord. *Experimental neurology* **88**, 135-149 (1985).
5. L. Noble, J. R. Wrathall, An inexpensive apparatus for producing graded spinal cord contusive injury in the rat. *Experimental neurology* **95**, 530-533 (1987).
6. W. Marcol *et al.*, Air gun impactor--a novel model of graded white matter spinal cord injury in rodents. *Journal of reconstructive microsurgery* **28**, 561-568 (2012).
7. S. Somerson, B. Stokes, Functional analysis of an electromechanical spinal cord injury device. *Experimental neurology* **96**, 82-96 (1987).
8. M. S. BEATTIE, Anatomic and behavioral outcome after spinal cord injury produced by a displacement controlled impact device. *Journal of neurotrauma* **9**, 157-160 (1992).
9. S. Kwo, W. Young, V. Decrescito, Spinal cord sodium, potassium, calcium, and water concentration changes in rats after graded contusion injury. *Journal of neurotrauma* **6**, 13-24 (1989).
10. J. A. Gruner, A monitored contusion model of spinal cord injury in the rat. *Journal of neurotrauma* **9**, 123-126; discussion 126-128 (1992).
11. W. Young, Spinal cord contusion models. *Prog Brain Res* **137**, 231-255 (2002).
12. S. W. Scheff, A. G. Rabchevsky, I. Fugaccia, J. A. Main, J. E. Lumpp, Jr., Experimental modeling of spinal cord injury: characterization of a force-defined injury device. *Journal of neurotrauma* **20**, 179-193 (2003).
13. W. L. Maxwell, Histopathological changes at central nodes of Ranvier after stretch-injury. *Microsc Res Tech* **34**, 522-535 (1996).
14. T. A. Gennarelli *et al.*, Traumatic damage to the nodal axolemma: an early, secondary injury. *Acta neurochirurgica. Supplementum* **57**, 49-52 (1993).
15. S. Constantini, W. Young, The effects of methylprednisolone and the ganglioside GM1 on acute spinal cord injury in rats. *J. Neurosurg.* **80**, 97-111 (1994).
16. D. M. Basso, M. S. Beattie, J. C. Bresnahan, Graded histological and locomotor outcomes after spinal cord contusion using the NYU weight-drop device versus transection. *Experimental neurology* **139**, 244-256 (1996).
17. D. M. Basso, M. S. Beattie, J. C. Bresnahan, A sensitive and reliable locomotor rating scale for open field testing in rats. *Journal of neurotrauma* **12**, 1-21 (1995).
18. A. Ibarra *et al.*, Effects of cyclosporin-A on immune response, tissue protection and motor function of rats subjected to spinal cord injury. *Brain research* **979**, 165-178 (2003).
19. H. Al-Nashash *et al.*, Spinal cord injury detection and monitoring using spectral coherence. *IEEE transactions on bio-medical engineering* **56**, 1971-1979 (2009).

20. T. P. Cameron, R. L. Hickman, M. R. Kornreich, R. E. Tarone, History, survival, and growth patterns of B6C3F1 mice and F344 rats in the National Cancer Institute Carcinogenesis Testing Program. *Fundam Appl Toxicol* **5**, 526-538 (1985).
21. M. F. Festing, Inbred strains should replace outbred stocks in toxicology, safety testing, and drug development. *Toxicologic pathology* **38**, 681-690 (2010).
22. J. Keller, F. Huang, W. Markesbery, Decreased levels of proteasome activity and proteasome expression in aging spinal cord. *Neuroscience* **98**, 149-156 (2000).
23. F. Josef Van Der Staay, A. Blokland, Behavioral differences between outbred Wistar, inbred Fischer 344, brown Norway, and hybrid Fischer 344× brown Norway rats. *Physiology & behavior* **60**, 97-109 (1996).
24. F. H. Gage *et al.*, Survival and differentiation of adult neuronal progenitor cells transplanted to the adult brain. *Proceedings of the National Academy of Sciences* **92**, 11879-11883 (1995).
25. E. Laconi *et al.*, Long-term, near-total liver replacement by transplantation of isolated hepatocytes in rats treated with retrorsine. *The American journal of pathology* **153**, 319-329 (1998).
26. M. H. Tuszynski *et al.*, Fibroblasts genetically modified to produce nerve growth factor induce robust neuritic ingrowth after grafting to the spinal cord. *Experimental neurology* **126**, 1-14 (1994).
27. R. Grill, K. Murai, A. Blesch, F. Gage, M. Tuszynski, Cellular delivery of neurotrophin-3 promotes corticospinal axonal growth and partial functional recovery after spinal cord injury. *The Journal of neuroscience* **17**, 5560-5572 (1997).
28. D. M. McTigue, P. J. Horner, B. T. Stokes, F. H. Gage, Neurotrophin-3 and brain-derived neurotrophic factor induce oligodendrocyte proliferation and myelination of regenerating axons in the contused adult rat spinal cord. *The Journal of neuroscience* **18**, 5354-5365 (1998).
29. P. Lu, L. L. Jones, M. H. Tuszynski, Axon regeneration through scars and into sites of chronic spinal cord injury. *Experimental neurology* **203**, 8-21 (2007).
30. J. E. Goodnight, D. A. Coleman, C. W. DeWitt, Strong and weak immune responses across the same major histocompatibility barrier in rats. *Immunogenetics* **7**, 63-71 (1978).
31. J. E. Marano, D. Sun, A. M. Zama, W. Young, M. Uzumcu, Orthotopic transplantation of neonatal GFP rat ovary as experimental model to study ovarian development and toxicology. *Reproductive Toxicology* **26**, 191-196 (2008).
32. S. Matsuda, S. Koyasu, Mechanisms of action of cyclosporine. *Immunopharmacology* **47**, 119-125 (2000).
33. T. Nguyen, S. Di Giovanni, NFAT signaling in neural development and axon growth. *International journal of developmental neuroscience : the official journal of the International Society for Developmental Neuroscience* **26**, 141-145 (2008).
34. D. M. Basso, M. S. Beattie, J. C. Bresnahan, A sensitive and reliable locomotor rating scale for open field testing in rats. *Journal of neurotrauma* **12**, 1-21 (1995).
35. J. R. Dimar, S. D. Glassman, G. H. Raque, Y. P. Zhang, C. B. Shields, The influence of spinal canal narrowing and timing of decompression on neurologic recovery after spinal cord contusion in a rat model. *Spine* **24**, 1623 (1999).
36. W. Young, M. B. Bracken, The Second National Acute Spinal Cord Injury Study. *Journal of neurotrauma* **9 Suppl 1**, S397-405 (1992).

37. C. D. Mills, B. C. Hains, K. M. Johnson, C. E. Hulsebosch, Strain and model differences in behavioral outcomes after spinal cord injury in rat. *Journal of neurotrauma* **18**, 743-756 (2001).
38. P. J. Horner *et al.*, Proliferation and differentiation of progenitor cells throughout the intact adult rat spinal cord. *The Journal of Neuroscience* **20**, 2218-2228 (2000).
39. L. L. Jones, M. H. Tuszynski, Chronic intrathecal infusions after spinal cord injury cause scarring and compression. *Microscopy research and technique* **54**, 317-324 (2001).
40. G. Agrawal, N. V. Thakor, A. H. All, Evoked potential versus behavior to detect minor insult to the spinal cord in a rat model. *Journal of Clinical Neuroscience* **16**, 1052-1055 (2009).
41. G. Agrawal, C. Kerr, N. V. Thakor, A. H. All, Characterization of graded multicenter animal spinal cord injury study contusion spinal cord injury using somatosensory-evoked potentials. *Spine* **35**, 1122-1127 (2010).
42. A. A. Webb, K. Gowribai, G. D. Muir, Fischer (F-344) rats have different morphology, sensorimotor and locomotor abilities compared to Lewis, Long-Evans, Sprague-Dawley and Wistar rats. *Behavioural brain research* **144**, 143-156 (2003).
43. P. M. VandenBerg, T. M. Hogg, J. A. Kleim, I. Q. Whishaw, Long–Evans rats have a larger cortical topographic representation of movement than Fischer-344 rats: A microstimulation study of motor cortex in naïve and skilled reaching-trained rats. *Brain research bulletin* **59**, 197-203 (2002).
44. W. Young. (Google Patents, 1993).
45. M. Banay-Schwartz, A. Lajtha, M. Palkovits, Changes with aging in the levels of amino acids in rat CNS structural elements I. Glutamate and related amino acids. *Neurochemical research* **14**, 555-562 (1989).
46. O. Raineteau, M. E. Schwab, Plasticity of motor systems after incomplete spinal cord injury. *Nature Reviews Neuroscience* **2**, 263-273 (2001).
47. D. M. Norden, J. P. Godbout, Review: microglia of the aged brain: primed to be activated and resistant to regulation. *Neuropathology and applied neurobiology* **39**, 19-34 (2013).
48. S. Kullberg, H. Aldskogius, B. Ulfhake, Microglial activation, emergence of ED1-expressing cells and clusterin upregulation in the aging rat CNS, with special reference to the spinal cord. *Brain research* **899**, 169-186 (2001).
49. M. J. Hooshmand, M. D. Galvan, E. Partida, A. J. Anderson, Characterization of recovery, repair, and inflammatory processes following contusion spinal cord injury in old female rats: is age a limitation? *Immunity & ageing : I & A* **11**, 15 (2014).
50. P. Schucht, O. Raineteau, M. E. Schwab, K. Fouad, Anatomical correlates of locomotor recovery following dorsal and ventral lesions of the rat spinal cord. *Experimental neurology* **176**, 143-153 (2002).
51. J. Müller-Ehmsen *et al.*, Survival and development of neonatal rat cardiomyocytes transplanted into adult myocardium. *Journal of molecular and cellular cardiology* **34**, 107-116 (2002).
52. H. Zhang, J. A. Stanford, Acute and rebound effects of lorazepam on orolingual motor function in young versus aged Fischer 344/Brown Norway rats. *Behav Pharmacol* **19**, 161-165 (2008).

53. J. E. Marano, D. Sun, A. M. Zama, W. Young, M. Uzumcu, Orthotopic transplantation of neonatal GFP rat ovary as experimental model to study ovarian development and toxicology. *Reprod Toxicol* **26**, 191-196 (2008).
54. G. Raisman, Repair of corticospinal axons by transplantation of olfactory ensheathing cells. *Novartis Foundation symposium* **231**, 94-97; discussion 97-109 (2000).
55. A. Ramon-Cueto, G. W. Plant, J. Avila, M. B. Bunge, Long-distance axonal regeneration in the transected adult rat spinal cord is promoted by olfactory ensheathing glia transplants. *The Journal of neuroscience : the official journal of the Society for Neuroscience* **18**, 3803-3815 (1998).
56. Y. Li, P. M. Field, G. Raisman, Repair of adult rat corticospinal tract by transplants of olfactory ensheathing cells. *Science* **277**, 2000-2002 (1997).
57. J. C. Bartolomei, C. A. Greer, Olfactory ensheathing cells: bridging the gap in spinal cord injury. *Neurosurgery* **47**, 1057-1069 (2000).
58. R. J. Franklin, S. C. Barnett, Olfactory ensheathing cells and CNS regeneration: the sweet smell of success? *Neuron* **28**, 15-18 (2000).
59. T. Imaizumi, K. L. Lankford, W. V. Burton, W. L. Fodor, J. D. Kocsis, Xenotransplantation of transgenic pig olfactory ensheathing cells promotes axonal regeneration in rat spinal cord. *Nature biotechnology* **18**, 949-953 (2000).
60. A. Ramon-Cueto, Olfactory ensheathing glia transplantation into the injured spinal cord. *Prog Brain Res* **128**, 265-272 (2000).
61. A. Ramon-Cueto, M. I. Cordero, F. F. Santos-Benito, J. Avila, Functional recovery of paraplegic rats and motor axon regeneration in their spinal cords by olfactory ensheathing glia. *Neuron* **25**, 425-435 (2000).
62. T. Imaizumi, K. L. Lankford, S. G. Waxman, C. A. Greer, J. D. Kocsis, Transplanted olfactory ensheathing cells remyelinate and enhance axonal conduction in the demyelinated dorsal columns of the rat spinal cord. *The Journal of neuroscience : the official journal of the Society for Neuroscience* **18**, 6176-6185 (1998).
63. G. Raisman, Olfactory ensheathing cells - another miracle cure for spinal cord injury? *Nature reviews. Neuroscience* **2**, 369-375 (2001).
64. A. Ramon-Cueto, F. F. Santos-Benito, Cell therapy to repair injured spinal cords: olfactory ensheathing glia transplantation. *Restorative neurology and neuroscience* **19**, 149-156 (2001).
65. J. Lu, F. Feron, S. M. Ho, A. Mackay-Sim, P. M. Waite, Transplantation of nasal olfactory tissue promotes partial recovery in paraplegic adult rats. *Brain research* **889**, 344-357 (2001).
66. J. Lu, K. Ashwell, Olfactory ensheathing cells: their potential use for repairing the injured spinal cord. *Spine* **27**, 887-892 (2002).
67. T. A. DeLucia *et al.*, Use of a cell line to investigate olfactory ensheathing cell-enhanced axonal regeneration. *Anatomical record. Part B, New anatomist* **271**, 61-70 (2003).
68. Y. Li, P. Decherchi, G. Raisman, Transplantation of olfactory ensheathing cells into spinal cord lesions restores breathing and climbing. *The Journal of neuroscience : the official journal of the Society for Neuroscience* **23**, 727-731 (2003).
69. G. W. Plant, C. L. Christensen, M. Oudega, M. B. Bunge, Delayed transplantation of olfactory ensheathing glia promotes sparing/regeneration of supraspinal axons in the contused adult rat spinal cord. *Journal of neurotrauma* **20**, 1-16 (2003).

70. J. Polentes, J. C. Stamegna, M. Nieto-Sampedro, P. Gauthier, Phrenic rehabilitation and diaphragm recovery after cervical injury and transplantation of olfactory ensheathing cells. *Neurobiology of disease* **16**, 638-653 (2004).
71. L. M. Ramer *et al.*, Peripheral olfactory ensheathing cells reduce scar and cavity formation and promote regeneration after spinal cord injury. *The Journal of comparative neurology* **473**, 1-15 (2004).
72. M. I. Chuah *et al.*, Olfactory ensheathing cells promote collateral axonal branching in the injured adult rat spinal cord. *Experimental neurology* **185**, 15-25 (2004).
73. M. Sasaki, K. L. Lankford, M. Zemedkun, J. D. Kocsis, Identified olfactory ensheathing cells transplanted into the transected dorsal funiculus bridge the lesion and form myelin. *The Journal of neuroscience : the official journal of the Society for Neuroscience* **24**, 8485-8493 (2004).
74. K. Fouad *et al.*, Combining Schwann cell bridges and olfactory-ensheathing glia grafts with chondroitinase promotes locomotor recovery after complete transection of the spinal cord. *The Journal of neuroscience : the official journal of the Society for Neuroscience* **25**, 1169-1178 (2005).
75. R. Deumens *et al.*, Olfactory ensheathing cells, olfactory nerve fibroblasts and biomatrices to promote long-distance axon regrowth and functional recovery in the dorsally hemisected adult rat spinal cord. *Experimental neurology* **200**, 89-103 (2006).
76. M. T. Moreno-Flores *et al.*, A clonal cell line from immortalized olfactory ensheathing glia promotes functional recovery in the injured spinal cord. *Molecular therapy : the journal of the American Society of Gene Therapy* **13**, 598-608 (2006).
77. A. Toft, D. T. Scott, S. C. Barnett, J. S. Riddell, Electrophysiological evidence that olfactory cell transplants improve function after spinal cord injury. *Brain* **130**, 970-984 (2007).
78. Y. B. Deng *et al.*, The co-transplantation of human bone marrow stromal cells and embryo olfactory ensheathing cells as a new approach to treat spinal cord injury in a rat model. *Cytotherapy* **10**, 551-564 (2008).
79. K. Iwatsuki *et al.*, Transplantation of olfactory mucosa following spinal cord injury promotes recovery in rats. *Neuroreport* **19**, 1249-1252 (2008).
80. M. D. Kubasak *et al.*, OEG implantation and step training enhance hindlimb-stepping ability in adult spinal transected rats. *Brain* **131**, 264-276 (2008).
81. K. W. Kafitz, C. A. Greer, Olfactory ensheathing cells promote neurite extension from embryonic olfactory receptor cells in vitro. *Glia* **25**, 99-110 (1999).
82. E. Woodhall, A. K. West, M. I. Chuah, Cultured olfactory ensheathing cells express nerve growth factor, brain-derived neurotrophic factor, glia cell line-derived neurotrophic factor and their receptors. *Brain research. Molecular brain research* **88**, 203-213 (2001).
83. L. A. Carter, A. J. Roskams, Neurotrophins and their receptors in the primary olfactory neuraxis. *Microsc Res Tech* **58**, 189-196 (2002).
84. B. Key, R. A. Akeson, Olfactory neurons express a unique glycosylated form of the neural cell adhesion molecule (N-CAM). *The Journal of cell biology* **110**, 1729-1743 (1990).
85. I. A. Franceschini, S. C. Barnett, Low-affinity NGF-receptor and E-N-CAM expression define two types of olfactory nerve ensheathing cells that share a common lineage. *Developmental biology* **173**, 327-343 (1996).

86. F. Miragall, G. Kadmon, M. Husmann, M. Schachner, Expression of cell adhesion molecules in the olfactory system of the adult mouse: presence of the embryonic form of N-CAM. *Developmental biology* **129**, 516-531 (1988).
87. R. Doucette, Immunohistochemical localization of laminin, fibronectin and collagen type IV in the nerve fiber layer of the olfactory bulb. *International journal of developmental neuroscience : the official journal of the International Society for Developmental Neuroscience* **14**, 945-959 (1996).
88. E. H. Franssen, F. M. de Bree, J. Verhaagen, Olfactory ensheathing glia: their contribution to primary olfactory nervous system regeneration and their regenerative potential following transplantation into the injured spinal cord. *Brain research reviews* **56**, 236-258 (2007).
89. A. Lakatos, P. M. Smith, S. C. Barnett, R. J. Franklin, Meningeal cells enhance limited CNS remyelination by transplanted olfactory ensheathing cells. *Brain* **126**, 598-609 (2003).
90. A. Ramon-Cueto, J. Avila, Olfactory ensheathing glia: properties and function. *Brain Res Bull* **46**, 175-187 (1998).
91. A. J. Vincent, A. K. West, M. I. Chuah, Morphological plasticity of olfactory ensheathing cells is regulated by cAMP and endothelin-1. *Glia* **41**, 393-403 (2003).
92. M. J. Wilby *et al.*, N-Cadherin inhibits Schwann cell migration on astrocytes. *Molecular and Cellular Neuroscience* **14**, 66-84 (1999).
93. F. T. Afshari, J. C. Kwok, J. W. Fawcett, Astrocyte-produced ephrins inhibit schwann cell migration via VAV2 signaling. *The Journal of neuroscience : the official journal of the Society for Neuroscience* **30**, 4246-4255 (2010).
94. F. T. Afshari, J. C. Kwok, L. White, J. W. Fawcett, Schwann cell migration is integrin-dependent and inhibited by astrocyte-produced aggrecan. *Glia* **58**, 857-869 (2010).
95. L. Cao *et al.*, Olfactory ensheathing cells promote migration of Schwann cells by secreted nerve growth factor. *Glia* **55**, 897-904 (2007).
96. M. W. Richter, P. A. Fletcher, J. Liu, W. Tetzlaff, A. J. Roskams, Lamina propria and olfactory bulb ensheathing cells exhibit differential integration and migration and promote differential axon sprouting in the lesioned spinal cord. *The Journal of neuroscience : the official journal of the Society for Neuroscience* **25**, 10700-10711 (2005).
97. K. A. Smale, R. Doucette, M. D. Kawaja, Implantation of olfactory ensheathing cells in the adult rat brain following fimbria-fornix transection. *Experimental neurology* **137**, 225-233 (1996).
98. W. C. Shyu *et al.*, Implantation of olfactory ensheathing cells promotes neuroplasticity in murine models of stroke. *The Journal of clinical investigation* **118**, 2482-2495 (2008).
99. S. Shukla, R. K. Chaturvedi, K. Seth, N. S. Roy, A. K. Agrawal, Enhanced survival and function of neural stem cells-derived dopaminergic neurons under influence of olfactory ensheathing cells in parkinsonian rats. *Journal of neurochemistry* **109**, 436-451 (2009).
100. O. Guntinas-Lichius *et al.*, Transplantation of olfactory mucosa minimizes axonal branching and promotes the recovery of vibrissae motor performance after facial nerve repair in rats. *The Journal of neuroscience : the official journal of the Society for Neuroscience* **22**, 7121-7131 (2002).

101. S. Y. Cheng, H. Z. Ruan, X. G. Wu, [Olfactory ensheathing cells enhance functional recovery of injured sciatic nerve]. *Zhongguo xiu fu chong jian wai ke za zhi = Zhongguo xiufu chongjian waike zazhi = Chinese journal of reparative and reconstructive surgery* **17**, 18-21 (2003).
102. C. Wang, Z. Shi, K. Wang, [Effect of olfactory ensheathing cells transplantation on protecting spinal cord and neurons after peripheral nerve injury]. *Zhongguo xiu fu chong jian wai ke za zhi = Zhongguo xiufu chongjian waike zazhi = Chinese journal of reparative and reconstructive surgery* **19**, 875-878 (2005).
103. Y. Li, M. Yamamoto, G. Raisman, D. Choi, T. Carlstedt, An experimental model of ventral root repair showing the beneficial effect of transplanting olfactory ensheathing cells. *Neurosurgery* **60**, 734-740; discussion 740-731 (2007).
104. J. S. Toma, L. T. McPhail, M. S. Ramer, Differential RIP antigen (CNPase) expression in peripheral ensheathing glia. *Brain research* **1137**, 1-10 (2007).
105. H. Delaviz *et al.*, Transplantation of olfactory mucosa improve functional recovery and axonal regeneration following sciatic nerve repair in rats. *Iranian biomedical journal* **12**, 197-202 (2008).
106. B. C. Li, S. S. Jiao, C. Xu, H. You, J. M. Chen, PLGA conduit seeded with olfactory ensheathing cells for bridging sciatic nerve defect of rats. *Journal of biomedical materials research. Part A* **94**, 769-780 (2010).
107. S. C. Barnett *et al.*, Identification of a human olfactory ensheathing cell that can effect transplant-mediated remyelination of demyelinated CNS axons. *Brain* **123 (Pt 8)**, 1581-1588 (2000).
108. P. M. Smith, F. J. Sim, S. C. Barnett, R. J. Franklin, SCIP/Oct-6, Krox-20, and desert hedgehog mRNA expression during CNS remyelination by transplanted olfactory ensheathing cells. *Glia* **36**, 342-353 (2001).
109. P. M. Smith, A. Lakatos, S. C. Barnett, N. D. Jeffery, R. J. Franklin, Cryopreserved cells isolated from the adult canine olfactory bulb are capable of extensive remyelination following transplantation into the adult rat CNS. *Experimental neurology* **176**, 402-406 (2002).
110. N. Keyvan-Fouladi, G. Raisman, Y. Li, Functional repair of the corticospinal tract by delayed transplantation of olfactory ensheathing cells in adult rats. *The Journal of neuroscience : the official journal of the Society for Neuroscience* **23**, 9428-9434 (2003).
111. F. F. Santos-Benito, A. Ramon-Cueto, Olfactory ensheathing glia transplantation: a therapy to promote repair in the mammalian central nervous system. *Anatomical record. Part B, New anatomist* **271**, 77-85 (2003).
112. R. Lopez-Vales, G. Garcia-Alias, J. Fores, X. Navarro, E. Verdu, Increased expression of cyclo-oxygenase 2 and vascular endothelial growth factor in lesioned spinal cord by transplanted olfactory ensheathing cells. *Journal of neurotrauma* **21**, 1031-1043 (2004).
113. C. Radtke *et al.*, Remyelination of the nonhuman primate spinal cord by transplantation of H-transferase transgenic adult pig olfactory ensheathing cells. *FASEB journal : official publication of the Federation of American Societies for Experimental Biology* **18**, 335-337 (2004).
114. G. Garcia-Alias, R. Lopez-Vales, J. Fores, X. Navarro, E. Verdu, Acute transplantation of olfactory ensheathing cells or Schwann cells promotes recovery after spinal cord injury in the rat. *Journal of neuroscience research* **75**, 632-641 (2004).

115. T. Takami *et al.*, Schwann cell but not olfactory ensheathing glia transplants improve hindlimb locomotor performance in the moderately contused adult rat thoracic spinal cord. *The Journal of neuroscience : the official journal of the Society for Neuroscience* **22**, 6670-6681 (2002).
116. V. M. Gomez *et al.*, Transplantation of olfactory ensheathing cells fails to promote significant axonal regeneration from dorsal roots into the rat cervical cord. *Journal of neurocytology* **32**, 53-70 (2003).
117. D. K. Resnick *et al.*, Adult olfactory ensheathing cell transplantation for acute spinal cord injury. *Journal of neurotrauma* **20**, 279-285 (2003).
118. J. S. Riddell, M. Enriquez-Denton, A. Toft, R. Fairless, S. C. Barnett, Olfactory ensheathing cell grafts have minimal influence on regeneration at the dorsal root entry zone following rhizotomy. *Glia* **47**, 150-167 (2004).
119. L. M. Ramer, M. W. Richter, A. J. Roskams, W. Tetzlaff, M. S. Ramer, Peripherally-derived olfactory ensheathing cells do not promote primary afferent regeneration following dorsal root injury. *Glia* **47**, 189-206 (2004).
120. D. J. Barakat *et al.*, Survival, integration, and axon growth support of glia transplanted into the chronically contused spinal cord. *Cell transplantation* **14**, 225-240 (2005).
121. O. Steward *et al.*, A re-assessment of the consequences of delayed transplantation of olfactory lamina propria following complete spinal cord transection in rats. *Experimental neurology* **198**, 483-499 (2006).
122. F. Bretzner, J. Liu, E. Currie, A. J. Roskams, W. Tetzlaff, Undesired effects of a combinatorial treatment for spinal cord injury--transplantation of olfactory ensheathing cells and BDNF infusion to the red nucleus. *The European journal of neuroscience* **28**, 1795-1807 (2008).
123. M. B. Bunge, Novel combination strategies to repair the injured mammalian spinal cord. *The journal of spinal cord medicine* **31**, 262-269 (2008).
124. A. B. Jackson, M. Dijkers, M. J. Devivo, R. B. Poczatek, A demographic profile of new traumatic spinal cord injuries: change and stability over 30 years. *Archives of physical medicine and rehabilitation* **85**, 1740-1748 (2004).
125. M. L. Sipski, A. B. Jackson, O. Gomez-Marin, I. Estores, A. Stein, Effects of gender on neurologic and functional recovery after spinal cord injury. *Archives of physical medicine and rehabilitation* **85**, 1826-1836 (2004).
126. B. D. Greenwald, R. T. Seel, D. X. Cifu, A. N. Shah, Gender-related differences in acute rehabilitation lengths of stay, charges, and functional outcomes for a matched sample with spinal cord injury: a multicenter investigation. *Archives of physical medicine and rehabilitation* **82**, 1181-1187 (2001).
127. J. C. Furlan, A. V. Krassioukov, M. G. Fehlings, The effects of gender on clinical and neurological outcomes after acute cervical spinal cord injury. *Journal of neurotrauma* **22**, 368-381 (2005).
128. E. Hauben, T. Mizrahi, E. Agranov, M. Schwartz, Sexual dimorphism in the spontaneous recovery from spinal cord injury: a gender gap in beneficial autoimmunity? *The European journal of neuroscience* **16**, 1731-1740 (2002).
129. M. Farooque *et al.*, Gender-related differences in recovery of locomotor function after spinal cord injury in mice. *Spinal cord* **44**, 182-187 (2006).
130. R. L. Roof, E. D. Hall, Estrogen-related gender difference in survival rate and cortical blood flow after impact-acceleration head injury in rats. *Journal of neurotrauma* **17**, 1155-1169 (2000).

131. E. D. Hall, T. R. Gibson, K. M. Pavel, Lack of a gender difference in post-traumatic neurodegeneration in the mouse controlled cortical impact injury model. *Journal of neurotrauma* **22**, 669-679 (2005).
132. K. R. Swartz *et al.*, Gender differences in spinal cord injury are not estrogen-dependent. *Journal of neurotrauma* **24**, 473-480 (2007).
133. D. B. Fee *et al.*, Effects of progesterone on experimental spinal cord injury. *Brain research* **1137**, 146-152 (2007).
134. C. Borras *et al.*, Mitochondria from females exhibit higher antioxidant gene expression and lower oxidative damage than males. *Free radical biology & medicine* **34**, 546-552 (2003).
135. S. Elkabes, A. B. Nicot, Sex steroids and neuroprotection in spinal cord injury: a review of preclinical investigations. *Experimental neurology* **259**, 28-37 (2014).
136. T. Y. Yune *et al.*, Systemic administration of 17beta-estradiol reduces apoptotic cell death and improves functional recovery following traumatic spinal cord injury in rats. *Journal of neurotrauma* **21**, 293-306 (2004).
137. E. A. Sribnick, D. D. Matzelle, S. K. Ray, N. L. Banik, Estrogen treatment of spinal cord injury attenuates calpain activation and apoptosis. *Journal of neuroscience research* **84**, 1064-1075 (2006).
138. P. Chaovipoch *et al.*, 17beta-estradiol is protective in spinal cord injury in post- and pre-menopausal rats. *Journal of neurotrauma* **23**, 830-852 (2006).
139. J. Y. Lee, S. Y. Choi, T. H. Oh, T. Y. Yune, 17beta-Estradiol inhibits apoptotic cell death of oligodendrocytes by inhibiting RhoA-JNK3 activation after spinal cord injury. *Endocrinology* **153**, 3815-3827 (2012).
140. E. A. Sribnick *et al.*, Estrogen attenuated markers of inflammation and decreased lesion volume in acute spinal cord injury in rats. *Journal of neuroscience research* **82**, 283-293 (2005).
141. E. A. Sribnick *et al.*, Postinjury estrogen treatment of chronic spinal cord injury improves locomotor function in rats. *Journal of neuroscience research* **88**, 1738-1750 (2010).
142. S. Kachadroka, A. M. Hall, T. L. Niedzielko, S. Chongthammakun, C. L. Floyd, Effect of endogenous androgens on 17beta-estradiol-mediated protection after spinal cord injury in male rats. *Journal of neurotrauma* **27**, 611-626 (2010).
143. A. Siriphorn, K. A. Dunham, S. Chompoopong, C. L. Floyd, Postinjury administration of 17beta-estradiol induces protection in the gray and white matter with associated functional recovery after cervical spinal cord injury in male rats. *The Journal of comparative neurology* **520**, 2630-2646 (2012).
144. A. J. Thomas, R. P. Nockels, H. Q. Pan, C. I. Shaffrey, M. Chopp, Progesterone is neuroprotective after acute experimental spinal cord trauma in rats. *Spine* **24**, 2134-2138 (1999).
145. P. A. McCombe, J. M. Greer, in *The Autoimmune Diseases*. (Academic Press, 2014), chap. 24, pp. 319-328.
146. W. W. Eaton, N. R. Rose, A. Kalaydjian, M. G. Pedersen, P. B. Mortensen, Epidemiology of autoimmune diseases in Denmark. *Journal of autoimmunity* **29**, 1-9 (2007).
147. S. T. Ngo, F. J. Steyn, P. A. McCombe, Gender differences in autoimmune disease. *Frontiers in neuroendocrinology* **35**, 347-369 (2014).
148. M. A. Choudhry *et al.*, Gender differences in acute response to trauma-hemorrhage. *Shock (Augusta, Ga.)* **24 Suppl 1**, 101-106 (2005).

149. H. Svarstad, H. C. Bugge, S. S. Dhillion, From Norway to Novartis: cyclosporin from Tolypocladium inflatum in an open access bioprospecting regime. *Biodiversity & Conservation* **9**, 1521-1541 (2000).
150. J. F. Borel, C. Feurer, H. U. Gubler, H. Stahelin, Biological effects of cyclosporin A: a new antilymphocytic agent. *Agents Actions* **6**, 468-475 (1976).
151. M. Dreyfuss *et al.*, Cyclosporin A and C. *European journal of applied microbiology and biotechnology* **3**, 125-133 (1976).
152. J. Borel, Comparative study of in vitro and in vivo drug effects on cell-mediated cytotoxicity. *Immunology* **31**, 631 (1976).
153. J. F. Borel, C. Feurer, C. Magnee, H. Stähelin, Effects of the new anti-lymphocytic peptide cyclosporin A in animals. *Immunology* **32**, 1017 (1977).
154. R. Y. Calne, D. J. White, K. Rolles, D. P. Smith, B. M. Herbertson, Prolonged survival of pig orthotopic heart grafts treated with cyclosporin A. *Lancet (London, England)* **1**, 1183-1185 (1978).
155. R. Y. Calne *et al.*, Cyclosporin A in patients receiving renal allografts from cadaver donors. *Lancet (London, England)* **2**, 1323-1327 (1978).
156. R. Calne *et al.*, Cyclosporin A initially as the only immunosuppressant in 34 recipients of cadaveric organs: 32 kidneys, 2 pancreases, and 2 livers. *The Lancet* **314**, 1033-1036 (1979).
157. T. Beveridge, Clinical transplantation–overview. (1986).
158. A. Von Wartburg, R. Traber, Chemistry of the natural cyclosporin metabolites. (1986).
159. F. C. Stevens, Calmodulin: an introduction. *Canadian journal of biochemistry and cell biology = Revue canadienne de biochimie et biologie cellulaire* **61**, 906-910 (1983).
160. C. B. Klee, H. Ren, X. Wang, Regulation of the calmodulin-stimulated protein phosphatase, calcineurin. *The Journal of biological chemistry* **273**, 13367-13370 (1998).
161. E. S. Masuda, R. Imamura, Y. Amasaki, K. Arai, N. Arai, Signalling into the T-cell nucleus: NFAT regulation. *Cellular signalling* **10**, 599-611 (1998).
162. A. Rao, C. Luo, P. G. Hogan, Transcription factors of the NFAT family: regulation and function. *Annual review of immunology* **15**, 707-747 (1997).
163. R. E. Handschumacher, M. W. Harding, J. Rice, R. J. Drugge, D. W. Speicher, Cyclophilin: a specific cytosolic binding protein for cyclosporin A. *Science* **226**, 544-547 (1984).
164. J. Liu *et al.*, Calcineurin is a common target of cyclophilin-cyclosporin A and FKBP-FK506 complexes. *Cell* **66**, 807-815 (1991).
165. M. Kronke *et al.*, Cyclosporin A inhibits T-cell growth factor gene expression at the level of mRNA transcription. *Proc Natl Acad Sci U S A* **81**, 5214-5218 (1984).
166. A. Granelli-Piperno, In situ hybridization for interleukin 2 and interleukin 2 receptor mRNA in T cells activated in the presence or absence of cyclosporin A. *The Journal of experimental medicine* **168**, 1649-1658 (1988).
167. D. J. Cohen *et al.*, Cyclosporine: a new immunosuppressive agent for organ transplantation. *Ann Intern Med* **101**, 667-682 (1984).
168. S. A. Survase, L. D. Kagliwal, U. S. Annapure, R. S. Singhal, Cyclosporin A—A review on fermentative production, downstream processing and pharmacological applications. *Biotechnology advances* **29**, 418-435 (2011).
169. P. J. Delves, I. M. Roitt, *Encyclopedia of immunology*. (ACADEMIC PRESS, San Diego, CA, ed. Second, 1998), vol. 2.

170. O. Lopez, A. Martinez, J. Torre-Cisneros, in *Transplantation proceedings*. (1991), vol. 23, pp. 3181.
171. Y. Shiga, H. Onodera, Y. Matsuo, K. Kogure, Cyclosporin A protects against ischemia-reperfusion injury in the brain. *Brain research* **595**, 145-148 (1992).
172. T. M. Dawson, J. Zhang, V. L. Dawson, S. H. Snyder, Nitric oxide: cellular regulation and neuronal injury. *Progress in brain research* **103**, 365-369 (1994).
173. T. M. Dawson *et al.*, Immunosuppressant FK506 enhances phosphorylation of nitric oxide synthase and protects against glutamate neurotoxicity. *Proc Natl Acad Sci U S A* **90**, 9808-9812 (1993).
174. H. Wakita, H. Tomimoto, I. Akiguchi, J. Kimura, Protective effect of cyclosporin A on white matter changes in the rat brain after chronic cerebral hypoperfusion. *Stroke* **26**, 1415-1422 (1995).
175. D. Ferrari, C. Stroh, K. Schulze-Osthoff, P2X7/P2Z purinoreceptor-mediated activation of transcription factor NFAT in microglial cells. *The Journal of biological chemistry* **274**, 13205-13210 (1999).
176. J. E. Miskin, C. C. Abrams, L. C. Goatley, L. K. Dixon, A viral mechanism for inhibition of the cellular phosphatase calcineurin. *Science* **281**, 562-565 (1998).
177. A. Kiani *et al.*, Regulation of interferon-gamma gene expression by nuclear factor of activated T cells. *Blood* **98**, 1480-1488 (2001).
178. C. Luo *et al.*, Recombinant NFAT1 (NFATp) is regulated by calcineurin in T cells and mediates transcription of several cytokine genes. *Molecular and cellular biology* **16**, 3955-3966 (1996).
179. G. W. Cockerill *et al.*, Regulation of granulocyte-macrophage colony-stimulating factor and E-selectin expression in endothelial cells by cyclosporin A and the T-cell transcription factor NFAT. *Blood* **86**, 2689-2698 (1995).
180. L. Rojanathammanee, K. L. Puig, C. K. Combs, Pomegranate polyphenols and extract inhibit nuclear factor of activated T-cell activity and microglial activation in vitro and in a transgenic mouse model of Alzheimer disease. *The Journal of nutrition* **143**, 597-605 (2013).
181. P. R. Montague, C. D. Gancayco, M. J. Winn, R. B. Marchase, M. J. Friedlander, Role of NO production in NMDA receptor-mediated neurotransmitter release in cerebral cortex. *Science* **263**, 973-977 (1994).
182. V. L. Dawson, V. M. Kizushi, P. L. Huang, S. H. Snyder, T. M. Dawson, Resistance to neurotoxicity in cortical cultures from neuronal nitric oxide synthase-deficient mice. *The Journal of neuroscience : the official journal of the Society for Neuroscience* **16**, 2479-2487 (1996).
183. A. Diaz-Ruiz *et al.*, Cyclosporin-A inhibits inducible nitric oxide synthase activity and expression after spinal cord injury in rats. *Neuroscience letters* **357**, 49-52 (2004).
184. A. Diaz-Ruiz *et al.*, Cyclosporin-A inhibits constitutive nitric oxide synthase activity and neuronal and endothelial nitric oxide synthase expressions after spinal cord injury in rats. *Neurochem Res* **30**, 245-251 (2005).
185. H.-G. Wang *et al.*, Ca2+-induced apoptosis through calcineurin dephosphorylation of BAD. *Science* **284**, 339-343 (1999).
186. N. Sachewsky *et al.*, Cyclosporin A enhances neural precursor cell survival in mice through a calcineurin-independent pathway. *Disease models & mechanisms* **7**, 953-961 (2014).

187. B. Gabryel, J. Bernacki, Effect of FK506 and cyclosporine A on the expression of BDNF, tyrosine kinase B and p75 neurotrophin receptors in astrocytes exposed to simulated ischemia in vitro. *Cell biology international* **33**, 739-748 (2009).
188. D. O. Okonkwo, J. T. Povlishock, An intrathecal bolus of cyclosporin A before injury preserves mitochondrial integrity and attenuates axonal disruption in traumatic brain injury. *Journal of cerebral blood flow and metabolism : official journal of the International Society of Cerebral Blood Flow and Metabolism* **19**, 443-451 (1999).
189. E. Suehiro, J. T. Povlishock, Exacerbation of traumatically induced axonal injury by rapid posthypothermic rewarming and attenuation of axonal change by cyclosporin A. *Journal of neurosurgery* **94**, 493-498 (2001).
190. C. Van Den Heuvel *et al.*, Downregulation of amyloid precursor protein (APP) expression following post-traumatic cyclosporin-A administration. *Journal of neurotrauma* **21**, 1562-1572 (2004).
191. S. W. Scheff, P. G. Sullivan, Cyclosporin A significantly ameliorates cortical damage following experimental traumatic brain injury in rodents. *Journal of neurotrauma* **16**, 783-792 (1999).
192. P. G. Sullivan, M. Thompson, S. W. Scheff, Continuous infusion of cyclosporin A postinjury significantly ameliorates cortical damage following traumatic brain injury. *Experimental neurology* **161**, 631-637 (2000).
193. D. Fee *et al.*, Activated/effector CD4+ T cells exacerbate acute damage in the central nervous system following traumatic injury. *J Neuroimmunol* **136**, 54-66 (2003).
194. K. Domanska-Janik *et al.*, Neuroprotection by cyclosporin A following transient brain ischemia correlates with the inhibition of the early efflux of cytochrome C to cytoplasm. *Brain research. Molecular brain research* **121**, 50-59 (2004).
195. P. G. Sullivan, M. B. Thompson, S. W. Scheff, Cyclosporin A attenuates acute mitochondrial dysfunction following traumatic brain injury. *Experimental neurology* **160**, 226-234 (1999).
196. P. E. Empey, P. J. McNamara, B. Young, M. B. Rosbolt, J. Hatton, Cyclosporin A disposition following acute traumatic brain injury. *Journal of neurotrauma* **23**, 109-116 (2006).
197. A. T. Mazzeo *et al.*, Brain metabolic and hemodynamic effects of cyclosporin A after human severe traumatic brain injury: a microdialysis study. *Acta neurochirurgica* **150**, 1019-1031; discussion 1031 (2008).
198. J. Hatton, B. Rosbolt, P. Empey, R. Kryscio, B. Young, Dosing and safety of cyclosporine in patients with severe brain injury. *Journal of neurosurgery* **109**, 699-707 (2008).
199. A. Diaz-Ruiz *et al.*, Cyclosporin-A inhibits lipid peroxidation after spinal cord injury in rats. *Neuroscience letters* **266**, 61-64 (1999).
200. A. Diaz-Ruiz *et al.*, Lipid peroxidation inhibition in spinal cord injury: cyclosporin - A vs methylprednisolone. *Neuroreport* **11**, 1765-1767 (2000).
201. A. G. Rabchevsky, I. Fugaccia, P. G. Sullivan, S. W. Scheff, Cyclosporin A treatment following spinal cord injury to the rat: behavioral effects and stereological assessment of tissue sparing. *Journal of neurotrauma* **18**, 513-522 (2001).
202. S. S. McMahon *et al.*, Effect of cyclosporin A on functional recovery in the spinal cord following contusion injury. *Journal of anatomy* **215**, 267-279 (2009).

203. N. Lonjon *et al.*, Potential adverse effects of cyclosporin A on kidneys after spinal cord injury. *Spinal cord* **49**, 472-479 (2011).
204. H.-Z. Lü, Y.-X. Wang, J.-S. Zhou, F.-C. Wang, J.-G. Hu, Cyclosporin A increases recovery after spinal cord injury but does not improve myelination by oligodendrocyte progenitor cell transplantation. *BMC neuroscience* **11**, 127 (2010).
205. A. Ibarra *et al.*, Cyclosporin-A enhances non-functional axonal growing after complete spinal cord transection. *Brain research* **1149**, 200-209 (2007).
206. T. Yoshimoto, B. K. Siesjo, Posttreatment with the immunosuppressant cyclosporin A in transient focal ischemia. *Brain research* **839**, 283-291 (1999).
207. F. Akhlaghi, A. K. Trull, Distribution of cyclosporin in organ transplant recipients. *Clinical pharmacokinetics* **41**, 615-637 (2002).
208. R. Kawai, D. Mathew, C. Tanaka, M. Rowland, Physiologically based pharmacokinetics of cyclosporine A: extension to tissue distribution kinetics in rats and scale-up to human. *The Journal of pharmacology and experimental therapeutics* **287**, 457-468 (1998).
209. C. Tanaka, R. Kawai, M. Rowland, Dose-dependent pharmacokinetics of cyclosporin A in rats: events in tissues. *Drug metabolism and disposition: the biological fate of chemicals* **28**, 582-589 (2000).
210. A. Bruelisauer, R. Kawai, P. Misslin, M. Lemaire, Absorption and disposition of SDZ IMM 125, a new cyclosporine derivative, in rats after single and repeated administration. *Drug metabolism and disposition: the biological fate of chemicals* **22**, 194-199 (1994).
211. L. Sangalli, A. Bortolotti, L. Jiritano, M. Bonati, Cyclosporine pharmacokinetics in rats and interspecies comparison in dogs, rabbits, rats, and humans. *Drug metabolism and disposition: the biological fate of chemicals* **16**, 749-753 (1988).
212. H. Mestre, T. Alkon, S. Salazar, A. Ibarra, Spinal cord injury sequelae alter drug pharmacokinetics: an overview. *Spinal cord* **49**, 955-960 (2011).
213. P. Garcia-Lopez, A. Martinez-Cruz, G. Guizar-Sahagun, G. Castaneda-Hernandez, Acute spinal cord injury changes the disposition of some, but not all drugs given intravenously. *Spinal cord* **45**, 603-608 (2007).
214. J. L. Segal *et al.*, Methylprednisolone disposition kinetics in patients with acute spinal cord injury. *Pharmacotherapy* **18**, 16-22 (1998).
215. H. Mestre, T. Alkon, S. Salazar, A. Ibarra, Spinal cord injury sequelae alter drug pharmacokinetics: an overview. *Spinal cord* **49**, 955-960 (2011).
216. A. Ibarra *et al.*, Alteration of cyclosporin-A pharmacokinetics after experimental spinal cord injury. *Journal of neurotrauma* **13**, 267-272 (1996).
217. K. Atkinson *et al.*, Cyclosporine-associated central nervous system toxicity after allogeneic bone marrow transplantation. *Transplantation* **38**, 34-36 (1984).
218. M. Bellet *et al.*, Systemic hypertension after cardiac transplantation: effect of cyclosporine on the renin-angiotensin-aldosterone system. *The American journal of cardiology* **56**, 927-931 (1985).
219. I. D. Roman, M. J. Monte, A. Esteller, R. Jimenez, Cholestasis in the rat by means of intravenous administration of cyclosporine vehicle, Cremophor EL. *Transplantation* **48**, 554-558 (1989).
220. S. Prasad, J. McCauley, G. Salama, T. Starzl, S. Murray, in *Transplantation proceedings*. (NIH Public Access, 1991), vol. 23, pp. 3128.

221. C. L. Truwit, C. P. Denaro, J. R. Lake, T. DeMarco, MR imaging of reversible cyclosporin A-induced neurotoxicity. *AJNR. American journal of neuroradiology* **12**, 651-659 (1991).
222. C. Ferguson *et al.*, Low-dose cyclosporin nephrotoxicity in the rat. *Nephrology Dialysis Transplantation* **8**, 1259-1263 (1993).
223. S. C. Textor *et al.*, Cyclosporine-induced hypertension after transplantation. *Mayo Clinic proceedings* **69**, 1182-1193 (1994).
224. K. Morozumi, A. Takeda, K. Uchida, M. Mihatsch, in *Transplantation proceedings*. (Elsevier, 2004), vol. 36, pp. S251-S256.
225. K. F. Akl, O. A. Samara, Posterior reversible encephalopathy syndrome. *Saudi journal of kidney diseases and transplantation : an official publication of the Saudi Center for Organ Transplantation, Saudi Arabia* **21**, 957-958 (2010).
226. J. R. Rogosheske *et al.*, Higher therapeutic CsA levels early post transplantation reduce risk of acute GVHD and improves survival. *Bone marrow transplantation* **49**, 122-125 (2014).
227. A. Hamwi *et al.*, Cyclosporine metabolism in patients after kidney, bone marrow, heart-lung, and liver transplantation in the early and late posttransplant periods. *American journal of clinical pathology* **114**, 536-543 (2000).
228. J. A. Augustine, M. A. Zemaitis, The effects of cyclosporin A (CsA) on hepatic microsomal drug metabolism in the rat. *Drug metabolism and disposition: the biological fate of chemicals* **14**, 73-78 (1986).
229. A. Diaz-Ruiz *et al.*, Cyclosporin-A inhibits lipid peroxidation after spinal cord injury in rats. *Neuroscience letters* **266**, 61-64 (1999).
230. A. Roozbehi, M. T. Joghataie, M. Mehdizadeh, A. Mirzaei, H. Delaviz, The effects of cyclosporin-A on functional outcome and axonal regrowth following spinal cord injury in adult rats. *Acta medica Iranica* **50**, 226-232 (2012).
231. S. Kumar *et al.*, Estrogen receptor beta ligand therapy activates PI3K/Akt/mTOR signaling in oligodendrocytes and promotes remyelination in a mouse model of multiple sclerosis. *Neurobiology of disease* **56**, 131-144 (2013).
232. J. Z. Hu, H. Long, T. D. Wu, Y. Zhou, H. B. Lu, The effect of estrogen-related receptor alpha on the regulation of angiogenesis after spinal cord injury. *Neuroscience* **290**, 570-580 (2015).
233. H. X. Nguyen, T. J. O'Barr, A. J. Anderson, Polymorphonuclear leukocytes promote neurotoxicity through release of matrix metalloproteinases, reactive oxygen species, and TNF-alpha. *Journal of neurochemistry* **102**, 900-912 (2007).
234. F. Bao *et al.*, A selective phosphodiesterase-4 inhibitor reduces leukocyte infiltration, oxidative processes, and tissue damage after spinal cord injury. *Journal of neurotrauma* **28**, 1035-1049 (2011).
235. H. Saiwai *et al.*, The LTB4-BLT1 axis mediates neutrophil infiltration and secondary injury in experimental spinal cord injury. *Am J Pathol* **176**, 2352-2366 (2010).
236. K. Kubota *et al.*, Myeloperoxidase exacerbates secondary injury by generating highly reactive oxygen species and mediating neutrophil recruitment in experimental spinal cord injury. *Spine* **37**, 1363-1369 (2012).
237. J. Kang *et al.*, IKK-beta-mediated myeloid cell activation exacerbates inflammation and inhibits recovery after spinal cord injury. *European journal of immunology* **41**, 1266-1277 (2011).

238. J. M. Daley, A. A. Thomay, M. D. Connolly, J. S. Reichner, J. E. Albina, Use of Ly6G-specific monoclonal antibody to deplete neutrophils in mice. *Journal of leukocyte biology* **83**, 64-70 (2008).
239. A. Diaz-Ruiz *et al.*, Lipid peroxidation inhibition in spinal cord injury: cyclosporin-A vs methylprednisolone. *Neuroreport* **11**, 1765-1767 (2000).
240. S. Yousuf, F. Atif, V. Kesherwani, S. K. Agrawal, Neuroprotective effects of Tacrolimus (FK-506) and Cyclosporin (CsA) in oxidative injury. *Brain and Behavior* **1**, 87-94 (2011).
241. Y. C. Shin, K. Y. Choi, W. G. Kim, Cyclosporin A has a protective effect with induced upregulation of Hsp70 and nNOS on severe spinal cord ischemic injury in rabbits. *J. Invest. Surg.* **20**, 113-120 (2007).
242. H. Z. Lu, Y. X. Wang, J. S. Zhou, F. C. Wang, J. G. Hu, Cyclosporin A increases recovery after spinal cord injury but does not improve myelination by oligodendrocyte progenitor cell transplantation. *BMC Neurosci.* **11**, 127 (2010).
243. A. Ibarra, A. Diaz-Ruiz, Protective effect of cyclosporin-A in spinal cord injury: an overview. *Curr. Med. Chem.* **13**, 2703-2710 (2006).
244. S. E. Romero, G. Bravo, E. Hong, G. Rojas, A. Ibarra, Acute, subacute and chronic effect of cyclosporin-A on mean arterial pressure of rats with severe spinal cord contusion. *Neurosci. Lett.*, (2008).
245. C. G. Yu, C. A. Fairbanks, G. L. Wilcox, R. P. Yezierski, Effects of agmatine, interleukin-10, and cyclosporin on spontaneous pain behavior after excitotoxic spinal cord injury in rats. *J. Pain* **4**, 129-140 (2003).
246. P. G. Sullivan, A. H. Sebastian, E. D. Hall, Therapeutic window analysis of the neuroprotective effects of cyclosporine A after traumatic brain injury. *J. Neurotrauma* **28**, 311-318 (2011).
247. S. N. Thompson, K. M. Carrico, A. G. Mustafa, M. Bains, E. D. Hall, A pharmacological analysis of the neuroprotective efficacy of the brain- and cell-permeable calpain inhibitor MDL-28170 in the mouse controlled cortical impact traumatic brain injury model. *Journal of neurotrauma* **27**, 2233-2243 (2010).
248. J. Sheehan, A. Eischeid, R. Saunders, N. Pouratian, Potentiation of neurite outgrowth and reduction of apoptosis by immunosuppressive agents: implications for neuronal injury and transplantation. *Neurosurg. Focus* **20**, E9 (2006).
249. A. G. Rabchevsky, I. Fugaccia, P. G. Sullivan, S. W. Scheff, Cyclosporin A treatment following spinal cord injury to the rat: behavioral effects and stereological assessment of tissue sparing. *J. Neurotrauma* **18**, 513-522 (2001).
250. P. G. Sullivan *et al.*, Intrinsic differences in brain and spinal cord mitochondria: Implication for therapeutic interventions. *The Journal of comparative neurology* **474**, 524-534 (2004).
251. P. G. Sullivan, A. G. Rabchevsky, P. C. Waldmeier, J. E. Springer, Mitochondrial permeability transition in CNS trauma: cause or effect of neuronal cell death? *Journal of neuroscience research* **79**, 231-239 (2005).
252. G. Guizar-Sahagun *et al.*, Lack of neuroprotection with pharmacological pretreatment in a paradigm for anticipated spinal cord lesions. *Spinal cord* **47**, 156-160 (2009).
253. S. Tsuruta *et al.*, The effects of cyclosporin a and insulin on ischemic spinal cord injury in rabbits. *Anesth. Analg.* **102**, 1722-1727 (2006).
254. H. Dube *et al.*, A mitochondrial-targeted cyclosporin A with high binding affinity for cyclophilin D yields improved cytoprotection of cardiomyocytes. *The Biochemical journal* **441**, 901-907 (2012).

255. A. Nicolli, E. Basso, V. Petronilli, R. M. Wenger, P. Bernardi, Interactions of cyclophilin with the mitochondrial inner membrane and regulation of the permeability transition pore, and cyclosporin A-sensitive channel. *The Journal of biological chemistry* **271**, 2185-2192 (1996).
256. O. N. Hausmann, Post-traumatic inflammation following spinal cord injury. *Spinal cord* **41**, 369-378 (2003).
257. J. R. Plemel, V. Wee Yong, D. P. Stirling, Immune modulatory therapies for spinal cord injury--past, present and future. *Experimental neurology* **258**, 91-104 (2014).
258. M. A. Lawson, F. R. Maxfield, Ca2+-and calcineurin-dependent recycling of an integrin to the front of migrating neutrophils. *Nature* **377**, 75-79 (1995).
259. B. Hendey, C. B. Klee, F. R. Maxfield, Inhibition of neutrophil chemokinesis on vitronectin by inhibitors of calcineurin. *Science* **258**, 296-299 (1992).
260. W. Wu *et al.*, Calcineurin B stimulates cytokine production through a CD14-independent Toll-like receptor 4 pathway. *Immunology and cell biology*, (2015).
261. M. B. Greenblatt, A. Aliprantis, B. Hu, L. H. Glimcher, Calcineurin regulates innate antifungal immunity in neutrophils. *The Journal of experimental medicine* **207**, 923-931 (2010).
262. J. Fric *et al.*, NFAT control of innate immunity. *Blood* **120**, 1380-1389 (2012).
263. S. Suzuki, L. Toledo-Pereyra, F. Rodriguez, D. Cejalvo, Neutrophil infiltration as an important factor in liver ischemia and reperfusion injury. Modulating effects of FK506 and cyclosporine. *Transplantation* **55**, 1265-1272 (1993).
264. H. Satonaka *et al.*, Calcineurin promotes the expression of monocyte chemoattractant protein-1 in vascular myocytes and mediates vascular inflammation. *Circulation research* **94**, 693-700 (2004).
265. L. Rojanathammanee, A. M. Floden, G. D. Manocha, C. K. Combs, Attenuation of microglial activation in a mouse model of Alzheimer's disease via NFAT inhibition. *Journal of neuroinflammation* **12**, 42 (2015).
266. C. Jennings, B. Kusler, P. P. Jones, Calcineurin inactivation leads to decreased responsiveness to LPS in macrophages and dendritic cells and protects against LPS-induced toxicity in vivo. *Innate immunity* **15**, 109-120 (2009).
267. K. Tsuda *et al.*, Calcineurin inhibitors suppress cytokine production from memory T cells and differentiation of naive T cells into cytokine-producing mature T cells. *PloS one* **7**, e31465 (2012).
268. S. Imashuku *et al.*, Management of severe neutropenia with cyclosporin during initial treatment of Epstein-Barr virus-related hemophagocytic lymphohistiocytosis. *Leukemia & lymphoma* **36**, 339-346 (2000).
269. I. Klusman, M. E. Schwab, Effects of pro-inflammatory cytokines in experimental spinal cord injury. *Brain research* **762**, 173-184 (1997).
270. T. Y. Yune *et al.*, Increased production of tumor necrosis factor-alpha induces apoptosis after traumatic spinal cord injury in rats. *Journal of neurotrauma* **20**, 207-219 (2003).
271. S. Zong, G. Zeng, B. Wei, C. Xiong, Y. Zhao, Beneficial effect of interleukin-1 receptor antagonist protein on spinal cord injury recovery in the rat. *Inflammation* **35**, 520-526 (2012).
272. K. Nagamoto-Combs, C. K. Combs, Microglial phenotype is regulated by activity of the transcription factor, NFAT. *The Journal of neuroscience : the official journal of the Society for Neuroscience* **30**, 9641-9646 (2010).
273. A. M. Fernandez, S. Fernandez, P. Carrero, M. Garcia-Garcia, I. Torres-Aleman, Calcineurin in reactive astrocytes plays a key role in the interplay between

proinflammatory and anti-inflammatory signals. *The Journal of neuroscience : the official journal of the Society for Neuroscience* **27**, 8745-8756 (2007).

274. L. Rojanathammanee, A. M. Floden, G. D. Manocha, C. K. Combs, Attenuation of microglial activation in a mouse model of Alzheimer's disease via NFAT inhibition. *Journal of neuroinflammation* **12**, 42 (2015).
275. A. E. Goldfeld *et al.*, Calcineurin mediates human tumor necrosis factor alpha gene induction in stimulated T and B cells. *The Journal of experimental medicine* **180**, 763-768 (1994).
276. Y. Hayashi *et al.*, Immunosuppression with either cyclosporine a or FK506 supports survival of transplanted fibroblasts and promotes growth of host axons into the transplant after spinal cord injury. *Journal of neurotrauma* **22**, 1267-1281 (2005).